



RIGA TECHNICAL  
UNIVERSITY

**Didzis Avišāns**

**THE EFFECT OF SHIELDING GAS ON THE WELDING  
PROCESS AND WELD SEAM IN SEMI-AUTOMATIC  
WELDING OF HIGH STRENGTH STEEL**

Doctoral Thesis



RTU Press  
Riga 2022

# **RIGA TECHNICAL UNIVERSITY**

Faculty of Mechanical Engineering, Transport and Aeronautics  
Institute of Mechanics and Mechanical Engineering

## **Didzis Avišāns**

Doctoral student of the doctoral study program "Production technology".

# **THE EFFECT OF SHIELDING GAS ON THE WELDING PROCESS AND WELD SEAM IN SEMI-AUTOMATIC WELDING OF HIGH STRENGTH STEEL**

## **Doctoral Thesis**

Field: Mechanical engineering and mechanics

Subfield: Mechanical Engineering Technology

Scientific supervisor

Professor Dr. sc. ing.

**IRĪNA BOIKO**

RTU Press

Riga 2022

# COOPERATION

The Doctoral Thesis was developed with the financial support from the European Social Fund project “Strengthening of the Academic Staff Members of Riga Technical University in Strategic Specialisation Areas” No. 8.2.2.0/18/A/017 (SAM 8.2.2.).

NACIONĀLAIS  
ATTĪSTĪBAS  
PLĀNS 2020



EIROPAS SAVIENĪBA  
Eiropas Sociālais  
fonds

---

IEGULDĪJUMS TAVĀ NĀKOTNĒ

## ANOTĀCIJA

Promocijas darbā “Aizsarggāzes ietekme uz metināšanas procesu un šuvi augstas izturības tēraudu pusautomātiskā metināšanā” pētīta aizsarggāzes ietekme uz augstas izturības tēraudu (650 MPa) metināšanas procesu un sametinātās šuves ķīmiskā sastāva un mehānisko īpašību (cietības) izmaiņām. Pamatota leģējošo elementu (Mangāns un Niķelis) un cietības parametru noteikšanas modeļa izvēle.

Veicot eksperimentālus mērījumus, iegūta principiāla teorijas un eksperimentu sakritība. Noteikta optimāla augstas izturības tēraudu metināšanas tehnoloģija pie strūklveida pārneses metināšanas režīmiem.

Promocijas darbs ir uzrakstīts angļu valodā un satur 71 lappusi, ievadu, 3 nodaļas, secinājumus, informācijas avotu sarakstu, 6 pielikumus, 9 tabulas un 48 attēlus.



## **ABSTRACT**

The influence of shielding gas on the welding process of high-strength steels (650 MPa) and changes in the chemical composition and mechanical properties (hardness) of welded seams is studied in the dissertation “Effect of shielding gas on the welding process and weld in semi-automatic welding of high-strength steels”. The choice of model for determination of alloying elements (Manganese and Nickel) and hardness parameters is justified.

By performing experimental measurements, a fundamental coincidence of theory and experiments was obtained. Optimal welding technology for high-strength steels has been determined for jet transfer welding modes.

The thesis is written in English and contains 71 pages, introduction, 3 chapters, conclusions, a list of information sources, 6 annexes, 9 tables and 48 figures.

## TABLE OF CONTENTS

Introduction.....	7
1. Literature Analysis.....	16
1.1. History of MAG welding technology .....	16
1.2. MAG welding equipment.....	17
1.3. Shielding gases.....	18
1.4. Filler Materials.....	23
1.5. Advantages and disadvantage of MAG welding process.....	25
1.6. Research results.....	25
2. Experimental studies.....	45
2.1. Materials and methods of investigation.....	45
2.2. Results of the investigation.....	49
2.2.1. Form of Welding Seam, Spatters and Penetration.....	49
2.2.2. Microstructure.....	51
2.2.3. Chemical composition.....	54
2.2.4. Hardness.....	59
3. Modeling of the hardness of the welding joint.....	62
3.1. Shielding gas and welding parameter influence on Mn content changes.....	62
3.2. Shielding gas and welding parameter influence on Ni content changes.....	62
Conclusion.....	67
Reference list.....	69
Annexes.....	72

## USED SYMBOLS AND TERMS

A – welding current in Amperes;

V – welding voltage in Volts;

m / min - melting electrode wire feed rate;

CO<sub>2</sub> - Carbon dioxide;

O<sub>2</sub> - Oxygen;

Ar - Argon;

Mn - Manganese;

Ni - Nickel;

Shielding gas - a mixture of gases containing Argon, Carbon dioxide, as well as Oxygen, which provides protection of the weld from the influence of the environment during the welding process;

Low-alloy high-strength steel - Steel in which the composition of the alloying elements does not exceed 2.5% and its minimum yield strength is reached at 450-750 MPa;

Welding pool - an area created by metal and a melting electrode during welding, where the metal is in the liquid phase;

High welding parameters – welding current increased between 265A to 365A that insures the welding wire transfer in spray-arc mode.

Spray arc - a mode of transformation of a molten electrode from a solid phase to a liquid before it comes into contact with the molten base material;

Penetration - the shape and depth of the newly formed weld in the base material of the molten and then hardened metal alloy;

MAG (Metal Active Gas) - fusion electrode welding in an active shielding gas environment;

HAZ – heat affective zone, which reflects the area of the base metal that has not been melted under the influence of the electric arc, which has been exposed to high temperatures and as a result its physical and structural properties have changed.

## INTRODUCTION

Steel production has been a very important field of manufacturing during last centuries. A lot of technologies have been used and implemented to join two metal parts together to make a complete construction. One of these technologies is welding.

Welding have taken a very important part in steel manufacturing during the second part of 20<sup>th</sup> century. Therefore, a lot of different welding technologies have been implemented each one differing from each other by their properties and application. Today most widely used technology in steel construction manufacturing is Metal Active Gas welding (MAG) because of its flexibility and fast welding speed.

There are several factors that influence processes in MAG welding. Steel properties and chemical content is the main component that is observed if looking on weldability of metals. The filler material that is used in MAG welding can make an influence on the process, equipment behavior, spatters and welding joint properties. One of the most important components in the welding process is shielding gas but it is not considered as an issue sometimes as its main task is to prevent an oxygen to get into the welding zone.

There have been developed different kind of shielding gases for mild steel welding during last half of 20<sup>th</sup> century. The first one shielding gas that was used in MAG welding was CO<sub>2</sub> that was implemented by Lyubavski and Novoshilov in 1953. Almost 10 years later in 1960s as small amount of oxygen was mixed with CO<sub>2</sub> that helped to provide a spray-type arc transfer. It took ten years till the new generation of shielding gases was made as new technologies like on-board computers, robots and highly sophisticated electrodes were implemented in MAG welding processes [1].

There are different mixtures of gases available in the market today and sometimes it's hard to decide which one should be used in the welding processes. This paper will include an analysis of the latest researches in field of shielding gases influence on MAG welding process. A short overview of the latest welding equipment used in MAG welding and how it influences behavior of shielding gases in the MAG process.

Not only shielding gases has changed through the years. There are also have been invented different materials that are used in steel production and nowadays they are becoming more available. Many steel production companies are looking for the ways how to make their constructions lighter and still durable and reliable. Therefore, different new materials with higher yield stresses are implemented in steel production. Ass these materials are high alloyed steels the welding process is becoming more complicated comparing to usual steel grades like S235 and S355.

There have been done a few researches about the welding processes of high alloyed steels. Many of these researches have been made about the filler materials and their influence on the welding joint. Only few researches were about the influence of shielding gas on the welding process and the joint of the high strength steels. A lot of researches have also been made using the short-arc welding process and its influence on welding joint. A spray-arc process and its influence will be researched in this investigation as well as the instructions will be provided how to weld the high strength steels correctly with less or no defects.

## **Actuality of the topic.**

Welding of high-strength steels is becoming more important in modern production. These materials allow to reduce the weight of structures with a minimal increase in costs. Semi-automatic gas shielded welding (MAG; Metal-Active-Gas) is widely used in the production of steel constructions. One of the main tasks during this process is not to lose the mechanical properties of the material. As metallurgical processes take place in the weld during welding - melting of the metal, change of the composition of chemical and alloying elements, re-formation of the metal micro structure as the metal cools down. These processes are significantly influenced by the used consumables, shielding gas and chosen welding parameters.

Many investigations till nowadays has focused on the short-arc welding of low-alloy steels (235 - 355MPa) with wire transfer in the form of droplets. As a result, slower seam formation occurs and the thermal effect or heat input to the weld is higher. On the other hand, changes in alloying materials as well as the mechanical properties of the material are not significantly affected. These studies also highlight the influence of shielding gas on welding process. Many studies suggest a mixture of 25% CO<sub>2</sub> (Carbon Dioxide) with Ar (argon) as one of the best mixtures [5], [14], [29], [31]. Similar studies have been performed on the welding of very high strength steels (890 - 1000 MPa) [38], [40], [42], [43]. These studies emphasize that shielding gas mixtures with a lower CO<sub>2</sub> content with Ar give better results. Some of these studies have been performed by welding with welding parameters that ensure the spray-arc transition of the melting electrode. This allows you to increase the welding speed, reduce heat input. As a result, the formation of the welding seam and metallurgical processes take place faster, the arc temperature rises, the molten material becomes more liquid, the seam formation process is not so easy to control [14]. However, the increased presence of CO<sub>2</sub> in the shielding gas and during welding increases the possibility of short-circuiting, which can result in the burning of significant alloying materials. This can lead to a deterioration of the mechanical properties of the weld, which can become the weakest point in the structure.

Analyzing the research carried out in recent years, it was concluded that there is a lack of research on welding of low-alloy, high-strength steels (420-850MPa). These materials are increasingly used and in demand not only in Latvia, but also in other markets. Therefore, it can be concluded that the study on the welding of low-alloyed high-strength steels and the effect of shielding gas on the process is actual. In recent years, welding equipment manufacturers have been offering high-capacity and high-performance equipment on the market, enabling companies to increase production capacity by increasing welding parameters. Therefore, the study of high welding parameters and welding in the spray-arc transfer mode and their effect on the mechanical properties of the welding joint is also very important.

## **Hypothesis.**

In MAG with spray-arc transfer welding of low-alloy high-strength steels (420-850MPa), the hardness of the welded joint material decreases due to the increase of CO<sub>2</sub> content, as well as the addition of O<sub>2</sub>. Based on this assumption, a study was conducted, which is presented in the Thesis.

### **The aim and tasks of the work.**

The aim of this Doctoral thesis is to investigate and find out the effect of MAG welding with spray-arc parameters and shielding gas mixture on the mechanical properties, microstructural changes and chemical composition of welded compounds in low-alloy high-strength steels. As a result of the research, it is planned to develop a mathematical model that would help to predict the mechanical properties and alloying materials like Mn of the welded joint depending on the welding parameters and the use of shielding gas.

Several tasks were performed to achieve the goal:

1. Research of previous investigations and their analysis.
2. Welding of samples with different shielding gases, with high welding parameters, which ensures the transfer of the melting electrode in spray-arc.
3. Analysis of visual testing of welded specimens, of the chemical composition and the newly created microstructure of the weld metal.
4. Examination of the mechanical (hardness) properties of the obtained compound.
5. Develop a mathematical model for predicting mechanical properties (hardness).
6. Approbation of the obtained research results.

### **Research methods.**

Qualitative and quantitative research methods were used to achieve the set goals and solve the tasks, as well as the technical support of the experiments is listed and described.

In order to ensure the high-quality results of the performed experiments, one of the best welding equipment *FRONIUS® (Switzerland)* was chosen for the tests. One of the most recently developed equipment, *Fronius®500i*, was used for the experiments, which ensures the fulfillment of the intended high current parameters, as well as stable transfer of the welding electrode, which is an essential condition for this study. It was mechanized with a *FRONIUS®FlexTrack 45 Pro (Switzerland)* welding tractor to ensure a stable welding process. For precise selection of welding parameters, the application *WeldConnect®* developed by *FRONIUS®* was used, with the help of which the appropriate welding parameters were selected, which would ensure the transfer of the melting electrode in a spray-arc, keeping the setted welding seam size.

Samples were prepared in such a way that it was possible to perform further research of the microstructure of the welded joint, penetration and melting, chemical analysis and hardness measurements after the performed experiments. Laboratory equipment *Texmet 2000 (Italy)* was used for sample preparation. The prepared samples were then etched with 9% nitric acid. It was then possible to see the shape of the weld and further studies and measurements of the welding joint were possible to be performed. The size and amounts of pores and other inclusions were determined using an *Axiovert 40 MAT optical microscope (Germany)* at 50x magnification. The location of the grains of the formed micro-structure and their formation was determined with a magnification of 200 times. Using the optical spectrometer *HITACHI PMI-MASTER Pro2 (Japan)*, the chemical composition of both the base material and the newly formed

weld was determined, after which further work conclusions were made. The hardness of the obtained samples was measured with a *Mitutoyo Micro Vickers hardness tester HM-210D (Japan)*.

Statistical methods used in data processing: descriptive / descriptive statistics, inferential statistical method used to determine correlations - multifactor regression analysis and correlation analysis. The results are displayed in the form of graphs, images and tables.

### **Scientific novelty**

- It has been proven that welding shielding gas with a reduced percentage of carbon dioxide in Argon provides the properties of the welded material and the proportions of the chemical composition more in line with the base material when welding with melting electrodes at high welding parameters.
- A new model has been developed, with the help of which it is possible to predict the influence of the selected welding parameters and the percentage of shielding gas on the properties of the welded joint.
- It has been found that the material formed in the thermal impact zone is weaker than the base material under the influence of high parameters, or the newly formed joint metal contradicts the previously established statement about the increased hardness of this zone in the case of welded joints of low-alloy structural steels.

### **Practical significance.**

The results obtained in the doctoral thesis can be used in steel construction companies and production of various metal structures. High-strength steel is one of the materials that manufacturing companies tend to avoid without knowing its properties and possibilities to process it. Such materials are increasingly being used to facilitate construction. While changes in technology other than the processing of low-alloy construction steels are leading to the abandonment of orders, which can lead to losses due to incorrect production.

Developing and presenting the obtained results to the companies of the steel manufacturing industry, as well as advising them on the possibilities of welding high-strength steels, would give them an advantage in the processing of such materials. It would also make it possible to reduce errors and eliminate the use of inappropriate technologies at the beginning of projects. The developed forecasting model is used in the production of Green Power Ltd products from high-strength steel (650 MPa), where it is necessary to significantly reduce the weight of the structure without losing its strength. This is confirmed by letter of Mārtiņš Grantiņš in Appendix 3.

In addition, in cooperation with the company *Speciāls Elektrods Ltd*, which is one of the leading distributors of MAG welding equipment Fronius® in Latvia, the study has been analyzed. Based on this analyse the solutions are evaluated and offered for metalworking companies in welding of high-strength steels. A letter confirming the cooperation is presented in Appendix 4.

## **Research results presented for the defense**

Results of experimental studies describing the correlation of the chemical composition and hardness of the weld between the welding parameters and the choice of shielding gas. In the performed experiments, welding parameters were chosen from 280A to 320A, but the shielding gas composition was chosen from 8% to 25% CO<sub>2</sub> mixtures with Argon, as well as 5% CO<sub>2</sub> and 5% O<sub>2</sub> mixture with Argon. With the increase of the percentage content of CO<sub>2</sub> gas, no significant changes in the alloyed elements were observed, as well as in the results of hardness measurements in the welded joint. With the decrease of CO<sub>2</sub> content, the decrease of alloying materials, as well as the decrease of the hardness of the indicated weld material was observed with the increase of welding parameters. As a result of the mixture of shielding gases containing 5% CO<sub>2</sub> and O<sub>2</sub>, the percentage of alloying elements in the weld was the lowest regardless of the welding parameters selected and set. No change or significant decrease in the indicated hardness was observed, regardless of the change in welding parameters.

A model developed for predicting the chemical composition and hardness of the welded joint, depending on the interaction of welding shielding gas and welding parameters. The interaction of the used shielding gas with the selected welding parameters under the conditions of spray-arc transfer significantly affects the hardness of the weld material. With the help of the developed model it is possible to predict the changes of hardness parameters (its stability or decrease) depending on the selected shielding gas and welding parameters.

A methodology developed for measuring and forecasting the strength of a welded joint depending on the choice of shielding gas and welding parameters. Using the methodology, the measurement results are within the absolute error limits. Using the developed methodology, the conformity assessment criteria of the forecasting model fall within the limits that indicate the development of a correct model. The methodology specifies guidelines for measurement procedures in the range of percentage of shielding gases from 8 to 25% CO<sub>2</sub> for the mixture, as well as 3% to 7% CO<sub>2</sub> and O<sub>2</sub> mixture in argon, and welding parameters from 260A to 360A.



**Approbation of obtained results.**

PUBLICATIONS IN A JOURNAL INDEXED IN INTERNATIONAL DATABASES

1. I.Boiko, D.Avisans "Study on Shielding Gases for MAG Welding", Journal "Materials Physics and Mechanics", Vol. 16, No 2 (2013), pp. 126-134, ISSN 1605-8119, Datu bāze: SCOPUS, Chemical Abstracts and Elsevier Bibliographic Databases

## PUBLICATIONS IN CONFERENCE PROCEEDINGS

1. D.Avišāns, I.Boiko „Защитные газы для МАG сварки: вопросы экономической эффективности”, Proceedings of 7th International Symposium „Surface Engineering. New Powder Composition Materials. Welding”, 2nd Part, 23-25 March 2011, Minsk, Belarus, p.226-232.
2. I.Boyko, V.Kulakova, D.Avisans “New approach for modeling of the welding processes”, Proceedings of 15th International Research/Expert Conference “Trends in the Development of Machinery and Associated Technology” TMT 2011, Prague, Czech Republic, 12-18 September 2011, Year 15, No 1, pp.809-812.
3. Avišāns, D., Boiko, I. “Review on Shielding Gases for Mag Welding of Mild Steel”. No: 12th International Symposium "Powder Metallurgy: Surface Engineering, New Powder Composite Materials. Welding": Proceedings, Baltkrievija, Minsk, 7.-9. aprīlis, 2021. Minsk: Belarusskaya Navuka, 314.-324.lpp. ISBN 978-985-08-2709-8.
4. D.Avišāns, I.Boiko, A. Avišāne „INFLUENCE OF 8% CO<sub>2</sub> AND ARGON SHIELDING GAS MIXTURE ON MAG WELDING OF HIGH STRENGTH STEEL (650 MPA) IN SPRAY ARC”, Proceedings of International Scientific Conference „Engineering for Rural Development 2022”, Jelgava, Latvija, 25-27.05.2022, p.936-942.

## PUBLICATIONS IN CONFERENCE ABSTRACT BOOKS

1. D.Avišāns, I.Boiko „Aizsarggāzes MAG metināšanā”, 50. RTU studentu zinātniskās un tehniskās konferences materiāli, 2009.g.aprīlī, Latvija, Rīga. – Rīgā: RTU Izdevniecība, 2009.g., 15. lpp.

2. D.Avisans, I.Boiko „Study of the Shielding Gas Influence on Costs of the Welding Joint”, Book of abstracts of the 20th International Baltic Conference „Materials Engineering 2011”, 27–28 October 2011, Kaunas, LITHUANIA, ISSN 2029-8307, p.56.

#### PARTICIPATION IN INTERNATIONAL CONFERENCES:

1. I.Boyko, V.Kulakova, D.Avisans "New approach for modeling of the welding processes", 15th International Research/Expert Conference "Trends in the Development of Machinery and Associated Technology" TMT 2011, Prague, Czech Republic, 12-18 September 2011
2. D.Avišāns, I.Boiko „Защитные газы для МАG сварки: вопросы экономической эффективности”, 7th International Symposium „Surface Engineering. New Powder Composition Materials. Welding”, 23-25 March 2011, Minsk, Belarus
3. D.Avisans, I.Boiko „Study of the Shielding Gas Influence on Costs of the Welding Joint”, 20th International Baltic Conference „Materials Engineering 2011”, 27–28 October 2011, Kaunas, LITHUANIA
4. D.Avisans „SHIELDING GASES IN MAG WELDING: ECONOMICAL ISSUES”, 8th INTERNATIONAL CONFERENCE MET-2013 Materials, Environment, Technology, June 19-20, 2013, Riga, Latvia

#### PRESENTATIONS IN INTERNATIONAL CONFERENCES ORGANISED BY RIGA TECHNICAL UNIVERSITY:

1. D.Avišāns, I.Boiko "Metināšanas ar kūstošu elektrodu aizsarggāzu vidē galvenie raksturojumi", 51. RTU starptautiskā zinātniski tehniskā konference, 2010. gada 11.-15. oktobris, Latvija, Rīga, Latvija
2. D. Avišāns, I. Boiko „Metināšanas ar kūstošu elektrodu aizsarggāzu vidē galvenie raksturojumi”, 52. RTU starptautiskā zinātniski tehniskā konference, 2011. gada 13.–16. oktobris, Rīga, Latvija
3. D.Avisans, I.Boiko „STUDY OF THE SHIELDING GAS INFLUENCE ON WELDING JOINT APPEARANCE”, Riga Technical University 53rd International Scientific Conference dedicated to the 150th anniversary and The 1st Congress of World Engineers and Riga Polytechnical Institute / RTU Alumni, 11-12 October 2012, Rīga, Latvija
4. D.Avišāns RESEARCH OF WELDING BY MELTING ELECTRODES IN PROTECTIVE GAS ENVIRONMENT, 54. RTU starptautiskā zinātniski tehniskā konference, 14. – 16. oktobrī 2013.g., Rīga, Latvija

## 1. LITERATURE ANALYSIS

There are a lot of researches on the MAG welding process done till today. They are mainly devoted to the study of welding processes for structural steels and stainless steels. In recent years, steels of other brands have become more and more available, which differ in their properties from structural steels - they are more durable and resistant to various types of loads. Welding of these high-strength steels may require a different approach to welding processes, and the choice of shielding gas can also affect both the welding process and the result.

In order to understand whether and how the choice of shielding gas affects the welding of different structures and high-strength steels, an analysis and research of various literature sources was performed. In addition to researching scientific publications, the technical literature recommended by high-strength steel manufacturers in addition to before and after welding was reviewed. Several manufacturers of additives have also been looking for the best solutions to ensure a successful welding process and result. Therefore, the literature review also included an analysis of information from some of the world's most popular raw material suppliers. This analysis of the information was supplemented by some studies on the effect of additives on the welding process of high-strength steels and the weld.

### 1.1. History of MAG welding technology

Since the second half of the last century, when metal processing developed more and more rapidly, MAG welding has become one of the most widely used welding technologies, which is currently the second most popular welding process in the world. It provides relatively fast and continuous melting of metal and can be done manually, mechanized or robotic.

MAG welding is a semi-automatic or automatic arc welding process in which a continuous and consumable wire electrode and a shielding gas are fed through a welding gun [1].

A constant voltage, direct current power source is most commonly used with GMAW, but constant current systems, as well as alternating current, can be used.

There are four primary methods of metal transfer in MAG:

- Globular
- Short-circuiting
- Spray
- Pulsed-spray

Each of which has distinct properties and corresponding advantages and limitations [2].

Originally developed for welding aluminum and other non-ferrous materials in the 1940s, MAG was soon applied to steels because it allowed for lower welding time compared to other welding processes. The cost of inert gas limited its use in steels until several years later, when the use of semi-inert gases such as carbon dioxide became common [2].

When it was discovered several years later in 1953 that it was possible to use semi-inert gases such as carbon dioxide in the MAG process, it became widespread and more economical, as well as more affordable. Further developments in the 1950s and 1960s gave the process more versatility and made it a very widely used industrial process. Today, the MAG welding process is the second most common industrial welding process. It is preferred because of its versatility, speed, and ability to adapt the process to automation and robotics. Especially in the automotive industry, the MAG welding process is most often used. Unlike shielding processes that do not use shielding gas, such as self-shielding arc welding (welding wire with self-shielding properties), it is rarely used outdoors or in other areas with changing conditions. In such cases, shielding gas is often not used in the welding process, instead using a hollow electrode wire that is filled with alloying element powder inside. [1]

## 1.2. MAG welding equipment.

MAG welding equipment consists of a welding gun, a power supply, a shielding gas supply, and a wire-drive system that pulls the wire electrode from a spool and pushes it through a welding gun.[2]

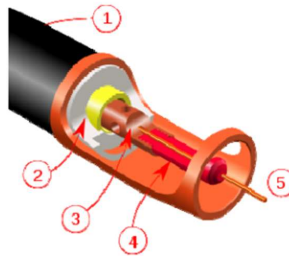


**Fig. 1.1.** Welding gun cross section [2].

- 1) Torch holder; 2) Ceramic (dielectric) insert (shown in white color) with threaded metal insert (yellow); 3) shielding gas separator (diffuser); 4) contact tip, (5) gas nozzle

The standard MAG welding gun (Fig. 1.1.) has several main parts - a control switch, a contact tip, a power cable, a gas nozzle, a wire electrode guide, and a gas hose. By pressing the control switch, the welder or operator activates the wire feed mechanism, the electrical power supply and the shielding gas flow, igniting the electric arc in an instant. The contact tip is usually made of copper, sometimes chemically treated to reduce splashes. It is connected to the welding power source via a power cable and transmits current to the electrode, directing it to the welding area. The nozzle must be firmly fixed and of the correct size, as it must at the same time ensure that the electrode moves smoothly while maintaining electrical contact. Before reaching the contact tip, the wire travels along a guide with a lining or coating that helps prevent bending and maintains a continuous supply of wire. The gas nozzle is used to distribute the shielding gas evenly in the welding area. If the flow is uneven, it may not provide sufficient protection for the weld. Larger nozzles provide higher shielding gas flow, which is useful for high current welding operations where the molten metal weld pool

is increased. Gas is supplied to the nozzle through a gas hose connected to a shielding gas cylinder. Sometimes the welding gun also has a built-in water hose that cools the gun during prolonged welding. The wire feed unit provides continuous supply of electrode to the work area by guiding it through the guide to the contact tip. Many welding machine models provide a constant speed of wire feed, but in more modern equipment, the wire feed speed can vary in response to arc length and tension. Some welding wire feed mechanisms can provide feed speeds of up to 30.5 m/min, but typically the wire feed speed of a semi-automatic MAG welding machine ranges from 2 to 10 m/min [1].

While simple in principle, a system of accurate controls is employed to initiate and terminate the shielding gas and cooling water, operate the welding contractor, and control electrode feed speed as required. The basic features of MAG welding equipment are shown in Fig. 1.2.

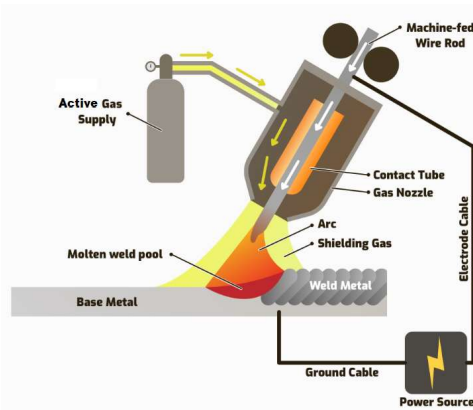


**Fig. 1.2.** MAG welding equipment [3].

A motor automatically unwinds a welding wire from spool and automatically feeds wire to the welding point. This wire is fed through the contact sleeve directly to the welding arc. At the same time shielding gas is fed through a nozzle, which protects the weld pool from the influence of oxygen and thus ensures an oxidation-free connection of the metal parts. The finished weld seam is also known as a welding bead [4].

The MAG process is used for semiautomatic, machine, and automatic welding. Semiautomatic MAG welding is often referred to as manual welding [2].

### 1.3. Shielding gases.

The role of the shielding gas in the welding process is not only to protect the welding pool from access to oxygen and to prevent the formation of pores in the welding bead. Shielding gases can also stabilize the arc and improve the type of metal transfer in arc welding [5], [6]. The quality, efficiency and overall compliance of the welding process with the standard requirements are highly dependent on the shielding gas, as it significantly affects the metal transfer mode [7]. The shielding gas also interacts with the base and filler metal and can thus change basic mechanical properties of the weld area, such as strength, toughness, hardness and corrosion resistance. Shielding gases moreover have important effects on the formation of the weld bead and

the penetration pattern. Oxygen, nitrogen and water vapor present in ambient air can cause weld contamination. Weld shielding, therefore, always involves removal of potentially reactive gases from the vicinity of the weld, preventing the detrimental effects on the molten metal of the surrounding atmosphere. Shielding gases can also stabilize the arc and enhance the metal transfer mode in arc welding processes [8].

Porosity in the weld is one of the most common welding defects related to the shielding atmosphere. Pores can be the initiation point for crack propagation in the welded joint and can considerably decrease the life cycle of joints under dynamic loads [6], [9]. Shielding gases have a distinct effect on the formation and the structure of the arc plasma. This plasma, composed of ionized gas, melted metals, slags, vapors and gaseous atoms and molecules, can be controlled by application of appropriate shielding gas [10].

Shielding gases are divided into two main groups according to their properties – inert, active gases. Inert and Active gases have an important role to play in MAG welding. Several studies have been conducted on the role of each shielding gas in welding processes.

As one of the most important technological processes in industry and construction - development of the method of welding with metal melting, is closely related to the search for various options to ensure the protection of molten metal from the air. The use of argon mixtures with oxidizing gases as CO<sub>2</sub> and O<sub>2</sub> opened up new applications in the welding process of steel in an active shielding gas environment. Most common mixtures are Ar + CO<sub>2</sub>, Ar + CO<sub>2</sub> + O<sub>2</sub> and Ar + O<sub>2</sub>. Depending on grade of welded steels, argon-based gas mixtures can contain 0.5 ... 8% O<sub>2</sub> and 3 ... 25% CO<sub>2</sub> [11].

**Argon** is the most widely used component of shielding gas mixtures, mainly used in TIG welding of non-ferrous, active and heat-resistant metals (Cu, Al, Ni, Mo, Ti, etc.) and their alloys, as well as alloyed and high-alloyed steels. Argon is not widely used in MIG welding of carbon and low-alloyed steels because it does not provide satisfactory transfer of the metal electrode and a stable electric arc, as well as cuts are formed on the metal edges of the welded joint. In addition to the above-mentioned disadvantages, it has been found that the MIG process in pure Argon media is prone to pore formation due to the incorporation of nitrogen, hydrogen and carbon monoxide. The low ionization potential of argon (15.75 eV) ensures stable arc combustion at low voltage, facilitates its excitation and increases stability. Arc plasma in Argon has a high energy inner core and a lower level of energy released in the outer zone, leading to the formation of an undesirable alloy finger shape [12].

Because argon allows operation at lower voltages in any current range, it is better suited for welding thin metals. Argon also has very little effect on the thermal effect during welding, where the arc length can change when the welding operator moves the welding torch [13].

**Carbon dioxide** has long been predominantly used in Eastern Europe and developing countries due to its relatively low cost and availability. However, such significant disadvantages of welding in CO<sub>2</sub> serial silicon-manganese wires as high spatter level and spattering of electrode metal, narrow and deep penetration of the base metal with a high bead, not always satisfactory mechanical properties of the weld metal and especially its impact strength at low temperatures have become the reason that recently and in these countries, there are steady trends towards replacement of CO<sub>2</sub> by



gas mixtures based on argon in those industries where increased attention is paid to the quality indicators of the weld metal and welded joints [14].

It should be noted that the welding process with CO<sub>2</sub> shielding gas is very sensitive to changes in welding parameters. For satisfactory formation of seams and reduction of spatters welding with CO<sub>2</sub> is preferably done with a small diameter wire (0.8 ... 1.4 mm) or at low (with short circuits) and high currents (spray arc), bypassing the medium welding parameter modes (globular arc), on which the maximum spatter amount are noted. For example, for wires with a diameter of 2.0 mm, unfavorable conditions are in the range of  $280 \text{ A} \leq I_w \leq 400 \text{ A}$ ,  $28 \text{ V} \leq U_w \leq 32 \text{ V}$ . Unfortunately, such recommendations are difficult to implement in practice, since in production conditions to ensure high performance and optimal heat input in welding of metals of medium thickness, it is precisely medium currents and wires that are required diameter 1.0...1.2 mm [14].

**Helium** from the gases used in welding ranks second in terms of density (0.178 kg/m<sup>3</sup>) after hydrogen (0.083 kg/m<sup>3</sup>). Compared to argon (1,784 kg/m<sup>3</sup>), helium has a higher thermal conductivity, which ensures an even distribution of energy in the cross-section of the arc, which allows to obtain a deep and wide parabolic weld, with a small joint reinforcement and a smooth transition to the base metal. Due to the high ionization potential in the Helium (24.58 eV) shielding environment, it is necessary to maintain an increased arc voltage compared to welding in a pure Argon environment, at the same arc length and welding current. Therefore, helium is commonly used in mixtures with argon for welding aluminum and other materials in cases where high heat concentrations are present in the welding area [14].

**Oxygen** is one of the components of shielding gas mixtures used in small quantities (from percentages to several percent) to activate metallurgical processes during steel welding. Its composition in the mixture can be used in an amount of 3 to 5% by volume. O<sub>2</sub> can be used as one of the components of the mixture with impurity-free argon (i.e. sufficiently purified in the air separation plant from nitrogen impurities and other gases in the production process) [14].

**Ar + O<sub>2</sub> mixtures** help to slightly improve the welding process and get rid of some of the disadvantages associated with welding in a clean Argon shielding environment. Impurity 3 ... 5% O<sub>2</sub>. A use of argon and the use of welding wire containing silicon and manganese allows to increase the resistance to pore formation in welded alloy steels, regardless of the welding process temperature. Although the mixture of oxygen with Argon practically does not change the shape of the welding arc during welding, it significantly improves its combustion stability and has a positive effect on the metal transfer nature of the electrode, and as a result, the number of drops per unit time increases with decreasing surface tension. The transfer of fine droplets (spray arc) is achieved with a lower welding current value compared to welding in a pure Argon environment, as well as significantly reduces spatter formation to a minimum [14].

The oxygen content of Ar + O<sub>2</sub> mixture can vary from 0.5 to 5.0%. When welding carbon and low-alloy steels, the optimal oxygen content of the mixture is 3 ... 5%. This mixture ensures a good appearance of the weld and the high mechanical properties of the weld metal, especially the impact resistance at negative operating temperatures. At oxygen contents above 5%, the loss of alloying elements during welding increases rapidly, while the technological and visual properties of the welding process do not

change. At the same time, the mixture Ar + O<sub>2</sub> the same as pure CO<sub>2</sub>, is not suitable for welding with a non-melting tungsten electrode (TIG), as it promotes its combustion, as well as contaminates the weld metal with tungsten oxides. Mixtures Ar + O<sub>2</sub> containing a minimum amount of oxygen (1 ... 2%) are of limited use in the welding of ferritic steels and are mainly used in the welding of austenitic steels. The rare use of this mixture is explained by its expensive cost, as it mixes two expensive pure gases, and by the fact that a low-oxygen mixture has the same disadvantages as welding with pure argon. They are narrow penetration root, low pore resistance of welds, uneven line along the edges of the weld, leading to the formation of cuts and insufficient metal alloy, intense arc heat and light radiation, ozone release in the welder's breathing zone is higher than the permissible concentration [14].

The use of **Ar + CO<sub>2</sub> mixtures** has led to a desire to find a protective gas environment that combines the benefits of argon, carbon dioxide and argon-oxygen mixtures. The shape of the arc and the transfer nature of the melting electrode when welding with Ar + CO<sub>2</sub> mixtures depend significantly on the composition of the mixture. By changing the CO<sub>2</sub> content of the mixtures under the same welding modes, a different type of electrode metal transfer can be obtained. It can be with droplets without short circuits (Fig. 1.3., a) or with arc gap short circuits (Fig. 1.3., b), fine droplets (Fig. 1.3., c), and spray arc (Fig. 1.3., d) [14].

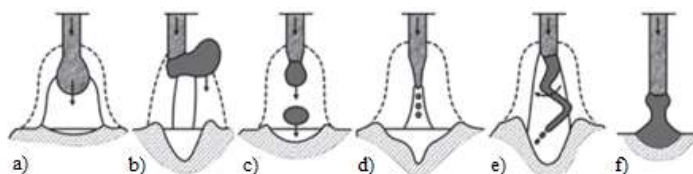


**Fig. 1.3.** Type of metal electrode transfer in welding pool:

- a) droplets without short circuits; b) droplets with arc gap short circuits; c) fine droplets; d) spray arc; e) spray-rotary arc; f) short circuit formation [14].

With a CO<sub>2</sub> content of 20% or more, welding with currents above the critical value changes the shape of the base metal penetration and eliminates the finger-shaped penetration (see Fig. 1.3.1, d). If the CO<sub>2</sub> content of the mixture is more than 35 ... 40%, the welding process is similar to welding with pure CO<sub>2</sub> in a protective medium, but with a lower amount of spatter.

Welding is improved by using mixtures with + 20 ... 25% CO<sub>2</sub>, and this is observed in a variety of modes. The height of the joint is significantly lower than with pure CO<sub>2</sub> welding, there is a smooth transition from spherical droplets to monolithic metal and in the current range at which jet transfer is formed (in the form of fine droplets), a fine surface is formed, as in welds using submerged arc welding technology, acceptable seam shape, low reinforcement height and reduced electrode metal spatter loss, as well as a significant reduction in electrode wire consumption per unit length of the weld. Recommendations for the optimal mixture of Ar + CO<sub>2</sub> usage among foreign companies are contradictory [15].

Structural steel joints welded in argon-based shielding gas mixtures with standard wires commonly used for CO<sub>2</sub> welding show high mechanical properties [16]. Particularly noteworthy are the values of impact resistance when welding metal at low

temperatures, as well as the metal resistance of welds welded in an Ar + CO<sub>2</sub> mixture values against creation and development of brittle fracture [17]. The improvement in the mechanical and performance properties of joints welded using argon-based mixtures can be explained by the reduced oxygen content in the joints, the formation of a favorable metal microstructure with a predominance of acicular ferrite and the favorable conditions in the joint formation process. The level of welding joint yield strength values at low temperatures and crack resistance indicators for joints welded at increased specific thermal input using Ar mixtures cannot be obtained by welding in CO<sub>2</sub> shielding environment at similar welding parameters [16], [18]. In general, data and results published by other researchers [5], [12] indicate that the properties of welded joints welded in argon-based gas mixtures meet the requirements of joints and structures operating under negative temperature conditions, dynamic loads and other adverse factors.

Welding with argon mixtures, in contrast to welding with CO<sub>2</sub> makes it possible to use the pulse-arc process with controlled droplet transfer and separation frequency drops corresponding to the frequency of superposition of current pulses [13], [19].

**Ar + CO<sub>2</sub> + O<sub>2</sub> mixtures** have become widespread in Germany and the United Kingdom [20]. The mixture "Coxogen" (with + 5% O<sub>2</sub> + 15% CO<sub>2</sub>) has lower oxidation capacity and better technological properties than pure CO<sub>2</sub>. Welding of carbon and low-alloy steels with welding wire containing manganese and silicon has the advantages of less spatter, better weld penetration, reduced tendency to form pores and cracks in the joints, as opposed to CO<sub>2</sub> welding. The mechanical properties of welded metal compounds are the same as when welding with Ar + 20 ... 25% CO<sub>2</sub>, whereas the impact resistance of the joints is higher when welding with Ar + O<sub>2</sub> + CO<sub>2</sub>.

**Ar + He + CO<sub>2</sub> mixtures**, in which argon is the main component, are used in welding with a stationary and pulsed arc, and mixtures with a predominant (60 ... 80%) content helium - when welding with short circuits. foreign publications [21], [22] consider various compositions of gas mixtures with helium (vol. %: (69...55) Ar + (40...30) He + (3...5) CO<sub>2</sub>) providing good technological performance. Practically, it is possible to increase the productivity when welding thick metal, reach wide and deep penetration of the base metal, improving the penetration and form of welding seams. The main feature of welding with shielding gas mixtures Ar + He + CO<sub>2</sub> is high performance process in modes with spray-rotary transfer of the electrode metal (see Fig. 1e). Such metal transfer occurs when using a welding wire with a diameter of 1.0 ... 1.2 mm, an electrode wire feed rate of up to 50 m/min and power supply with good dynamic characteristics [23], [24].

**Ar + He + CO<sub>2</sub> + O<sub>2</sub> mixtures** require special technology, power sources and mechanisms wire feed. So, for the T.I.M.E process [24], [25] a mixture of gases is used (vol. %: 65 Ar + 26.5 He + 8 CO<sub>2</sub> + 0.5 O<sub>2</sub>), providing a high wire melting rate (up to 25 kg/h) at a feed rate of up to 50 m/min at a welding current of about 600 A. High-performance methods as Rapid Arc and Rapid Melt are also known [22, 26, 27], which are performed in protective mixtures with helium (vol. %: (65...60) Ar + (25...30) He + 10 CO<sub>2</sub>), when using the wire feed speeds that exceed the classic limit of 20 m/min and provide various types of electrode metal transfer including spray-rotary arc (see Fig. 1, e). Strict restrictions on the composition of the protective environment, provided by the technological recommendations of the developers of the T.I.M.E process [24]

are not reasonable, since similar performance and quality indicators can be obtained with using cheaper and easier to manufacture gas mixtures based on argon without helium, for example, Ar + CO<sub>2</sub> + O<sub>2</sub>, and careful selection of welding parameters and parameters correction [20], [27], [28].

Due to the fact that the MAG welding process is dominant in Europe, the focus is on the choice of shielding gas composition. Its optimization criteria are the level of spatter and the amount of slag on the surface of the welded joint, the process of joint formation (penetration and form of welding seam). Based on these requirements, it is proposed to use weakly oxidizing mixtures based on argon with a low content of oxidizing gases (1 ... 4% O<sub>2</sub> and up to 10% CO<sub>2</sub>) [12]. It should also be noted that welding of low alloyed steels in easily oxidizable argon-based mixtures has all the above-mentioned disadvantages of pure argon [14].

#### 1.4. Filler materials.

Several sources of information emphasize that the correct choice of raw materials and the preparation of the metal are very important for the successful bonding of two separate materials. As technologies, both in the production of raw materials and in welding equipment, have changed in recent years, new research has also been conducted to find the best parameters and raw materials that provide faster and higher quality welding.

Since the wire electrode also serves as the weld filler material, the wire diameter and composition will vary. Which you use depends on variables like the type of metal, its thickness, and the joint configuration [Te var ielikts pāris no tiem neieliktajiem].

The solid electrode wire comes on different size spools, and the MAG welder feeds it to the torch where it is consumed. Therefore, one of the key MAG welder settings is the wire feed speed (WFS), which must be set to provide the right amount of weld metal for the intended joint [3].

There are two types of melting electrode wires used in MAG welding. The name wire is usually understood to mean solid (monolithic) wire and wire with powder filling (flux-cord wire). There is one meaning in Europe MAG welding that include using both types of welding wires. Nevertheless, there are two different meanings in America that describes welding by using solid wire and flux-cord wire.

**GMAW (Gas Metal Arc Welding)** is understood as a MAG welding process where the solid wire is used.

**FCAW (Flux-Cord Arc Welding)** is stated as a MAG welding process where wire with powder filling is used in America.

**Solid wires** are made for MIG / MAG welding with different diameters (0.6: 2.4 mm) and different chemical composition. Steel wire the surface is usually covered with a thin copper layer that protects the wire from rusting during storage and facilitates power supply to the wire. Wire is supplied to consumers in cartridges of a certain size. Each batch of wire must be attached a certificate stating the chemical composition of the wire in question. Compact wire for MIG / MAG arc welding of non-alloy and fine-grained steels in a shielding gas environment is classified according to LVS EN ISO 14341: 2008 [48].

These wires are classified by welding seam strength limits and stiffness 27 J. Usually, solid wires are made with the copper coating to ensure proper contact during the wire movement through the contact nozzle. There are also copper-free coating wires used nowadays. These wires have some advantages against copper coated wire electrodes: higher allowable current strength, more stable arc, less spatters, copper-free smoke and better seam quality (no copper inclusions) [48]. One more practical issue by using this type of wires is that copper coating is not separating from the wire while it is unrolled from the drum. These copper particles can get stuck in the guiding coil. Electrode wire is guided and pushed through that coil from the welding machine to the welding gun. By using copper-free welding wire that have homogeneous surface structure, which together with the special coating provide safe wire supply through the guiding coil and more stable power supply. The special coating also protects the copper-free wire from corrosion at long-term storage.

**Wires with powder filling (Flux-cord)** are made of tape by bending and filling with specially prepared powder mass. (Fig. 1.4.). The filling in the welding process is partially performing the same functions as the electrode cover in MMA (Manual Metal Arc) welding, i.e.:

- forms gases that protect the molten metal from the effects of ambient air;
- forms impurities that protect the liquid metal bath;
- performs alloying of metal [48].

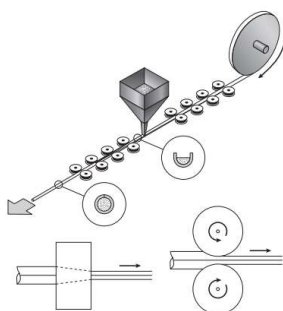


**Fig. 1.4.** Production process technology of flux-cord wire [48].

There are three types of filler materials according to their chemical composition: rutile, basic and metallic powder fillings.

**Rutile** type filling provides spray arc transfer, small amounts of spatters and rutile - a basic type of slag that completely closes the welding bath. You can use PA and PB positions.

**P** - type wires are similar to rutile type, but produce fast-curing slag, which allows them to be used in all positions.

**Basic** type filling provides high mechanical properties of the seam and good resistance cracking. Weld with this filling is harder, probably only at the bottom yes and in a horizontal position. For other positions it is necessary to use a pulsating circle.

**Metal powder** filling does not contain any contaminants, only the metal powder. That gives higher productivity. The arc is stable and spatters are small. These wires

commonly used mechanized and robotic welding. Can be welded in PA and PB positions, other positions need pulse-arc [48].

Different sources of information emphasize that the correct choice of raw materials and the preparation of the metal are very important for the successful welding of two separate materials [3], [14], [42], [44], [56], [57]. As technologies, both in the production of raw materials and in welding equipment, have changed in recent years, new research has also been conducted to find the best parameters and raw materials that provide faster and higher quality welding of high strength steels [41], [42].

### **1.5. Advantages and Disadvantages of MAG welding process.**

The major advantage of gas metal-arc welding is that high-quality welds can be produced much faster than with other manual welding methods like MMA (Manual Metal Arc) or TIG (Tungsten Inert Gas) welding [4], [14]. It gives a possibility to increase the productivity of the welding process.

Since a flux is not used, there is no chance for the entrapment of slag in the weld metal [14]. For the same reason there is less possibility to have pores in the welding joint even when making multi-layer welding.

The shielding gas protects the arc so that there is very little loss of alloying elements as the metal transfers across the arc. Only minor weld spatter is produced, and it is easily removed [4], [12], [14], [36]. In this case it is very important to use appropriate shielding gas, welding parameters and equipment to insure spatter-free welding.

This process is versatile and can be used with a wide variety of metals and alloys, including aluminum, copper, magnesium, nickel, and many of their alloys, as well as iron and most of its alloys. The process can be operated in several ways, including semi- and fully automatic [6], [12], [14], [18]. MAG welding is the second most common welding process used by many industries for welding a broad variety of materials, parts, and structures.

The major disadvantage of this process is that it cannot be used in the vertical or overhead welding positions due to the high heat input and the fluidity of the weld pool [4]. In this case the welder should use special flux-cored melting electrode to reduce the welding pool temperature and increase the hardening speed of welded metal.

The equipment is more complex compared to equipment used for the manual metal-arc welding process that can be used [5]. It is also hard to afford shielding gases on places where welding has to be done. Wind is also very serious factor that can influence MAG welding process as it can blow away the shielding gas and decrease the defense of welding pool against creation of pores.

### **1.6. Research results.**

There have been made different researches during last years that were related to research of MAG welding process. Almost all of them are related to search the influence of shielding gas on created welding joint. Different materials have been used and overviewed in the investigations as well as different shielding gases and welding parameters.

A wide overview of different shielding gas influence on different types of welding technologies was done by scientists P. Kah and J. Martikainen. Four different Argon and CO<sub>2</sub> mixtures were tested on steel grade ST37-2 that is equivalent to S235JR according to EN ISO 10025-2 standard. It was stated that the amount of inclusions in

welding joint decreases as the volume of CO<sub>2</sub> is increased [5]. Similar conclusion was made in another two researches [55], [56].

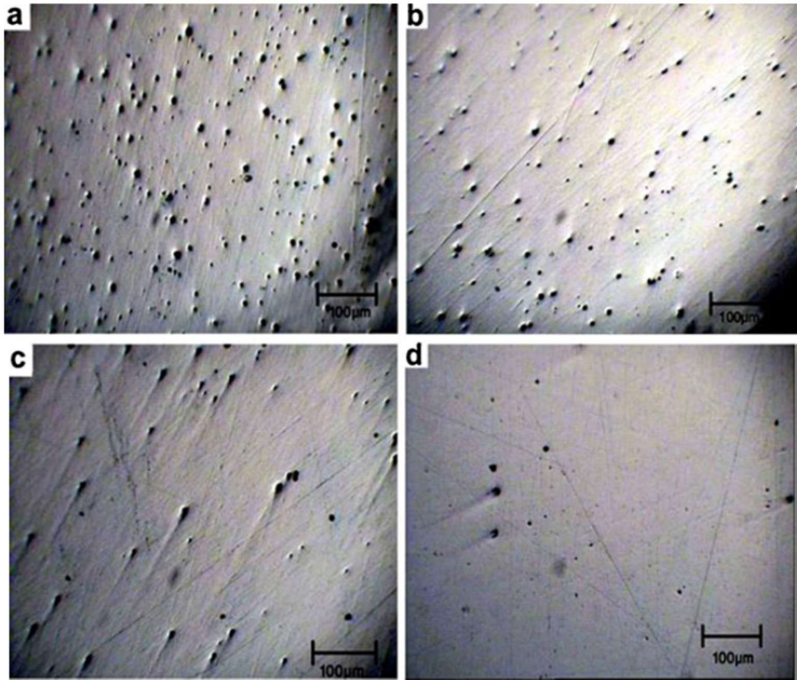


**Fig. 1.6.** Inclusion in samples with different shielding gas composition. a) 97.5 % Ar+2.5 %CO<sub>2</sub>, b) 90 % Ar+10 % CO<sub>2</sub>, c) 82 % Ar+18 % CO<sub>2</sub> and d) 75 % Ar+25 % CO<sub>2</sub>.

Samples are in unetched state. Material ST37-2. Process MAG [5].

Inclusions in the weldment initiate and direct cracks and promote brittle fracture. Increasing the CO<sub>2</sub> percentage also enhances the formation of acicular ferrite, which improves weld toughness and decreases hardness [5].

Authors haven't used three component gas mixture in their research as well as there is no information about the parameters that were used during welding procedures. The steel that was observed is low alloyed carbon steel that has different properties compared to high strength steels.

Authors have also overviewed another research of shielding gas influence on the impact strength and tensile strength of ST37-2 welded joint [6]. The results are illustrated in Fig. 1.7. As the oxidation potential of the shielding gas increases, the toughness and the tensile strength of the weld deposit decrease.

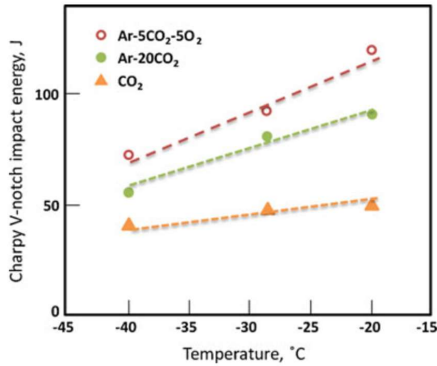
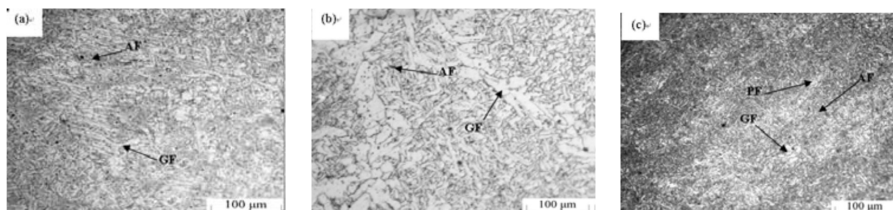


**Fig. 1.7.** Weld metal impact energy as a function of shielding gas composition for MAG welding of carbon steel [6].

Argon blends with lower oxidizing gas content will generally produce weld properties superior to those obtained by shielding with CO<sub>2</sub> only. There appears to be an optimal oxygen content, since too low oxygen levels can also be detrimental to toughness [6]. Here authors have also used ST37-2 (S235JR) steel with only three shielding gases. No influence on welded joint composition and hardness was done.

A research on ST37-3 steel by using the flux-cored welding wire with seven different shielding gases was done by scientist Ramy Gadallah and his colleagues [29]. They claim that 75% Ar – 25% CO<sub>2</sub> shielding gas composition has the optimum deposition rate among other shielding gases for B.O.P (bead-on-plate). Furthermore, for complete real welded joints, the absorbed energy in the Charpy impact toughness test of weld metal (W.M) decreases with increase of the CO<sub>2</sub> percent in the shielding gas composition. Additionally, the hardness of W.M decreases with the increase of the CO<sub>2</sub> percent in the shielding gas composition [29]. Similar conclusion was also made by S.A. Rizvi in his research of welding mixture influence on structural steel welding [57].

The microstructures of investigated samples as a function of the shielding gas compositions are shown in the Fig. 1.8. The W.M microstructure in case of pure Ar shielding gas is a solidified columnar structure associated with fine grains of GF and AF, as shown in Fig. 1.8. a. The W.M microstructure in case of pure CO<sub>2</sub> shielding gas is also a columnar structure consisting of GF and AF, as shown in Fig. 1.8. b with larger grain sizes than that observed for pure Ar shielding gas. Thus, this change in microstructure could be related to the effect of arc stirring force [37], which is much higher in the case of pure Ar shielding gas as compared to the case of pure CO<sub>2</sub>.





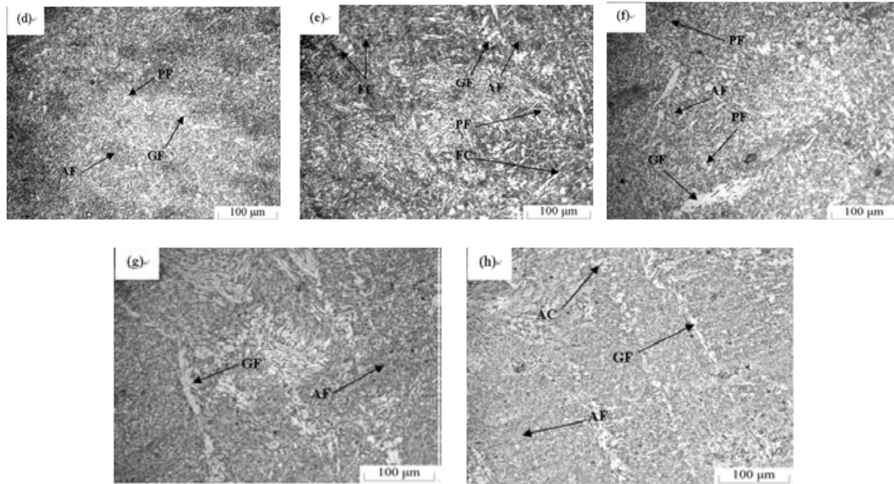


**Fig. 1.8.** Microstructure of W.M of B.O.P specimens. (a) Pure Ar, (b) Pure CO<sub>2</sub>, (c) 95% Ar – 5% CO<sub>2</sub>, (d) 90% Ar – 10% CO<sub>2</sub>, (e) 82% Ar – 18 CO<sub>2</sub>, (f) 80% Ar – 20% CO<sub>2</sub>, (g) 75% Ar – 25% CO<sub>2</sub>, and (h) 50% Ar – 50% CO<sub>2</sub>. Where AF: Acicular ferrite, GF: Grain boundary ferrite, PF: Polygonal ferrite, FC: Ferrite carbide and AC: Aligned carbide [29].

Authors have made following conclusions:

- 1) The shielding gas compositions have a significant effect on the arc stability and efficiency, deposition rate, microstructure, chemical and mechanical properties of mild carbon steel welds.
- 2) Among the investigated shielding gas compositions in case of FCAW the shielding gas composition 75% Ar – 25% CO<sub>2</sub> is the best economic shielding gas composition, because of its high arc efficiency and deposition rate, thus it can reduce the number of weld layers and also reduce the welding time (i.e. reduce the costs)
- 3) The W.M microstructure in case of 75% Ar – 25% CO<sub>2</sub> shielding gas is homogenous due to the balance of cooling rate and the formation of a high amount of AF which leads to the improvement of strength and toughness.
- 4) Increasing the amount of CO<sub>2</sub> in the shielding gas, decreases the hardness of W.M.
- 5) As the CO<sub>2</sub> percent in the shielding gas increases, the required absorbed energy (impact toughness) of W.M decreases due to the decrease of the amount of AF [29].

The authors have done a good research by using low carbon steel and experiments were done with the flux-cord wire. It gives a possibility to weld with lower parameters to reach the spray-arc metal transfer during the process. There are no experiments done with the solid wire and also three component gas tests are not included and Argon mixture with low CO<sub>2</sub> content is not taken into count in further investigations.

Opposite view on inclusion formation were reported by A.F. Moreira and J. Gallego. They were welding structural steel A36 (Equivalent to S235JR) with four different shielding gases that were pure argon and mixture of argon-carbon dioxide

(92%Ar+8%CO<sub>2</sub>, 85%Ar+15%CO<sub>2</sub> and 75%Ar+25%CO<sub>2</sub>) [30]. In their conclusion we can find the table that shows the amount of inclusions in the welding joint that increases as the volume of CO<sub>2</sub> increases in the shielding gas mixture. Results of the investigation are collected in table 1.1.

**Table 1.1.**  
Gas composition and values of volume fraction of inclusion [30].

Sample	Gas composition	Volume fraction of inclusion [%]
S1	Pure Argon	2,32 ± 0,4
S2	92%Ar + 8% CO <sub>2</sub>	2,94 ± 0,3
S3	85%Ar + 15% CO <sub>2</sub>	3,12 ± 0,3
S4	75%Ar + 25% CO <sub>2</sub>	3,48 ± 0,2

Pictures from transmission electron micrographs of typical inclusions was confirming the same (Fig. 1.9.).

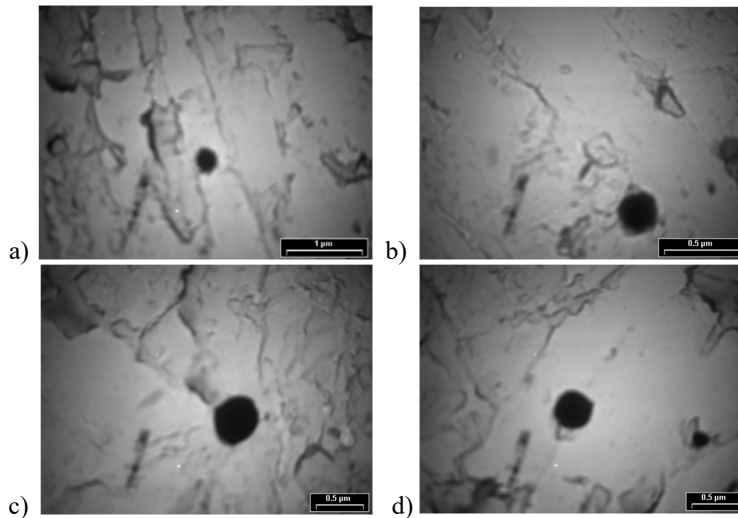


**Fig.1.9.** Transmission electron micrographs of typical inclusions: a) sample S1, b) sample S2, c) sample S3, d) sample S4 [30].

Authors have concluded that there is an influence of CO<sub>2</sub> content on appearance of pores and inclusions in the welding joint. Structural steel and two component gases were used in the investigation and there are no other conclusions done according to weld hardness, microstructure and chemical composition.

In recent study of shielding gas influence on welding of structural steel S275 B. Çevik was testing the shielding gas with Argon mixture with CO<sub>2</sub> and a little content of O<sub>2</sub> (Ar 86 %, CO<sub>2</sub> 12 %, O<sub>2</sub> 2 %) [31]. This mixture was compared with pure Argon. Tests showed that there is an influence on Tensile strength on the welding joint. Tensile strength of 589.8MPa was determined in the joint welded by mixed gas. There was a decrease of 3.8 % in tensile strength compared to the base metal. % elongation ratio of the sample welded by mixed gas was 30.7% and a decrease of 9.7% was observed

compared to % elongation value of base metal [32]. The tensile strength of the joint performed by using pure Ar gas was 481.4MPa. When tensile strength of this sample was compared with base metal, it decreased at the rate of 21.4%. % elongation value of the sample joined by using pure Ar was 23.9%, and a decrease of 29.7% was observed compared to. % elongation value of the base metal [31].

There was an influence on microstructure of welding joint noticed during examination of the microscope inspection. Author of the report states that the reason of these changes is the different behavior of the arc. An easy arc ignition was ensured, a stable arc was formed, and when pure Ar gas was used, a no spatter welding seam was obtained. When a CO<sub>2</sub> gas of 12% and 2% of O<sub>2</sub> was added to Ar gas, the amounts of spatters increased [31].

We can find the results of the formed microstructure in Fig. 1.10. The microstructure of both weld metals consisted of thin acicular grains. However, weld metal sample welded by pure Ar gas had finer grain structure compared to the sample joined by mixed gas [31] as heat input for Ar + CO<sub>2</sub> + O<sub>2</sub> mixture was bigger during the welding process.

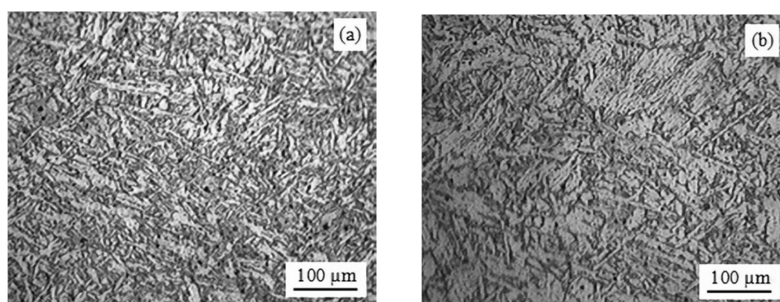


**Fig. 1.10.** Microstructure of weld metal: (a) pure Ar gas, (b) mixed gas [6].

Literature sources [33], [34], [35] report that the structures formed in the welding pool are ferrite, Widmanstätten ferrite, acicular ferrite, bainite and perlite. As microstructures of weld metal were examined. It was observed that mainly grains of Widmanstätten ferrite and acicular ferrite (acicular parts) formed [31].

Authors have used only one three component gas mixture and pure argon with flux-cord wire on standard structural steel in this investigation. There were no two component (Ar + CO<sub>2</sub>) mixtures used and no influence on welding joint chemical composition or hardness investigated during the research. Better results with Ar mixture than with pure Ar was achieved in this investigation compared to other investigations were pure Ar was showing the best results among other shielding gases.

Different mixtures of Ar + CO<sub>2</sub>, Ar + CO<sub>2</sub> + O<sub>2</sub> and pure CO<sub>2</sub> were tested on structural steel S235 with MAG welding and solid wire in one of the reports. Short arc parameters were chosen to create smooth welding joints on each sample. Microstructure inspection as well as chemical analysis of the welding joint were carried out during the research. Difference in the shielding gas composition showed the influence on microstructure changes as well as on chemical composition of the welding pool. It is possible to find in Fig. 1.11. that the size of grains is growing as the volume of CO<sub>2</sub> gas increases in the gas mixture. It is also stated that the degree of oxidation is high for pure CO<sub>2</sub> and increases with higher quantities of CO<sub>2</sub> and/or O<sub>2</sub> in the shielding gas. The

presence of a high-volume fraction of inclusions may initiate premature ductile fracture [36]. This confirms the inclusions that can be found in Figure 1.11. b), c) and also e).

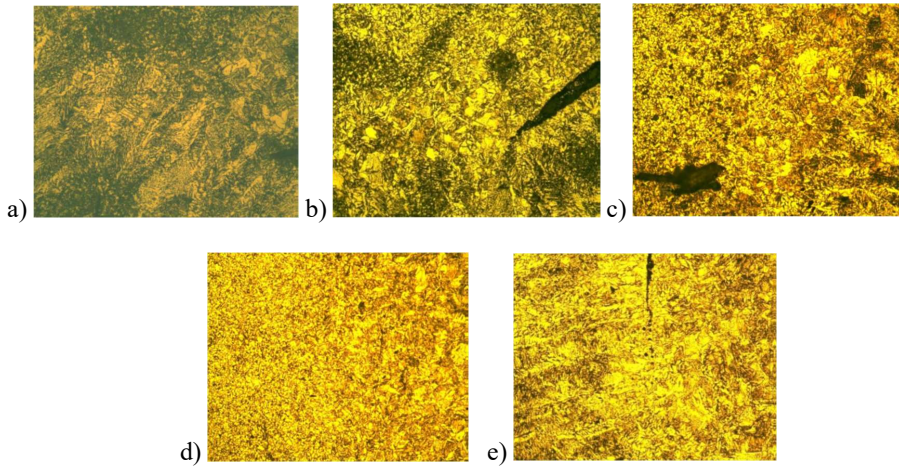


**Fig. 1.11.** Microstructure of the weld metal using different shielding gases (200x): a) Ar+CO<sub>2</sub> 18%; b) Ar+CO<sub>2</sub> 25%; c) Ar+CO<sub>2</sub> 5% + O<sub>2</sub> 5%; d) Ar+CO<sub>2</sub> 8%; e) CO<sub>2</sub> [36].

The most homogeneous structure is received, using shielding gas with the lowest content of CO<sub>2</sub> (Fig. 1.11. d). It is evident that an increase in CO<sub>2</sub> content in the shielding gas as well as applying of O<sub>2</sub> in the mixture of gases (Fig. 1.11. c) increases the grain size due to the higher heat input [36].

Authors also concluded that Better results were performed using Argon mixtures with CO<sub>2</sub> and or O<sub>2</sub> – good welding performance, not much spatters, good welding speed. In general, the content of micro alloying elements in the welding joint is less when the oxygen is involved in shielding gas and with increasing carbon dioxide content in the shielding gas [36].

This investigation was carried out on structural low carbon steel with MAG process and short arc parameters. It was also stated that there is an influence of shielding gas on alloying material chemical composition in welding joint.

One of the investigations including the high welding parameters was done by scientist M. Gouda, M. Takahashi and K. Ikeuchi. They were testing five different shielding gases on 950MPa class steel that was alloyed with Mn and Ni.

Authors also made similar conclusion to previous research that the addition of CO<sub>2</sub> to the shielding gas resulted in reductions in hardness and Charpy energy as shown in Fig. 1.12. [38]. According to the empirical law correlating the yield strength with hardness [39] a weld metal hardness below 360 HV does not meet the strength requirement of 950 MPa class steel. In this sense, the weld metal obtained in this study meets the strength requirement, only when the shielding gas is pure Ar [38].

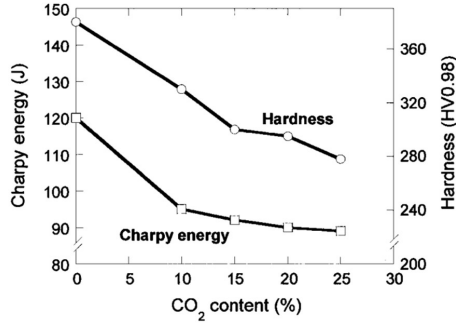


**Fig. 1.12.** Charpy energy and hardness test results depending on CO<sub>2</sub> content in shielding gas [38].

M. Gouda and his team claims that chemical composition of the weld metal was significantly influenced by the CO<sub>2</sub> content in the shielding gas. The O<sub>2</sub> content increased with CO<sub>2</sub> content in the shielding gas. On the other hand, Mn, Si, Al, and Ti content decreased as the CO<sub>2</sub> content was increased. Other alloying elements such as C, Mo, Cr, and Ni were almost independent of O<sub>2</sub> content. The simultaneous decrease in Mn, Si, Al, and Ti content can be attributed to their oxidation in the weld pool, considering their high affinity for oxygen and the higher O<sub>2</sub> content with the addition of CO<sub>2</sub> [38]. Changes in chemical composition are reflected in Fig 1.13.

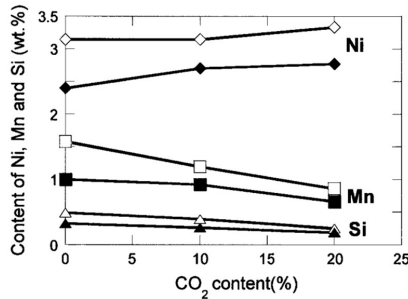


**Fig. 1.13.** Contents of Ni, Mn and Si detected from the bright (open symbols) and dark (closed symbols) areas observed in the microstructures revealed by LePera's solution [38].

Authors did the experiments on investigating the optical microstructure revealed by LePera's solution. Thanks to that method they found out that with an increase in the CO<sub>2</sub> content of the shielding gas, white areas were decreased, and black areas were increased. As described in the experimental procedure, this suggests that the bainitic area became dominant compared with the martensitic, as the CO<sub>2</sub> content of the shielding gas was increased. The microhardness of both areas against the CO<sub>2</sub> content of the shielding gas is shown in Fig. 1.14. The hardness of the white area was higher than that of the black one, supporting the view that the white area was martensitic and the black area bainitic [38].

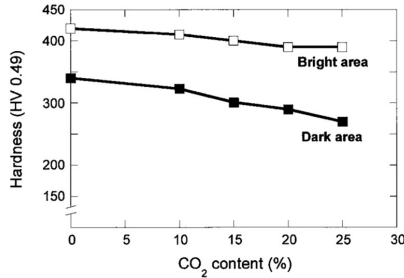


**Fig. 1.14.** Hardness parameters of bright and dark areas depending on CO<sub>2</sub> content in shielding gas [38].

The hardness in the bainitic area decreased with increasing CO<sub>2</sub> content, probably because the granular bainite became more dominant in this area. The decrease in the hardness of the white areas with increasing the CO<sub>2</sub> content is probably due to the influence of the lower hardness of the increased bainitic area [38].

Authors concluded following facts from their investigations:

- 1) The O content in the weld metal increased with increasing CO<sub>2</sub> content in the shielding gas, while Mn, Si, Al, and Ti contents decreased due to their oxidation.
- 2) The hardness and absorbed energy of the weld metal decreased as CO<sub>2</sub> content of the shielding gas was increased.
- 3) With the addition of CO<sub>2</sub> to the shielding gas, the bainite structure became more dominant than martensite in the weld metal microstructure, which consisted primarily of martensite and bainite. The bainite structure became more granular involving the MA constituent with CO<sub>2</sub> addition to the shielding gas. These microstructural changes with the addition of CO<sub>2</sub> to the shielding gas can be explained as resulting from the reduction in the hardenability of the weld metal due to the losses of Mn, Si, Ti, and Al [38].

This investigation was done by using low weld parameters (short arc) with low alloyed 950 MPa class steel, by using five different shielding gases with Ar + CO<sub>2</sub>. Three component mixtures were not used in this research as well as steel grade and alloying elements differ from the investigation that is used in doctoral thesis. Nevertheless, the conclusions made by M. Gouda has to be taken into account during further research work.

The relationship between microstructure and mechanical properties of MAG weld metal with strength over 890MPa was discussed in Y. Peng and his team scientific article [40]. They have been using totally different approach comparing to previous articles. There have been used only one shielding gas (Ar + CO<sub>2</sub> 20%) with three different welding wires to insure the weld of high strength steel properties in this case. Authors have used spray-arc parameters in the experiments by reaching rather high heat input. It is normal in this case as they were using 20mm thick plates for the tests.

Authors has stated that there is more influence of microstructure on hardness than the chemical composition in the weld. As we can find in the Fig. 1.15. the smaller grain size of the structure is in the third sample but larger is in the first.

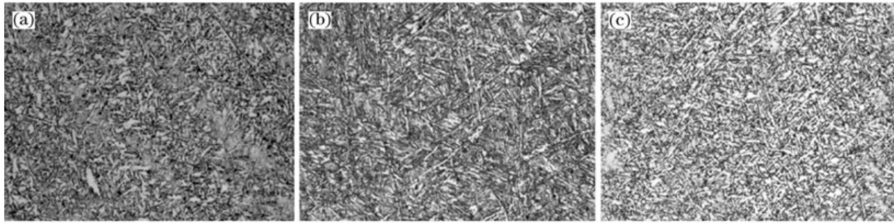


**Fig. 1.15.** Microstructure of weld metals: a) sample No. 1, b) sample No. 2, c) sample No. 3 [40].

Even with the higher Ni and Mn content in the welding joint hardness is higher in the second sample as well as the Yield stress. Nevertheless, toughness in Charpy tests were achieved higher in the sample No. 1 [40].

Finally, authors have concluded following statements:

- 1) at the level of tensile strength; from 800 - 900MPa, the welded metal microstructure mainly consists of a mixture of lath bainite and martensite. The yield strength is related to the promotion of martensite.
- 2) The effective grain size and ductile phase of austenitic films are main factors to improve the toughness of weld metal.
- 3) A fine microstructure of bainite and proper amount of martensite plays a key role in good mechanical properties. [40]

This investigation gives a good understanding of the importance of the welding microstructure on the yield strength and toughness of the weld. Chemical composition influences hardness of high strength steel of 890 MPa class steel. However, there is no influence of shielding gas observed in this investigation as well as different parameters are not taken into count.

A research of shielding gas influence on pulsed arc and weld morphology was carried out by scientist group that was led by Y. Zhao [41]. They were using three different three gas component mixtures and one mixture with Ar + CO<sub>2</sub>. The welding was done on structural steel Q345E (equivalent to S355J2+N) with pulsed current st 260A. The experiments after welding were carried out to measure the weld penetration and weld width, observe the changes of weld microstructure and coarse grained HAZ microstructure [41].

Authors found out that the best influence on pulsed arc stability was achieved by using three gas component mixtures. It means that oxygen gives the arc better stability then the CO<sub>2</sub>. The arc length was increased but the spatter amount decreased by the increase of Ar in the shielding gas mixture. Argon finger weld penetraton shape was achieved by the increase of Ar content in the mixtutre.

Fig. 1.16. shows that weld metal consists of acicular ferrite and pearlite with four different kinds of shielding gases. The proeutectoid ferrite was distributed in the columnar grain boundary. For different shielding gases, ferrite-pearlite ratio may change by affecting the heat input.



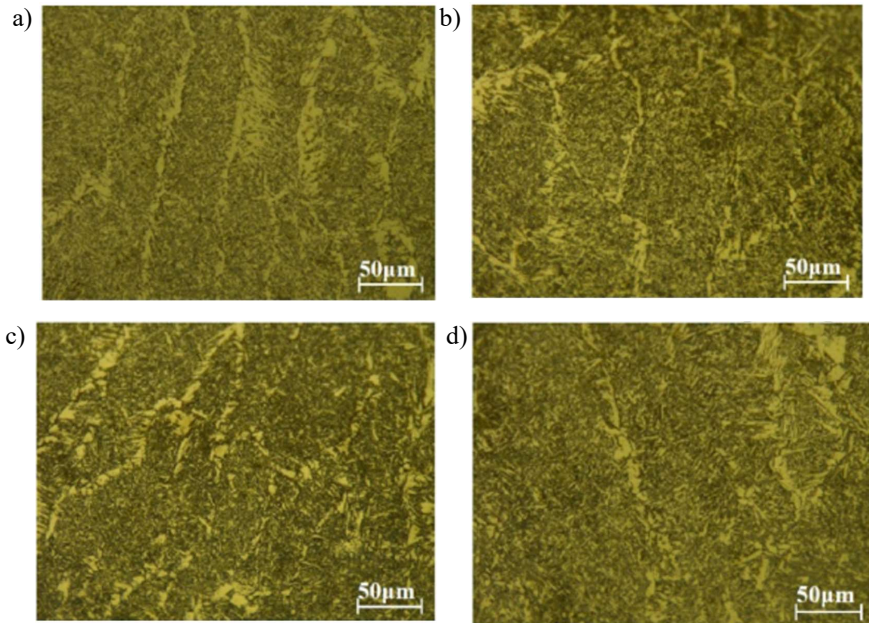


**Fig. 1.16.** Microstructure of evolution of weld metal for different shielding gases:  
 a) Ar + 18%CO<sub>2</sub>; b) Ar + 13%CO<sub>2</sub> + 3%O<sub>2</sub>; c) Ar + 10%CO<sub>2</sub> + 3%CO<sub>2</sub>;  
 d) Ar + 4%CO<sub>2</sub> + 3%O<sub>2</sub> [41].

For reducing the accidental error, the center of the weld metal was marked and taken photos of the surrounding metallograph. By analyzing the ratio between ferrite and pearlite, it can be obtained that the ferrite content slightly increased from 54.9% to 60.4% with the augment of CO<sub>2</sub> concentration in the ternary shielding gas. This can be explained in terms of chemical composition and cooling speed [41].

The hardness of weld metal and HAZ was measured during the investigation. Slightly different results were achieved in HAZ of the welding joint (see Fig. 1.17.) but the hardness in welding joint was almost even for all of the samples.

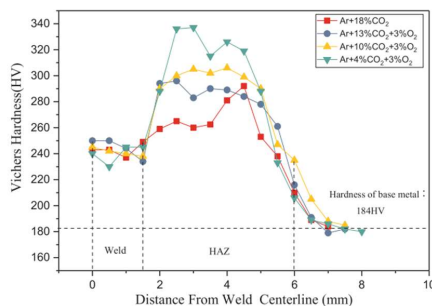


**Fig. 1.17.** The hardness profile of the weldment for different shielding gases [41].

Authors investigated the effects of four kinds of shielding gases on metal transfer mode, arc behavior, weld morphology and weld microstructure used in pulsed current



MAG welding of carbon steel in this study. The primary results and conclusions stated following:

- 1) Compared with the binary shielding gas (Ar+CO<sub>2</sub>), the ternary shielding gas (Ar+CO<sub>2</sub>+O<sub>2</sub>) can obtain less splash quantity, the stable metal transfer, the stable arc combustion, the refinement of metal droplet by the addition of oxygen. A stable pulsed streaming spray transfer was obtained when the shielding gas of Ar +4%CO<sub>2</sub>+3%O<sub>2</sub> was used, but the change of metal transfer mode had a tight relationship with the bell-shaped arc rather than critical current when a mixture of Ar+13%CO<sub>2</sub>+3%O<sub>2</sub> was as shielding gas.
- 2) The higher concentration CO<sub>2</sub> has obvious compression effect on arc shape. With increasing CO<sub>2</sub> concentration, bright arc area and arc length decreased. The longer neck of electrode tip and arc jumping phenomenon determined whether a stable pulsed streaming spray transfer can occur for MDPP.
- 3) With the increase of CO<sub>2</sub> concentration in the ternary shielding gas, weld width and weld penetration increased slightly due to the higher arc force.
- 4) The ferrite content in the weld metal increased slightly by affecting chemical composition and cooling rate with the increase of CO<sub>2</sub> concentration in the shielding gas. The low-carbon lath martensite was distributed in HAZ [41].

From this investigation it is possible to find out that the oxygen that is used in shielding gas can slightly increase the stability of the welding arc. An increase of CO<sub>2</sub> content in shielding gas can influence spatter appearance even in pulse arc. It is not possible to know if the content of the same amount of Ar and CO<sub>2</sub> mixture (for instance 7 or 8%) could give the same result as Ar + 4%CO<sub>2</sub> + 3% CO<sub>2</sub> on arc stability and the microstructure of the welding joint. It is also important to know how these parameters and mixtures would influence the high strength steel welding.

Another research on shielding gas influence on MAG welding of 1000 MPa grade steel was made by A. Tongbang, W. Jinshan, S. Jiguo and T. Zhiling. The effect of four different shielding gas compositions (Ar + (5%~30%)CO<sub>2</sub> volume fraction) on the general compositional and microstructural characteristics of deposited metals, including non-metallic inclusions was carried out in their investigation [42]. Tests were made on 20mm thick plate samples with several passes by using high welding parameters reaching the heat input 13 kJ/cm during the welding process.

Authors examined the chemical composition of the welding joints and the results are displayed in table 1.2.

**Table 1.2.**

Chemical composition of deposited metals with  
different shielding gases [42].

Shielding gas	C	Si	Mn	Ni+Cr+Mo	Ti	O	N	Fe
95%Ar+5%CO <sub>2</sub>	0.097	0.52	1.67	3.88	0.070	0.021	0.0034	Bal.
90%Ar+10%CO <sub>2</sub>	0.089	0.48	1.54	3.83	0.065	0.027	0.0032	Bal.
80%Ar+20%CO <sub>2</sub>	0.089	0.47	1.46	3.80	0.045	0.032	0.0036	Bal.
70%Ar+30%CO <sub>2</sub>	0.087	0.43	1.38	3.69	0.043	0.040	0.0034	Bal.

There were also made tests on the weld mechanical properties. It is possible to see the results of the yield strength and hardness of welding joint decreases by the increase of CO<sub>2</sub> content in the shielding gas mixture. However, Charpy absorbed energy is better

on samples welded with shielding gases with higher CO<sub>2</sub> content in both – room temperature and -40°C tests. The results of the mechanical tests are displayed in Table 1.3.

**Table 1.3.**

**Mechanical properties of the deposited metals with different shielding gases [42].**

Shielding gas	$R_m$ MPa	$R_{p0.2}$ MPa	Charpy absorbed energy / J		Vickers hardness kg · mm <sup>-2</sup>	$\gamma$
			RT	-40 °C		
95%Ar+5%CO <sub>2</sub>	1173	1038	49.3	17.3	404.25	0.88
90%Ar+10%CO <sub>2</sub>	1101	942	55.0	33.0	381.47	0.86
80%Ar+20%CO <sub>2</sub>	1160	980	72.6	52.0	366.71	0.84
70%Ar+30%CO <sub>2</sub>	1044	921	57.6	47.6	358.39	0.88

Note:  $R_m$ —tensile strength,  $R_{p0.2}$ —yield strength, RT—room temperature,  $\gamma$ —yield ratio

Authors of this research have also paid attention to the inclusions in the welding joint. The difference on the amount and size of inclusions are displayed in Fig. 1.18. The picture shows the opposite result as it was stated in one of the previous researches [5]. The size and amount of the inclusion are growing by the increase of CO<sub>2</sub> content in shielding gas.



**Fig. 1.18.** Images of inclusions in the deposited metal with different shielding gases: (a) 95%Ar+5%CO<sub>2</sub> (b) 90%Ar+10%CO<sub>2</sub> (c) 80%Ar+20%CO<sub>2</sub> (d) 70%Ar+30%CO<sub>2</sub> [42].

A microstructure of the welding joints was also examined during the investigation. The mixture of bainite and martensite structures were observed in the welding joints (Fig. 1.19).

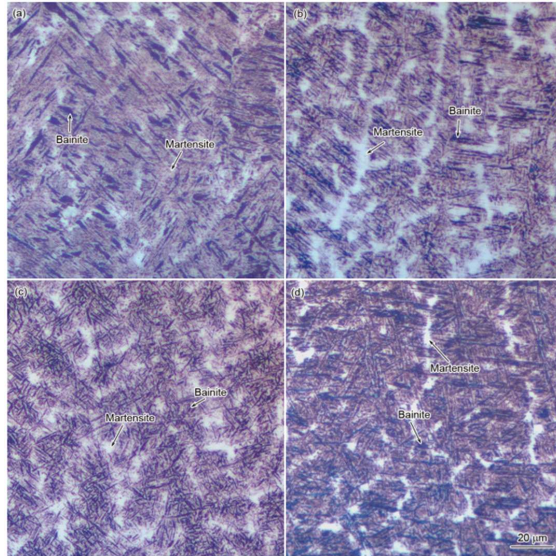


**Fig. 1.19.** Color OM images of the as-deposited top beads with different shielding gases: (a) 95%Ar+5%CO<sub>2</sub> (b) 90%Ar+10%CO<sub>2</sub> (c) 80%Ar+20%CO<sub>2</sub> (d) 70%Ar+30%CO<sub>2</sub> [42].

Authors claim that the quantitative statistics show that when the CO<sub>2</sub> content in the protective gas rises from 5% to 30%, the bainite content in the deposited metal increases, respectively 8%, 15.4%, 23.8% and 29.6% (volume fraction). The same time martensite structure becomes bigger with the increase of CO<sub>2</sub> content [42].

Concluding the investigation authors have stated that:

(1) With the increase of CO<sub>2</sub> content in the shielding gas, the 1000 MPa grade weld metal metallization strength decreased slightly, while the impact toughness first increased and then decreased. When the shielding gas was Ar+20%CO<sub>2</sub>, the deposited metal has the best strength properties, the yield strength is 980 MPa, the impact energy at room temperature is 72.6 J, the impact energy at -40 °C is 52.0 J, and the yield ratio is 0.84.

(2) Different shielding gas deposited metals are composed of martensite/bainite mixture, composed of combined formations with retained austenite between laths. With the increase of CO<sub>2</sub> content in shielding gas, the B<sub>50</sub> and M<sub>s</sub> phase transition temperature range of deposited metal increases. Large number of inclusions suitable for bainite nucleation increases, and the bainite content increased from 8% to 29.6% by the increase of CO<sub>2</sub> content in shielding gas. The nucleation position is from the original austenite grain boundary transform to common nucleation at the original austenite grain boundaries and intragranular inclusions. The distribution morphology changes from "parallel" to "interlaced", dividing and thinning groups. Weaving is conducive to improvement of material toughness [42].

This investigation describes the changes of microstructure depending on the shielding gas content. Authors have used only two component shielding gases. There is still a question of oxygen mixture influence on the welding process, arc stability and the weld metal metalurgy of high strength steel with lower grade. Nevertheless, this investigation gives different point of view on the result comparing to previous research on high strength steels.

A scientific investigation was carried out to find the relationship between alloying content, microstructure, and properties has been clarified for highstrength steel weld metals with 7 to 9 wt-% nickel by E. Keehan and his colleagues [43]. Neural network modeling suggested that manganese reductions and nickel additions in a controlled manner with respect to manganese lead to increased impact toughness. Carbon additions were predicted to enhance yield strength at limited loss to impact toughness. Following these predictions, shielded metal arc welding was used to produce experimental welds with manganese at 0.5 or 2 wt-% and nickel at 7 or 9 wt-%, while carbon was varied between 0.03 and 0.11 wt-%.

Authors have done modeling of the SMAW (Self-shielded Metal Arc Welding) process of high strength steel 1000 MPa to find the coincidence between Mn and Ni content of the chemical composition and the microstructure of welding material. They made seven experimental weld metals using SMAW technology. It was decided to study the changes in mechanical and microstructural behavior in detail for manganese concentrations of 0.5 or 2.0wt-%, nickel levels at 7 or 9 wt-%, and carbon additions from 0.03 to 0.11 wt-% with nickel at 7 wt-% and manganese at 0.5 wt-%. These compositional variations were chosen since modeling predicted significant effects on mechanical properties [43].

As the result of investigation and from *Thermo-Calc* modeling and observed segregation behavior, it was concluded that the weld metals solidified completely as austenite. Nickel and carbon additions were found to stabilize austenite to lower transformation temperature, while manganese reductions promote the decomposition of austenite at higher temperatures [43].

Combinations of high-resolution microstructural characterization techniques were employed to assess the microstructures. For a combination of high Ni and Mn, a mixture of upper and coalesced bainite was found in dendrite core regions with mainly martensite present in interdendritic regions. A Mn reduction reduced the amount of coalesced bainite and promoted greater amounts of upper bainite within the microstructure while carbon additions were found to promote martensite [43].

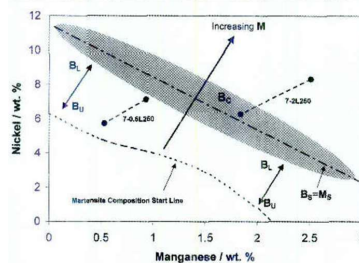


**Fig. 1.20.** Constitutional diagram showing the dominant microstructure as a function of Ni and Mn content for the base composition 0.034 C, 0.25 Si, 0.5 Cr and 0.62 Mo [43].

A constitutional diagram has been constructed summarizing the effects on microstructure of varying manganese and nickel contents (Fig. 1.20.).

As this research was done without using shielding gases the only thing that can be taken is the idea of the modeling of the microstructure of the weld metal depending on Ni and Mn content in the welding joint. However, the modeling of hardness or other mechanical properties of the weld metal was not discovered in this investigation.

Several more investigations were done by using same SMAW technology. M. Lord did the research of special composition consumable (ESAB OK 75.78 with 3 Ni, 2 Mn, 0.5 Cr, 0.6 Mo, 0.05 C) as the basis of development. The Author increased Ni concentrations to 4 wt-% and decreased Mn levels to 0.8 wt-% of the melting electrode. He found that impact toughness increased to 74 J at -60°C, and the yield strength was reduced to 809 MPa [44].

B.Y. Kang together with his team used similar solution of increasing Ni and reducing Mn content in the metal cored wires. They discovered that the impact toughness of 55J at -60°C was reached with nickel at 6.95 wt-% and manganese at 0.52 wt-% with the SMAW technology. They also reached the tensile strength of 684 MPa for this alloy on low-carbon steel weld metal from hardness results [45].

It is possible to conclude from both of these investigations that the Ni content is playing a great role in increasing the strength of the weld metal by keeping the impact toughness rather high at very low temperature. It is important to find out how the shielding gas and MAG welding process can influence both Mn and Ni content in the welding joint for high strength steel.

R.E. Francis, J.E. Jones and D.L. Olson in the end of last century came out with the investigation where the wire composition, oxygen activity of the shielding gas, and heat input were varied to study the effects of each on MAG welding process of high strength steel [46]. Several mixtures of Ar + O<sub>2</sub> or Ar + CO<sub>2</sub> were used in welding of molybdenum-niobium microalloyed HSLA pipeline steel X-70 (equivalent to L485). Shielding gases were mixed from pure Ar to 100%CO<sub>2</sub>. Oxygen was added from 1 to 5% of the mixture. Authors used high welding parameters, reaching the 390A as the wire diameter was used 1.6mm. They also have tested two types of welding wire (ER70S-3 and ER70S-6) that contained different amount of alloying materials.

Two separate studies were conducted in this investigation. First, the gas/metal reactions were studied to determine the effect of cover gas composition on the final weld metal composition (Fig. 1.21.). Second, the effect of changes in weld metal chemical composition on the resultant weld metal microstructure was examined [46].

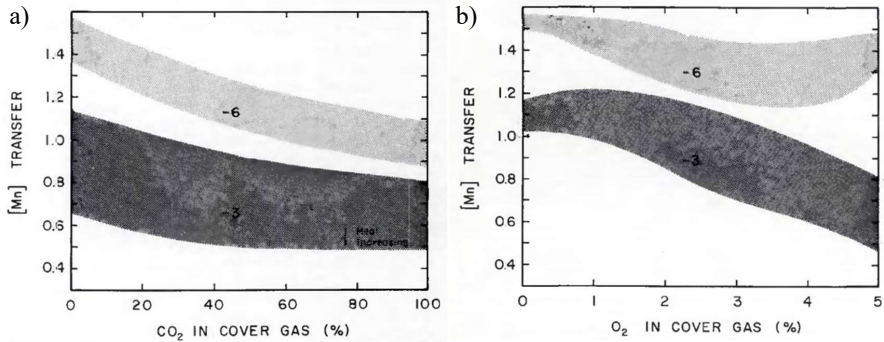


**Fig. 1.21.** Plots of data bands: a) for wt-% Mn Transfer as a function of the percentage CO<sub>2</sub> in the cover gas; b) for wt-% Mn Transfer as a function of the percentage O<sub>2</sub> in the cover gas [46].

Depending on the Mn content in welding wire and composition of shielding gas two graphs were created (Fig. 1.6.16). As the content of CO<sub>2</sub> and O<sub>2</sub> increases the Mn wt-% is dropping. Interesting phenomena appears with the ER70S-6 welding wire where the Mn wt-% is reducing a little and after reaching 3,5% of O<sub>2</sub> content in shielding gas the graph is not dropping any more. By the increase of CO<sub>2</sub> in the shielding gas mixture the drop of Mn wt-% is constant.

Authors also created diagrams by plotting the microstructure results obtained in this study using the MAG welding process with Ar + CO<sub>2</sub> cover gas, a diagram similar to that of Y. Kikuta [47] is produced. However, the two chemical compositions from the two wires map separately as seen in Fig. 1.6.17. Each wire composition gives a band of coarse microstructure at the upper left, a center band of fine acicular ferrite, and another band of aligned carbide at the lower right, having the ER70S-3 welding wire toward the left and the ER70S-6 welding wire toward the right side of the diagram [46].

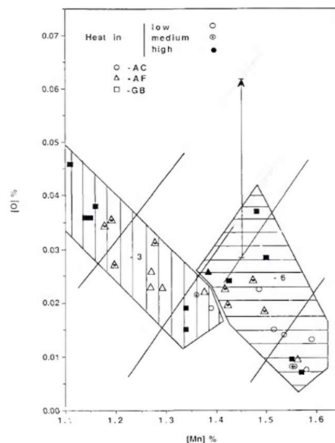


**Fig. 1.22.** Diagram of the derived weld microstructure as a function of the weld oxygen and manganese composition [46]

Fig. 1.23. a) and b) show the regions of preferred microstructure as a function of heat input and cover gas composition for each of the welding wires used. It is apparent



that each wire has an optimum region. Thus, it is important that the choice of welding wire for a particular application be coupled with the choice of shielding gas. For example, it can be seen from this work that with the argon-oxygen cover gas, a greater range in heat input can give acceptable welds between 2-4% oxygen in argon with either welding wire, and the use of an argon-carbon dioxide cover gas will restrict both the heat input and the choice of wire composition [46].

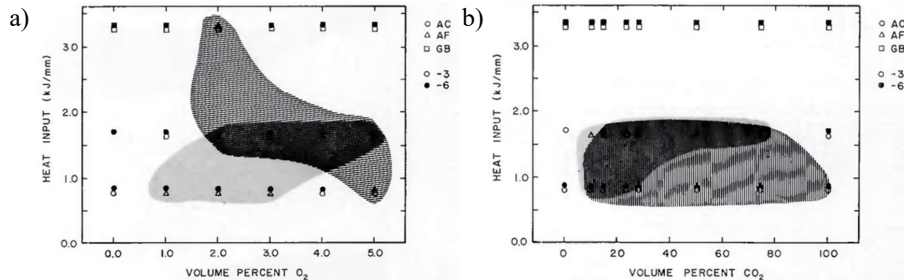


**Fig. 1.23.** Map of microstructure as a function of heat input, cover gas and welding wire type: a) shielding gas Ar + O<sub>2</sub>; b) shielding gas Ar + CO<sub>2</sub>. The shaded area delineates the areas of acicular ferrite. The lined area silhouettes the ER70S-6 produced welds, and the dotted area the ER70S-3 produced welds [46].

Finally, authors made following statements after their investigation:

- 1) The volume fraction of acicular ferrite is definitely influenced by the oxygen and carbon dioxide content in the argon cover gas.
- 2) Plots of inclusion-forming agent vs. hardenability agent can be used to predict microstructure of MAG weld metal.
- 3) MAG welding can achieve acceptable weld metal microstructures in niobium microalloyed steels only with the proper combination of welding wire, shielding gas and heat input [46].

Authors have done an interesting research by using a very wide range of shielding gas mixtures. There has been discovered some advantages and drawbacks of both double gas mixtures Ar + O<sub>2</sub> and Ar + CO<sub>2</sub>. However, there were no conclusions done about the influence of all three gas mixtures. The hardness and other mechanical properties were not tested or predicted in this research and the welding parameters were increased due to the increased wire diameter that is not commonly used in MAG welding nowadays.

After a review of different researches about MAG welding and the influence of shielding gas on this process a summary of all found useful literature sources was made (Table 1.4.). There is a description and summary about the used base materials as well as types of electrode materials that were used in different researches as they influence the welding parameters, process and weld joint. Types of shielding gases that were involved are also included in the summary of the investigations. There are also some notes if gases were not used there. An important role on the research and conclusions take place the mechanical properties of the welds like Yield Strength, Tensile Strength and Hardness. These issues are also included and outlined in the summary. Finally, all investigations, where some kind of modeling was carried out, are outlined in the conclusion of all research works.

**Table 1.4.**

Summary of studied literature sources.

Experiment	Reference	Metals	Shielding gas	Welding parameters	Mechanical properties	Chemical composition	Developed model
MAG + Solid wire	Kah [5]	S235	Ar+2.5%CO <sub>2</sub> , Ar+10%CO <sub>2</sub> , Ar+18%CO <sub>2</sub> , Ar+25%CO <sub>2</sub>	Short arc	Pore size and quantities	?	?
MAG + Solid wire	Knovel [6]	S235	Ar+5%CO <sub>2</sub> + +5%O <sub>2</sub> , Ar+20%CO <sub>2</sub> , 100%CO <sub>2</sub>	Short arc	Charpy test	?	?
MAG + Flux-cord wire	Gadallah [29]	S235	100%Ar, 100%CO <sub>2</sub> , Ar+5%CO <sub>2</sub> , Ar+10%CO <sub>2</sub> , Ar+18%CO <sub>2</sub> , Ar+20%CO <sub>2</sub> , Ar+25%CO <sub>2</sub>	Puls-arc	Charpy test not for all samples 100%Ar, Ar+25%CO <sub>2</sub>	Microstructure,	?
MAG + Solid wire	Moreira [30]	S235	100%Ar, Ar+8%CO <sub>2</sub> , Ar+15%CO <sub>2</sub> , Ar+25%CO <sub>2</sub>	Short arc	Pore size and quantities	?	?
MAG + Flux-cord wire	Çevik [31]	S275	100%Ar, Ar+12%CO <sub>2</sub> +2%O <sub>2</sub>	Short arc	Tensile strength, spatter	Microstructure	?
MAG + Solid wire	Boiko [36]	S235	Ar+8%CO <sub>2</sub> , Ar+18%CO <sub>2</sub> , Ar+25%CO <sub>2</sub> , 100%CO <sub>2</sub>	Short arc	?	Chemical composition	Model of economical calculation
MAG + Solid wire	Gouda [38]	S950	100%Ar, Ar+10%CO <sub>2</sub> , Ar+15%CO <sub>2</sub> , Ar+20%CO <sub>2</sub> , Ar+25%CO <sub>2</sub>	Spray-arc	Charpy test, Hardness	Microstructure, Chemical composition	?
MAG + 3 Solid wire	Peng [40]	S890	Ar+20%CO <sub>2</sub>	Spray-arc	Yield and Tensile Strength, Hardness	Microstructure	?
MAG + Solid wire	Zhao [41]	S355J2+N	Ar+18%CO <sub>2</sub> , Ar+13%CO <sub>2</sub> +3%O <sub>2</sub> , Ar+10%CO <sub>2</sub> +3%O <sub>2</sub> , Ar+4%CO <sub>2</sub> +3%O <sub>2</sub>	Puls-Arc	Penetration size and form, Hardness	Microstructure	?
MAG + Solid wire	Tongbang [42]	S1000	Ar+5%CO <sub>2</sub> +5%O <sub>2</sub> , Ar+10%CO <sub>2</sub> , Ar+20%CO <sub>2</sub> , Ar+30%CO <sub>2</sub>	Spray-arc	Yield and Tensile Strength, Hardness, Charpy, Pores	Microstructure, Chemical composition	?
SMAW + 3 Flux-cord wires	E. Keehan [43]	S1000	?	Spray-arc	Yield and Tensile Strength	Microstructure	Model of structure formation depending on Mn and Ni content
SMAW + Flux-cord wire	M. Lord [44]	S460	?	Spray-arc	Yield strength, Charpy test	?	?
SMAW + Flux-cord wire	B.Y.Kang [45]	S355	?	Spray-arc	Yield strength, Charpy test	?	?



MAG + 2 Solid wires (1.6mm)	R.E. Francis [46]	L485	100%Ar, Ar+1%O <sub>2</sub> , Ar+2%O <sub>2</sub> , Ar+3%O <sub>2</sub> , Ar+4%O <sub>2</sub> , Ar+5%O <sub>2</sub> , Ar+10%CO <sub>2</sub> , Ar+14%CO <sub>2</sub> , Ar+23%CO <sub>2</sub> , Ar+28%CO <sub>2</sub> , Ar+52%CO <sub>2</sub> , Ar+75CO <sub>2</sub> , 100%CO <sub>2</sub>	Spray-arc	Penetration size and form	Microstructure, Chemical composition	Diagram of creation of structure as a function of Mn and O content
-----------------------------------	-------------------------	------	---	-----------	------------------------------	--	--

In summary, it can be concluded that various studies have been performed on the effect of shielding gas on carbon steels such as S235, S275, S355, which are standard structural steels. In most cases these investigations are done by using short arc except those where the flux-cord wire was used in. However, a couple of studies were made without using shielding gas. Authors in these studies have focused on the reinforcement of welded joints in standard structural steels using an alloyed melting electrode. It is possible to find there the overview that not only Mn content influences the mechanical properties of welding joint. The same influence is also on Ni content in the welding joint that was not taken into count in my previous research.

Low-alloy steels with a yield strength of 890 - 1000 MPa are also considered in latest investigations. All authors have used high welding parameters in these studies. This should also be taken into count during investigation of this work.

Thus, it was concluded that structural steels in the range of 420 - 850 MPa are not considered, although currently these materials are increasingly used in production, helping to lighten the weight of structures, ensuring their sufficient strength. It is important to find out the influence of different processes.

The above conclusions open the way for a new study on the effect of shielding gas on high-strength steel (650MPa) with MAG welding technology. Taking into account the previous research, it was decided to perform the research by welding with high welding parameters.

## 2. EXPERIMENTAL STUDIES.

### 2.1. Materials and methods of investigation.

The material that was chosen for the investigation should be within 420 and 850 MPa class as it was discovered from the summary of literature sources. For this reason, the steel grade 650 MPa as the middle range was chosen to be used in further investigations. It is low alloyed high strength structural steel that has Yield strength at least 650 MPa. According to the certificate given by steel production company (Appendix 1) the Yield strength of the material is 702 MPa. However, the hardness of the material is not given by the producer. It is possible to replace the 6 to 8mm thick plate of steel grade S235 or S355 by using only 2 or 3mm steel plates of 650 MPa class steel. This advantage gives the opportunity to decrease the weight of the construction by 50 to 60%. There are more advantages from economical point of view by choosing this type of steel that are described later in the investigation.

As it was mentioned before the base metal that was choosed for the experiments was 650 MPa class steel. In this case STRENX®650MC delivered by company SSAB was taken to create the samples for welding experiments. The chemical composition of the material was tested in the laboratory was different as given by the producer (see Apprndix 1). The results after testing by optical emissionspectrometer are given in Table 2.1.

**Table 2.1.**

Composition of Base and Filling Material.

	C	Si	Mn	S	Cr	Mo	Ni	Al	Nb	Ti	V
Base material	0,0581	0,157	1,56	0,0162	0,0451	<0,0030	0,0251	0,0191	0,0416	0,102	0,0165
Electrode wire	0,075	0,63	1,63	0,007	0,28	0,22	1,42	0,006	0,002	0,001	0,09

As per certificate the  $C_{ekv}$  for the material is 0.35 taking into count chemical composition from certificate, it is important to calculate this value once more to be sure that the material is weldable without any extra treatment.  $C_{ekv}$  is calculated according to formula:

$$C_{ekv} = \%C + \frac{\%Mn}{6} + \frac{\%Ni + Cu}{15} + \frac{\%Cr + \%Mo + \%V}{5} \quad [48]$$

After the calculation of results from chemical composition test the real  $C_{ekv}$  is 0,22. According to the literature [47], these amterials are with good weldability without any extra treatment. According to certificate the steel has satisfactory weldability, as  $C_{ekv}$  was in the group up to 0.35%. Usually, when welding these steels, above 0°C no special conditions need to be met, but at a reduced temperature preheating required and slow cooling [48]. It means that the chosen material is weldable in room temperature without any extra treatment or preheating.

As it was decided after the review of literature sources the high welding parameters should be taken into count during welding experiments. For this reason, the 10mm thick plate was chosen to create welding samples. It gives the opportunity to increase welding parameters such as welding current and wire speed to not burn through the steel plate. Samples then were laser cut into welding pieces of 100x200mm according to EN ISO

9606-1 (Welder Approval Testing). They were stick together creating a T-joint with two spot welds on the opposite side of the welding experiment seam. No extra preparation (chamfering) was done on any of welding specimens.

Welding equipment of company FRONIUS® TPS500i (Fig 2.1.) and welding tractor Fronius® FlexTrack 45 Pro (Fig. 2.2.) was used to create smooth movement of the welding torch and regular welding joint.



**Fig. 2.1.** Welding machine  
Fronius®MIG500i [49]



**Fig. 2.2.** Welding tractor  
Fronius® FlexTrack 45 Pro

Welding process was done according to EN ISO 6947 in PB (Plate Horizontal Vertical) position and a welding seam was created with a height of 5mm ( $a=5$ ). Figure 2.3. shows the welding set-up of the experiments.



**Fig. 2.3.** Welding set-up of the experiments.

Experimental samples were fixed on the even welding table. Before each experiment the welding torch that was fixed on the welding tractor was moved along the sample to check the constant height and distance between the sample and the welding wire. Welding tractor was put on 1000mm long rail to afford the movement of 200mm across the welding sample. It was also possible to regulate the welding speed before and during the welding process.

From the literature overview it was concluded that the wire electrode plays an important role on welding parameters and also on the result of the weld. For this reason, the welding wire electrode was used according to base material properties with proper manganese content. Chemical composition of the welding wire is given in Table 2.1. It is also possible to find that there is an increased Ni content in the welding wire chemical composition. As there was no possibility to make a chemical composition test the only evidence of the alloying material content is the certificate given by the producer of the welding wire electrode (Appendix 2). The diameter of the electrode was chosen 1.2mm that gives higher deposition rate. It also gives a possibility to increase the welding speed that helps to decrease the heat input during the welding process [48].

As the last and one of the main necessary chosen components for all experiments was the shielding gas. To afford the stable welding in high welding parameters there should be chosen Argon mixtures as pure Ar and pure CO<sub>2</sub> is not suitable for welding in spray arc conditions [14]. Therefore, the investigation was carried out with four different shielding gases. Argon mixtures with CO<sub>2</sub> (Carbon dioxide) and O<sub>2</sub> (oxygen) were used in experiments. The composition of these gases is given in Table 2.2. and can be found in Appendix 4.

**Table 2.2.**

Compositions of Shielding Gases.

Gas	Argon	CO <sub>2</sub>	O <sub>2</sub>
MISON®25 (M25)	75%	25%	-
MISON®18 (M18)	82%	18%	-
MISON®8 (M8)	92%	8%	-
CORGON®3 (C3)	90%	5%	5%

All of these shielding gases are commonly used in different metalworking companies in Latvian market and also widely spreaded across the world [14], [36]. As there is an Ar content in the shielding gas there is a possibility to create a stable plasma arc during the welding process. CO<sub>2</sub> addition to the mixture still gives a possibility create short arc during the welding process. Gas flow rate was held at constant 15l/min. The flow rate control was carried out before each welding experiment separately for each sample according to example shown in the Fig. 2.4. a.

High welding parameters should be used to reach the spray arc [14]. For this reason, the welding parameter matrix was chosen by using special welding parameter modeling application WeldConnect® (Fig 2. 4 b). To reach the previously mentioned parameters of welding joint size a=5mm following parameters were set to reach the results: 280A at 28V, 300A at 29V and 320A at 30V. To reach constant height for all the samples as wire speed increases the traveling speed was set for each experimental weld accordingly: 350; 380 and 420 mm/min.

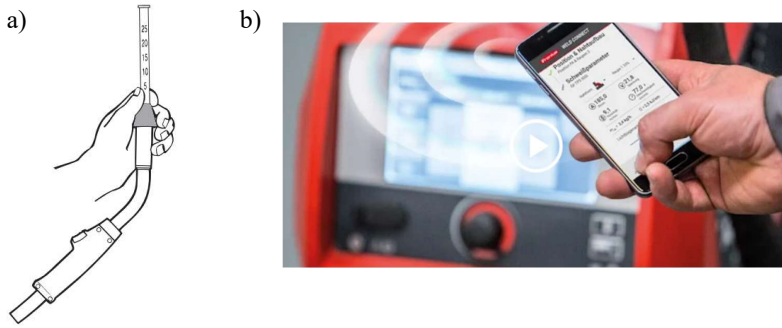


**Fig. 2.4.** a) testing of shielding gas consumption [48]; b) WeldConnect® application [50].

Arc stability was checked after setting the welding parameters before each block of experiments (at 280 A/28 V, 300 A/29 V and 320 A/30 V). The stick-out of the welding wire electrode was set 19 mm before each weld.

After welding of each specimen, they were photographed, cut into pieces of thickness of 10mm and prepared according to procedures described in referenced studies [51, 52]. The evident pictures of all specimen were also made before and after preparation (Fig. 2.5.).

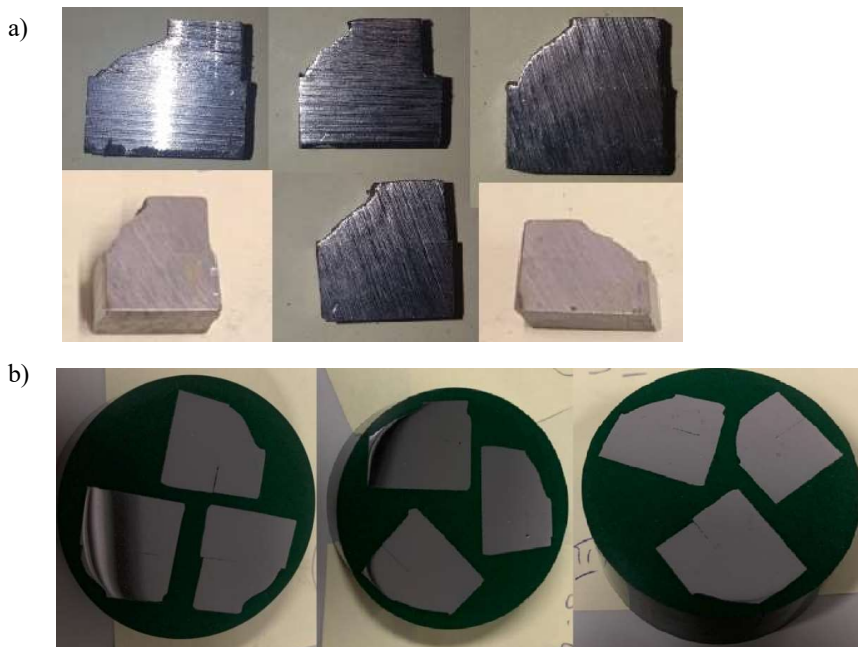


**Fig. 2.5.** Welding specimen prepared for following experiments:  
a) after cutting; b) after grinding and polishing.

After polishing all samples, they were treated with liquid of 9% nitrogen acid. After this procedure it is possible to see the size and form of penetration. It is also possible to see and measure the heat affective zone (HAZ). Finally, it is possible to do photomicrography of the welding joint. It was done by Axiovert 40 MAT optical microscope. It was possible to identify microstructural changes for each weld sample and the pixctures were taken from the middle of the welding joint. All of the pictures were taken and described in further research. Chemical composition of the welding joints was determined using Optical spectrometer PMI-MASTER Pro2. Finally, the tests of mechanical properties (hardness) was carried out by using Mitutoyo Micro Vickers hardness tester HM-210D. Testing of the hardness was made using the multi-step punctures according to EN ISO 9015-1 including base metal, HAZ (Heat Affective Zone) and the welding joint. Photographs of all puncture lines were captured to evidence and measure the hardness of each zone in every sample.

## 2.2. Results of the investigation.

Four different studies were conducted in this investigation. First, was the visual control of the welding seam, created spatters during welding and the penetration. Second, the change of microstructure of the weld with different shielding gases and different Spray arc parameters. Third, the effect of shielding gases on chemical composition of the weld. Finally, mechanical properties of the welding joint by the influenced shielding gas and spray arc conditions were evidenced, as three different heat inputs were achieved during the welding process.

### 2.2.1. Form of Welding Seam, Spatters and Penetration.

Welding parameters can influence the formation of the welding pool and form of the welding joint. Shielding gas can influence the form of metal transfer of melted electrode and arc stability. It is also stated that the amounts of spatters are affected by the stability of the welding process [14].

It is visible in pictures of the welding joints that all shielding gases show rather good stability of the arc (Fig. 2.6.). There were no spatters observed on all samples welded with M8 and C3 shielding gases.

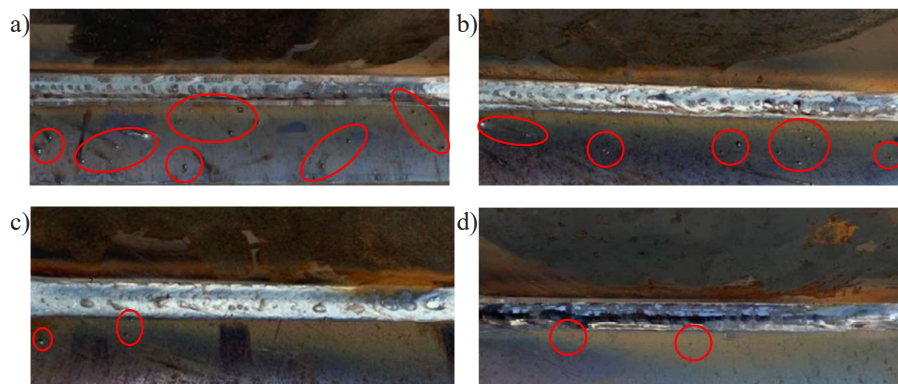


**Fig. 2.6.** Amounts of spatters on welding seams with different shielding gases welded at 300 A parameters: a) M25; b) M18; c) M8; d) C3.

There was more spatters more on the samples welded with shielding gases M25 and M18 at all of welding parameters. According to previous studies [14], [36] CO<sub>2</sub> gas provides and supports creation of short arc. The increase of its content in argon mixture increases the possibility of spatter creation. It appears that the influence of CO<sub>2</sub> still gives the possibility to create a short arc at high welding parameters. This leads to appearance of spatters after welding with these two shielding gases.

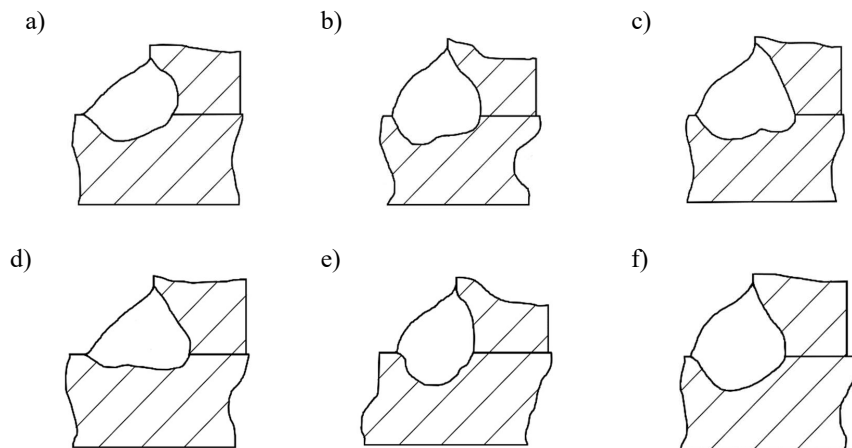
An interesting phenomenon was observed on the welding seam where mixture C3 was used (Fig. 2.7.).



**Fig. 2.7.** Phenomena of SiO<sub>2</sub> on the welding seam.

A layer of thin and transparent substance was covering the welding joint all across it. It appears to be the SiO<sub>2</sub> (siliceous oxide or glass) layer. The siliceous that was burned out from the welding pool made a reaction with oxygen that was in the shielding gas and brought it to the upside of the welding joint.

All samples were treated with liquid of 9% nitrogen acid after polishing. It is then possible to see the form of weld penetration. Smooth and stable form of penetration was made by using mixtures M25 and M18 (Fig. 2.8. a), b), c), d), e), f)). Good penetration and welding seam form combination was achieved with samples welded with M8 shielding gas at 280 A and 300 A parameters (Fig. 2.8. g), h)). The shape of the penetration was becoming unregular according as welding parameters were increased to 320 A with the same mixture (Fig. 2.8. i).





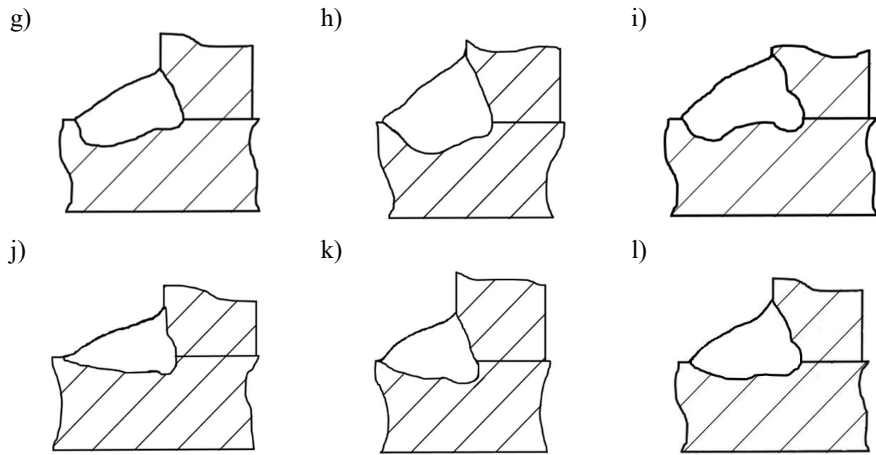


**Fig. 2.8.** Welding Seam Form and Shape of Penetration of the welded Samples: M25 - a) 280 A, b) 300 A, c) 320 A; M18 – d), e), f); M8 – g), h), i); C3 – j), k), l).

Similar issue appeared with all samples that were welded with C3 mixture (Fig. 2.8. j), k), l).). It can be explained with higher temperature of welding pool that melted the base material not only where the electrode was directed, but also on the horizontal base plate away from the corner. The side plate was almost not melted at 280 A sample because of that reason.

It was also impossible to keep regular shape of welding seam as the temperature of welding pool was hot when welding with C3 mixture.

### 2.2.2. Microstructure.

Microstructure of all welded samples was captured by optical microscope Axiovert 40 MAT. One of the defects that can be recognize at 50 times (50x) increase of the picture are the inclusions in the welding joint. According to Fig. 2.9. it appears that more inclusions were captured in welding joints that were welded with M25 and C3 shielding gases.

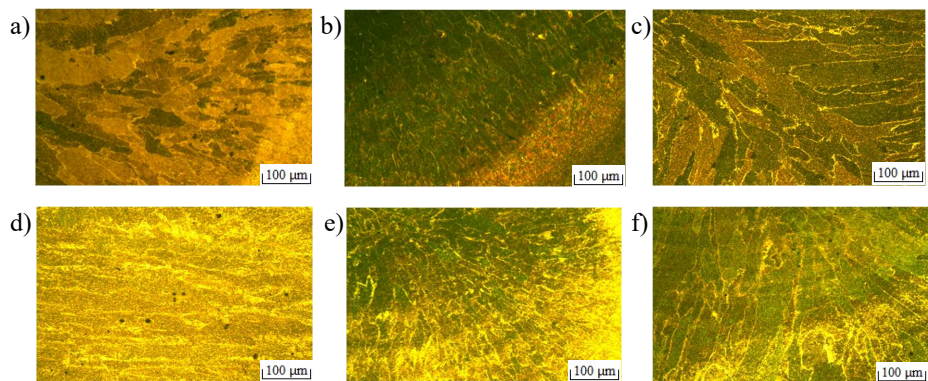


**Fig. 2.9.** Welding seam microstructure (50x) from samples welded with M25 and C3 shielding gases: a) M25 -280 A; b) M25 – 300 A; c) M25 – 320 A; d) C3 – 280 A; e) C3 – 300 A; f) C3 – 320 A.



Smaller amount and smaller size of the inclusions were found in welds that were made with mixture M18 (Fig. 2.10.).

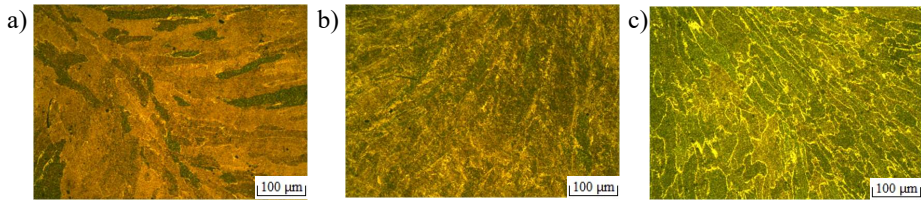


**Fig. 2.10.** Welding seam microstructure (50x) from samples welded with M18 shielding gas: a) M18 - 280 A; b) M18 – 300 A; c) M18 – 320 A

The least amount of inclusions but with a little bigger size appeared in welds that were welded with M8 shielding gas (Fig. 2.11.).

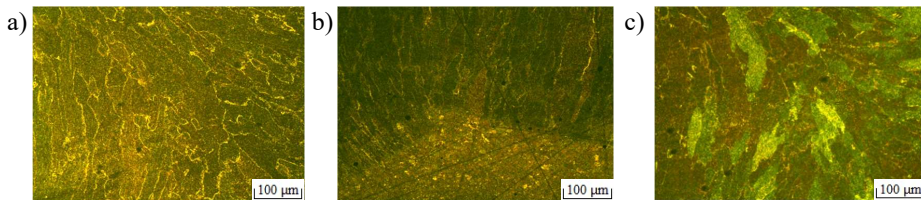


**Fig. 2.11.** Welding seam microstructure (50x) from samples welded with M8 shielding gas: a) M8 -280 A; b) M8 – 300 A; c) M8 – 320 A

After the comparison of the inclusions a 200x increased view was investigated. A structure of the welding joint was possible to observe in the samples. As from Fig. 2.9. – 2.11. it can be observed that the structure in general is formed by different size boundaries. As it was stated in different studies [29], [31], [38], [39], [40], it is important to find out of what kind of grains the structure consists of. In most cases grains of ferrite, bainite and martensite creates structure of the welding joint according to previously mentioned studies.

Thanks to 200x increased view it is now possible to see the grain size, shape and location of the created joint structure. The grain size of a metal structure can affect the strength of the metal and the formation of various types of defects [59].

After the performed experiments it can be concluded that the structure of smaller grains is formed in samples M25 320 A and M8 280 A (Fig. 2.12.). In the structure formed by M25 320 A, a number of wider and longer grain formations can also be observed. As bigger the ferrite boundaries the bigger possibility for weld to become fragile [62]. This can be a reason to cause the intercrystal cracking.

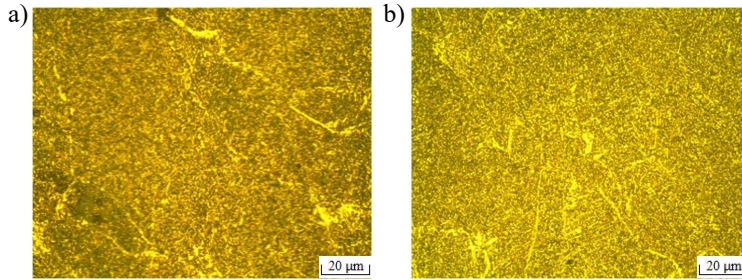


**Fig. 2.12** Material microstructure (200x): a) M25 320A; b) M8 280A.

In the microstructure of samples M8 280 A, these grain formations are much thinner and shorter, thus the structure is more even and ensures the strength of the welded joint [40].

For several welded samples, such as M25 300 A, M18 320 A, M8 300 A, M8 320 A, and C3 320 A, uneven formation of martensite and ferrite-perlite formations with ferrite grain boundaries can be observed in the welded joint structure (Fig. 2.13.). As can be seen, such a structure is formed at higher welding parameters, which can be explained by faster cooling of the samples and the occurrence of metallurgical processes in the joint [63]. Such created martensite boundaries may cause cold cracks in the weld [59, 62].

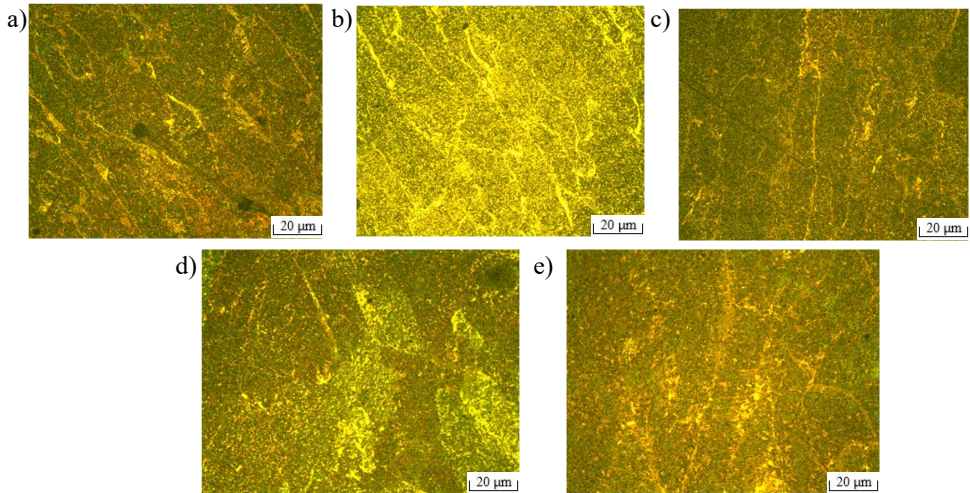


**Fig. 2.13.** Material microstructure (200x): a) M25 300 A; b) M18 320 A; c) M8 300 A; d) M8 320 A; e) C3 320 A

Similar structures have formed in samples M25 280 A and M18 280 A (Fig. 2.14.). The grain size of the microstructure is small, but martensite formations are placed with uneven distance between each other. This may cause the formation of different internal stresses in the weld [62].

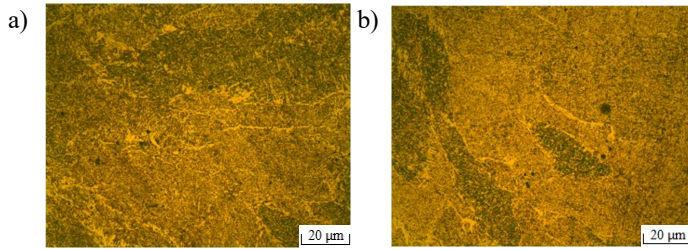


**Fig. 2.14.** Material microstructure (200x): a) M25 280 A; b) M18 280 A.

In the microstructure of the welded samples C3 280 A, C3 300 A and M18 300 A, the grains form elongated shapes and form regular layers, which are separated by grain ferrites (Fig. 2.15.). All these structures are with regular form however, the elongated grain shape of the stratification may adversely affect the strength properties of the weld metal [60].

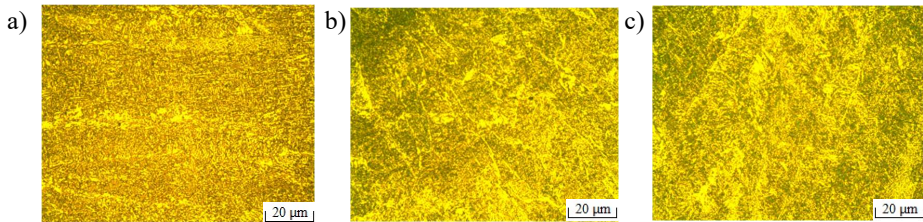


**Fig. 2.15.** Material microstructure (200x): a) C3 280 A; b) C3 320 A; c) M18 320 A.

As it can be observed from fig. 2.15. the ferrite grains are formed more. As per literature sources [61], [62] this can make the welding joint more fragile and may influence the formation of intercrystal or laminar cracks.

Smaller grain size was achieved with lower welding parameters and shielding gas that contains less CO<sub>2</sub>. Shielding gas containing O<sub>2</sub> shows the tendency to create more ferritic structure at lower welding parameters. However, as the temperature in welding joint rises the structure turns to create more martensite and bainite mixture and ferrite contamination is decreasing. Similar conclusions were made and calculated in previous researches [42], [46].

### 2.2.3. Chemical composition.

Chemical composition of the welding joint plays a big role on the mechanical properties of the weld as it was stated in different studies. Therefore, the investigation of chemical composition of all welds was carried out. Shielding gas can influence the amounts of alloys that might be burned out from the welding joint as it was stated in previous research [52]. Manganese (Mn) is one of the most important alloying elements that is responsible for hardness properties of the high strength steels [54, 58]. It is possible to find how different shielding gases and welding parameters do influence chemical composition of the 650MPa steel grade welding joint in this research. Graphs in Figure 2.16. show changes of Mn content in welding joint with each gas at all three welded parameters.

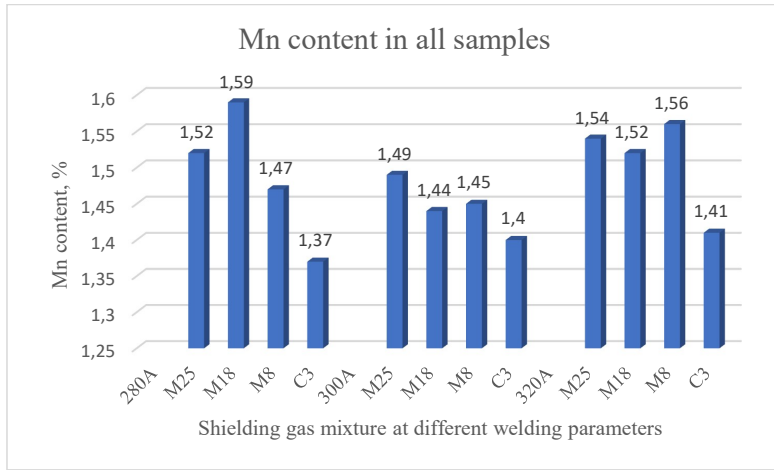
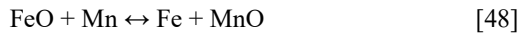


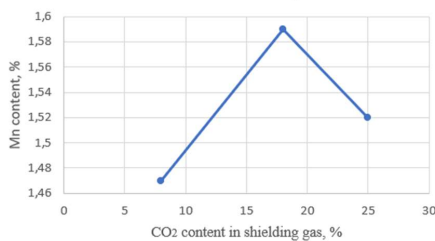
**Fig. 2.16.** Chart of Mn content in welding joints with different shielding gases at different welding parameters.

As it was stated in previous investigations that more alloys were burned out of the welds that were made by using shielding gas mixture C3 with short arc parameters [36]. The same phenomena also appear in this investigation. All samples that were welded with this gas mixture contains less Mn alloy then other welded samples. Content of Mn decreases by more than 16% against wire electrode and more than 12% against base material in samples welded by this mixture. A little increase was observed in samples that were welded with higher parameters then with lower ones. It can be explained with the Mn property to create MnO during the welding process [48]. Mn can make a reaction with FeO to take the O molecule and burn faster from the welding joint.

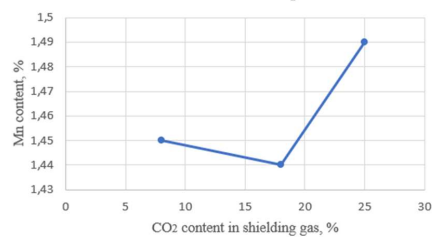


Rather opposite view on the Mn level according to increase of CO<sub>2</sub> level in shielding gas [38], [45] was observed in this study (Fig. 2.17. a). As the gas content was containing 25% CO<sub>2</sub> the more stable and higher level of Mn was achieved in welds. The Mn content was more depending on the welding parameters here. Decrease of 6-9% against wire and 1- 4% against base material was observed with M25 mixture in all three chosen welding parameters.

a) Mn content in weld at 280A parameters



b) Mn content in weld at 300A parameters





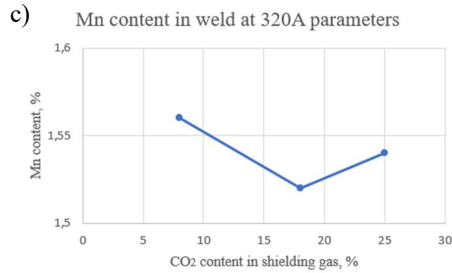


**Fig. 2.17.** Mn content depending on CO<sub>2</sub> content at different welding parameters: a) at 280 A; b) at 300 A; c) at 320 A.

Rather similar results were achieved with the mixture M18 (Fig. 2.17. b). Results again showed the opposite view as it was stated in the observed studies [38], [45]. Lowest decrease against wire material (only 2%) and even increase against the base material was observed in samples welded with M18 mixture at 280 A. At 300 A parameters this mixture showed a bigger drop in Mn content (12% against wire; 8% against base material).

As parameters increased to 320 A the shielding gas M8 mixture showed the best result in this investigation between the other CO<sub>2</sub> mixtures at these parameters (Fig. 2.17.c). Mn content in these welding joints was decreased only by 2% against wire material and no changes against base material. At lower parameters this mixture showed lower content of Mn in the welding joint (10- 11% against wire; 6- 7% against base material).

None of the previous charts do not show the same results as it was stated in previous researches except the higher parameters where the tendency of the decrease of Mn is negative. At the same time the line of the Mn content depending on welding parameters looks rather similar for all of the samples welded with CO<sub>2</sub> gases (Fig. 2.18.).

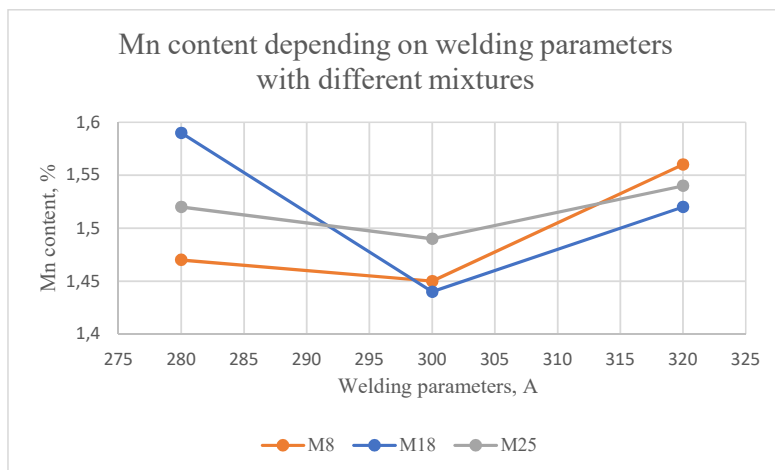


**Fig. 2.18.** Change of Mn content depending on welding parameters.

It is now possible to state that the influence of the welding parameters that also can influence the heat input of the welding process gives a possibility to keep higher Mn content in welding joint. So, there can be a possibility to find the correlation between the welding parameters including heat input and the Mn content in the welding joint.

Content of Ni as an alloying element is also important for high strength steel as it was stated in previous studies [42], [43], [44]. Because of this reason the same investigation was carried out on the influence of shielding gas on Ni content in the 650 MPa steel grade welding joint. As it can be found in Table 1, there is a difference of Ni content in base metal and wire electrode. It is used to keep the mechanical properties of the weld close to the base metal as the structure of the welding joint is slightly changing [42]. There is also stated that Ni content is important alloying element that helps to increase the strength of the welding joint without sacrificing the impact toughness [64].

From the investigation appeared that the Ni content was behaving opposite to the Mn when welding with C3 mixture. The content of Ni was the highest between all the samples compared to all shielding gas mixtures containing CO<sub>2</sub> (Fig. 2.19.).

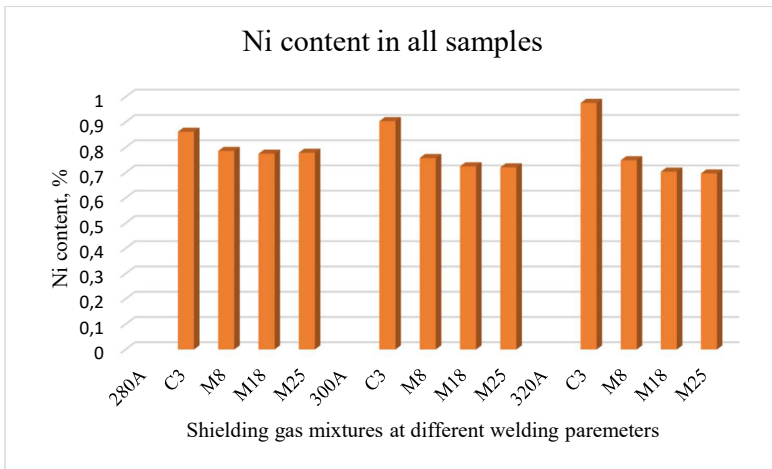


**Fig. 2.19.** Chart of Mn content in welding joints with different shielding gases at different welding parameters.

As it can be observed from the obtained results, as the current parameters increase, the Ni content in the weld also increases when the O<sub>2</sub> takes part in the welding process (Fig. 2.20.).

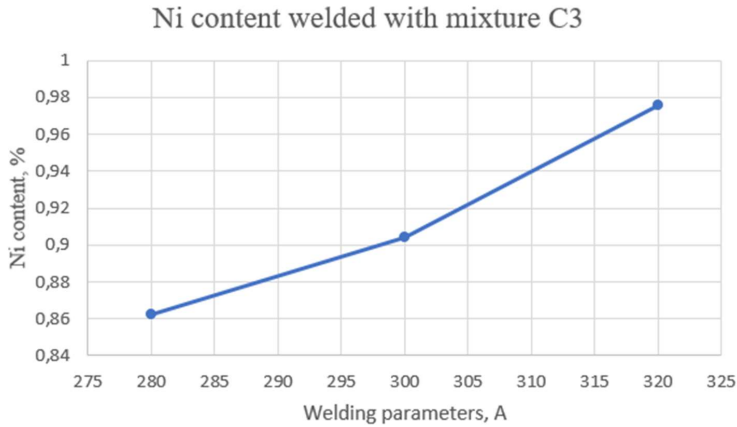


**Fig. 2.20.** Ni content depending on welding parameters with C3 mixture.

This phenomenon is not described in any of the overviewed researches where the oxygen mixture was used as a shielding gas. The increase of Ni content with this shielding gas was found to be 14% between 280 A to 320 A parameters. This correlation of the Ni content and the welding parameter increase looks rather similar to the previously raised idea about the Mn dependency on welding parameters.

However, the Ni content is decreasing in welding joints created by CO<sub>2</sub> mixtures. Though, the changes of the content were not so sufficient as in the samples welded by C3 mixture. Similar insufficient changes were also observed in other investigations [38]. Another scientist [42] chose to not take into account changes of Ni by using Ni+Cr+Mo complex changes of chemical composition in the weld that were also fluctuating not much.

Charts in Fig. 2.21. show the changes of Ni content with each shielding gas containing only mixture with CO<sub>2</sub> shielding gas.

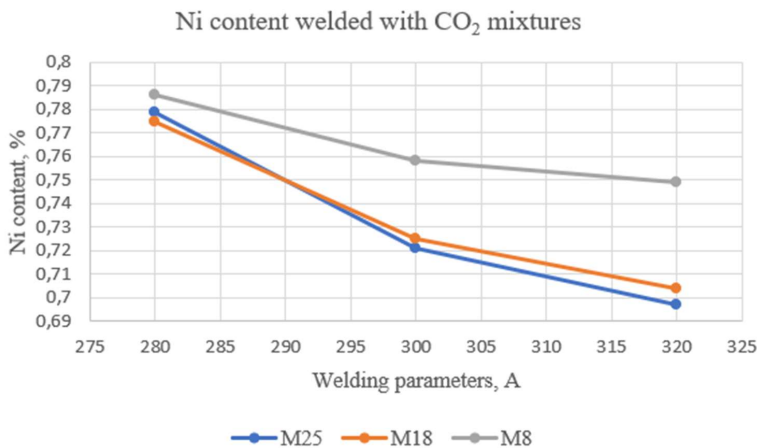
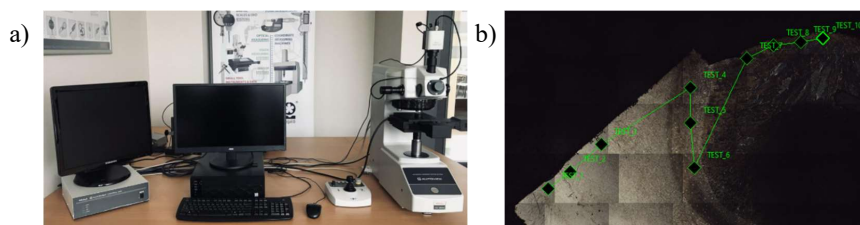


**Fig. 2.21.** Ni content depending on welding parameters with CO<sub>2</sub> mixtures.

It is possible to observe the insufficient decrease of Ni content by 4% in welding joint by increase of welding parameters with M8 shielding gas. The correlation looks descending in all of the charts and can be described with the increased temperature of the welding joint that influences the possibility to burn out Ni from the welding joint. Burning of Ni can also be explained by the short arc creation possibility that was observed previously with M8 and M25 shielding gases. However, the decrease of Ni in welding joints created by M18 and M25 looks more sufficient as the changes are approximately 10%. This decrease might show some influence on mechanical parameters of the welding joint as it was stated before [38].

#### 2.2.4. Hardness.

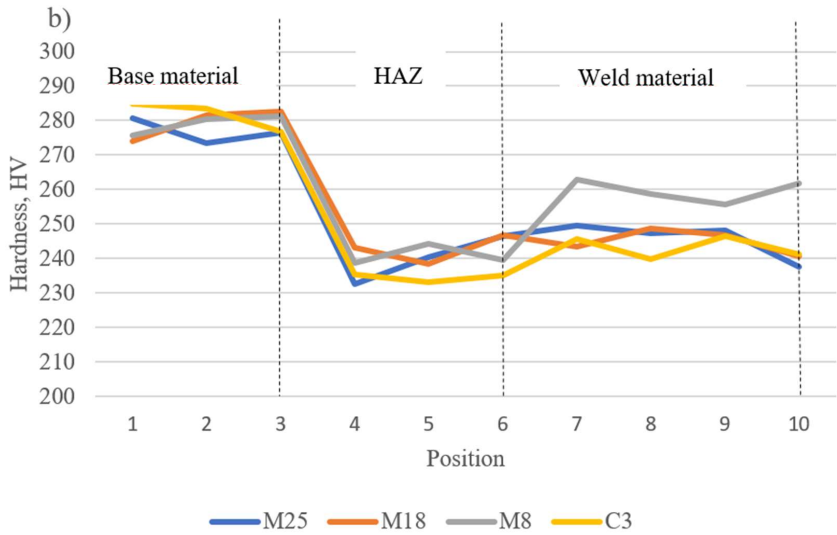
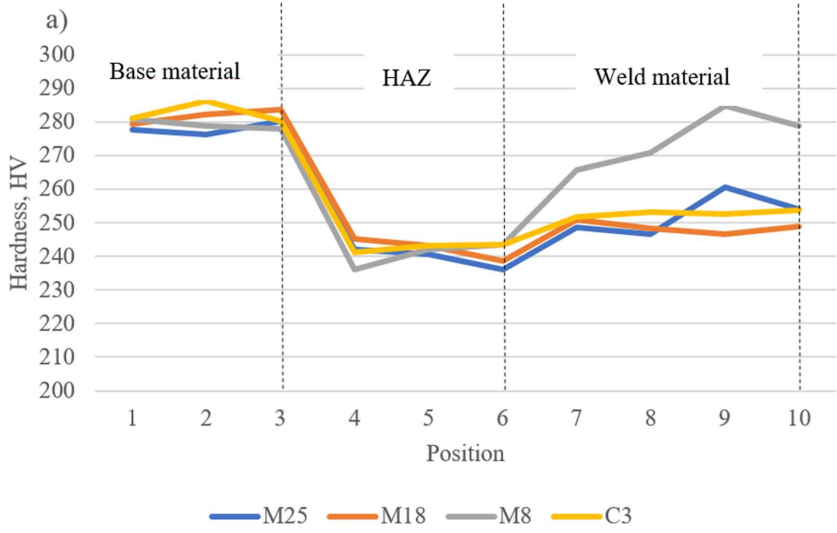
High strength steels are mainly used for their properties. One of the main features that influence the material toughness is the hardness. It is important to keep this property in the welding joint as high as possible to the base metal also after welding. All welded samples were tested with an automated hardness testing machine Mitutoyo Micro Vickers hardness tester HM-210D (Fig. 2.22. a) according to standard EN ISO 9015-1 procedures.



**Fig. 2.22.** Hardness testing setup: a) Mitutoyo Micro Vickers hardness tester HM-210D; b) hardness testing technology.

The welding joint was divided in the middle the same as it was done in one of the previous studies [41]. Ten stitches one by one after 0,5mm were made into every sample covering base material (3 stitches), HAZ (3 stitches) and weld metal (4 stitches) (Fig. 2.22. b). The changes in hardness of the material after welding are described in chart (Fig. 2.23.)





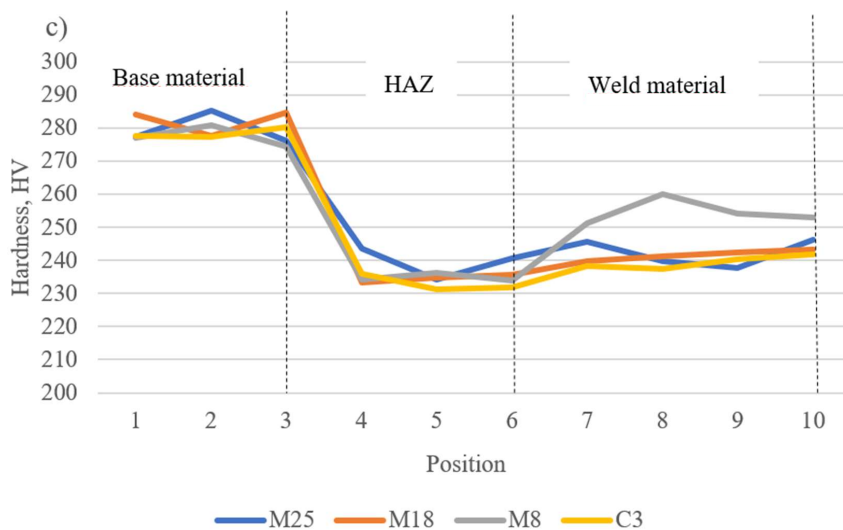


**Fig. 2.23.** Weld metal hardness at different welding parameters:  
a) 280 A; b) 300 A; 320 A.

Each parameter set was highlighted separately with the graph that shows the tested hardness of the samples. From these graphs it appears that the hardness in HAZ is almost the same for every welded specimen. The difference is visible only in the welding pool. Hardness was the highest in samples welded with M8 shielding gas. Other Ar+CO<sub>2</sub> mixtures (M18 and M25) showed smaller values of hardness in the welding seam as well as the C3 mixture. Similar graphs with rather similar values was carried out with all three used parameters. It was also possible to see that in one part of the welding pool at 280 A parameters the hardness was reached similar to base metal. This sample was welded with M8 shielding gas. Hardness close to the base metal was also reached at 300 A regime. As the parameters were rising the hardness of the weld did not reach the same values as the base metal, but still showed higher level than it was reached with other gases.

It is also possible to see that the HAZ of all welds made with gas mixtures M18 and M25 was a little bit longer than for other two shielding gases. It was approximately 1 – 1,5 mm wider compared to other samples. It can be explained with the CO<sub>2</sub> increase in shielding as that supports the creation of short arc during the welding process.

### 3. MODELING OF THE HARDNESS OF THE WELDING JOINT.

In order to compile the data and to find the relationship between the obtained result and the predicted content of alloying materials in the welded joint and its hardness. Obtained research results were compiled and the graphs were created using *Microsoft Excel 2019* program (Fig. 2.16, 2.19, 2.23). The mathematical model describing the influence of shielding gas and welding parameters on hardness of the weld was obtained with the *Microsoft Excel 2019* computer program. The results and each member of the model was also validated. Extra inspection was done by computer program *SPSS@Statistics* and the results is provided in Table 3.3.

#### 3.1. Shielding gas and welding parameter influence on chemical composition changes.

After review of different studies above, it was concluded that the investigations have been more focused on changes in the Mn and Ni content in the weld [36], [38], [42], [46]. R.E. Francis has also created a diagram showing the dependence of Mn on the content of oxygen molecules in the shielding gas [46]. From the results of this study (Fig. 3.1.a) it can be concluded that the results obtained in this study do not exactly coincide with the changes of the previously developed diagram at 280 A and 300 A parameters, while they coincide with 320 A parameters (Fig. 3.1.b). Thus, it can be concluded that the Mn content is influenced not only by the CO<sub>2</sub> content in the shielding gas, but also by the welding parameters.

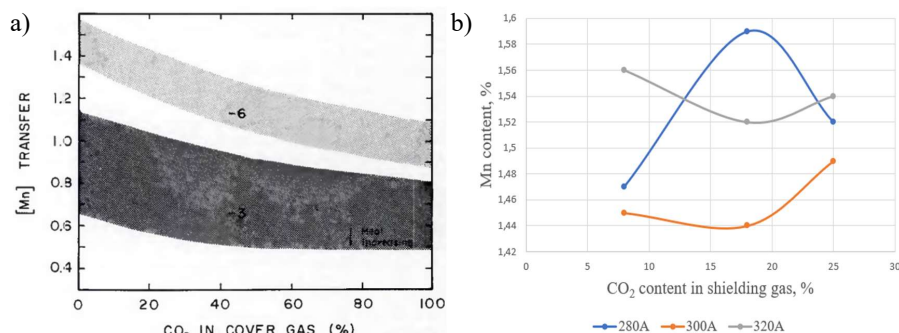


**Fig. 3.1.** Diagram of dependance of Mn on the composition CO<sub>2</sub> in the shielding gas: a) the studied model [46]; b) data obtained in this study.

After reviewing the above-mentioned studies, it was decided not to develop a model that could predict changes in the percentage of Mn and Ni content in the weld depending on the choice of shielding gas composition and welding parameters as the previously made studies were already including this kind of reasearch. Similar models are also generated for calculating Ni content in welded material.

#### 3.2. Modeling of hardenss of the welding joint influenced by shielding gas and welding parameters.

As it was stated before, one of the most important mechanical properties of high-strength steels is its hardness. This property also characterizes the wear resistance of

the material. Many studies have been carried out looking at the different mechanical properties of the weld and it has been found that the hardness of the material decreases with the increase of CO<sub>2</sub> in the shielding gas mixture. This conclusion has been stated in both studies with low-alloy structural steels [29] and high-strength steels (950 MPa) [38], [42], and a relationship between metal hardness and impact resistance has yet to be found, which is an important statement for high-strength steels research [38]. This phenomenon can also be observed in the study conducted in this work. In contrast to the study by M. Gouda [38], where it was stated that the hardness level was achieved identical to the base material only with pure Ar as shielding gas, in this study it was achieved with a mixture of Ar and 8% CO<sub>2</sub> at 280 A parameters.

Although, a relationship between hardness and the percentage of CO<sub>2</sub> in the shielding gas has been found before, no relationship has been found involving welding parameters. Therefore, in this work, a model was developed to help predict changes in the hardness of the weld, depending on the shielding gas and welding parameters used.

As the base model of finding the forecasting formula of hardness was chosen the linear regression. The independent parameters that influences the hardness result were chosen the welding current ( $I_w$ ) and the CO<sub>2</sub> and O<sub>2</sub> concentration. Results of the hardness measurements were also used as dependent parameters for the model calculation.

Following equation was created to determine the linear regression:

$$HV_w = a_{CO_2} \cdot CO_2 + a_{O_2} \cdot O_2 + a_I \cdot I_w + b \quad (3.1.)$$

where,

$HV_w$  – Hardness of the weld metal,

$a_{CO_2}, a_{O_2}, a_I$  – regression coefficient

$I_w$  – welding current (A)

$O_2$  – oxygen concentration in shielding gas (%)

$CO_2$  – carbon dioxide concentration in shielding gas (%)

$b$  – independent coefficient

Following table was drawn after entering the data in the *Microsoft Excel* calculation model:

**Table 3.1.**

Obtained results from *Microsoft Excel* calculation

Coefficient	CO <sub>2</sub>	O <sub>2</sub>	$I_w$	b
$a_{1,2,3...n}; b$	-1,02	-3,74	-0,32	364,31
a standart deviation	0,14	0,51	0,05	15,78
$R^2$	0,70			
$HV_w$ standart deviation	5,87			
Degree of freedom	44			

From these data the coefficients for the formula can be found and the equation 3.1. looks following:

$$HV_w = (-1,02) \cdot CO_2 + (-3,74) \cdot O_2 + (-0,32) \cdot I_w + 364,31 \quad (3.2)$$

The obtained equation was then checked for conformity by using obtained data in table 3.1. The resulting corrected coefficient of determination ( $R^2$ ), taking into account the number of independent variables and the number of measurements was determined  $R^2 = 0,70$ . It shows rather close relationship between calculated values and measurement results, namely 70% of the measurements can be explained by the linear regression model used.

To verify statistical significance of the obtained coefficients, the  $t$ -statistic and associated P-value for 2-tailed Student distribution was calculated by using following formula:

$$t = \frac{a_{CO_2, O_2, I}}{S_{a_{CO_2, O_2, I}}} \quad \text{and} \quad t = \frac{b}{S_b} \quad (3.3)$$

$a_{CO_2, O_2, I}$  – regression coefficient

$b$  – independent coefficient

$S_{a_{CO_2, O_2, I}}, S_b$  – standard deviation of residual

It is now possible to find the residual sum of squares as the coefficients of the obtained model are calculated and the results of experimental hardness tests are summarized.

$$SS_{res} = \sum_i (H_i - a_I \cdot I_i - a_{O_2} \cdot O_i - a_{CO_2} \cdot CO_i - b)^2 \quad (3.4)$$

Standart deviation of residual can be calculated by using the obtained results from formula 3.4.

$$S_{res} = \sqrt{\frac{SS_{res}}{n - m - 1}} \quad (3.5)$$

$n$  – degree of freedom (from table 3.1)

$m$  – number of variables

From formula 3.5  $S_{a_{CO_2, O_2, I}}, S_b$  values can be calculated as following:

$$S_b = \frac{S_{res}}{\sqrt{n - m - 1}} \quad (3.6)$$

$$S_{a_I} = \frac{S_{res}}{S_I \sqrt{n - m - 1}} \quad (3.7)$$

$$S_{a_{O_2}} = \frac{S_{res}}{S_{O_2} \sqrt{n - m - 1}} \quad (3.8)$$

$$S_{a_{CO_2}} = \frac{S_{res}}{S_{CO_2} \sqrt{n-m-1}} \quad (3.9)$$

The  $t$ -statistic values and the  $P$ -value now can be calculated. Obtained results are shown in the table 3.2.

**Table 3.2.**

Calculated  $t$ -distribution and  $P$  Values

	CO <sub>2</sub>	O <sub>2</sub>	I <sub>w</sub>	b
$t$	7,26	7,24	6,13	23,09
$P$	4,79E-09	5,02E-09	2,2E-07	3,16E-26

The accuracy and reliability of the model can be now verified from analyzed data in table 3.2. If the  $P$ -value associated with a regression coefficients does not reach 0.05, then the developed regression model is statistically significant [65], [66] In this case  $P$ -value is less then prescribed figure for all of the coefficients. It means that the resulting coefficients are correct and reliable.

More expanded formula was created to find more accurate linear regression model to insure the accuracy of received data.

$$HV_w = a_1 \cdot I_w + a_2 \cdot O_2 + a_3 \cdot CO_2 + a_4 \cdot I_w \cdot O_2 + a_5 \cdot I_w \cdot CO_2 + a_6 \cdot O_2 \cdot CO_2 + a_7 \cdot I_w \cdot O_2 \cdot CO_2 + b \quad (3.10)$$

where:

$HV_w$  – hardness of the weld metal

$a_{1,2,3,4,5,6,7}$  - regression coefficients

$b$  – independent coefficient

$I_w$  – welding current

$O_2$  – Oxygen content in shielding gas (%)

$CO_2$  – Carbon dioxide content in shielding gas (%)

Following the previous analysis of the model by using  $t$ -distribution test it was stated that the  $P$ -value of coefficients  $a_4, a_5, a_6, a_7$  are bigger than figure 0,05. Therefore, these coefficients where removed from the formula. The final result of the model was then obtained the same as formula 3.2.

Fig. 3.4. shows the obtained linear model according to the linear regression modeling method, as well as the predicted deviations from the theoretical values using different shielding gas.

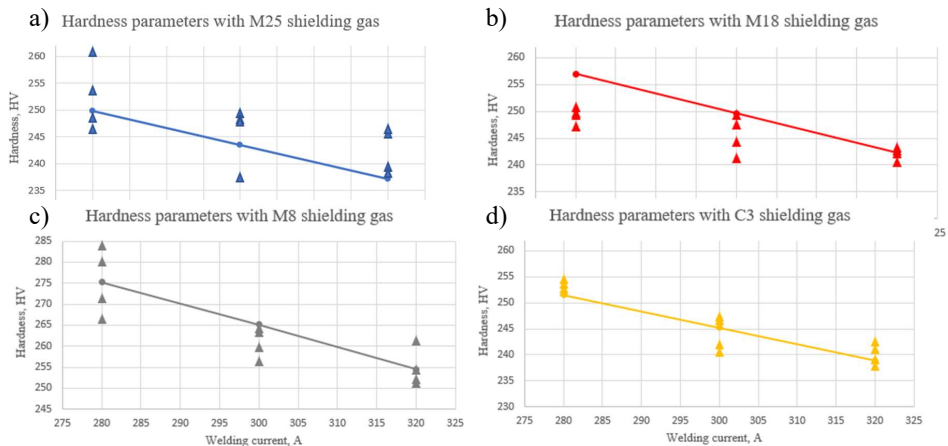


**Fig. 3.2.** Comparison of the calculated hardness of the welded seam material with the experimentally measured data: a) M25; b) M18; c) M8; d) C3.

It can be concluded that the generated model (3.2.) show rather precise calculated results that give a possibility to predict the welded metal hardness parameters as the calculated tolerance of the model was 6 HV hardness units. It is the same tolerance that was found during measuring process of the base material and weld material almost for all samples (except for four points).

An additional inspection of obtained model was carried out by computer programm *SPSS@Statistics*. After all the data were collected and put in the model following results were obtained.

**Table 3.3.**

Coefficients Obtained with *SPSS@Statistics*.

Coefficients <sup>a</sup>													
Model		Unstandardized Coefficients		Standardized Coefficients	t	Sig.	95.0% Confidence Interval for B		Correlations			Collinearity Statistics	
		B	Std. Error	Beta			Lower Bound	Upper Bound	Zero-order	Partial	Part	Tolerance	VIF
1	(Constant)	364.310	15.776		23.093	.000	332.517	396.104					
	ampers	-.318	.052	-.508	-6.126	.000	-.422	-.213	-.508	-.678	-.508	1.000	1.000
	co2_perc	-101.781	14.023	-.795	-7.258	.000	-130.042	-73.520	-.277	-.738	-.602	.575	1.740
	o2_perc	-373.885	51.612	-.793	-7.244	.000	-477.902	-269.868	-.275	-.738	-.601	.575	1.740

a. Dependent Variable: cietlba

From the data that are captured in first column it is possible to conclude that they look similar to the coefficients in the Formula (3.2). Similar result can be found with *t*-distribution in column number four. All *t* values are almost the same.

As the created models look similar as well as created graphs show very close results to experimentally achieved ones it can be concluded that the obtained mathematical model is correct and significant.

## CONCLUSIONS

1. The effect on spatter formation when welding with shielding gases M18 and M25 is still observed in the spray-arc material transfer modes. Despite the high plasma temperature in the welding arc, the high CO<sub>2</sub> content still supports the potential for short-circuit formation during the welding process, resulting in droplets forming in the welding bath, which can be seen as a spatter on the surface of the material. When welding with M8 and C3 mixtures, no spatters occur, as the Argon content is at least 90%, ensuring less CO<sub>2</sub> impact on the welding process and the formation of short circuits.

2. Deeper penetration was achieved in all samples welded with M18 and M25 shielding gases. This is possible due to the above-mentioned characteristics of short-circuit formation due to the higher CO<sub>2</sub> content of the shielding gas. It is possible that by reducing the wire feed rate, and thus the welding current, the amount of spatter would be reduced if it were also possible to insure the smooth flow of the molten electrode wire into the bath by reducing the welding speed. As a result, the potential of increasing the heat input to the weld becomes more eventual. It can lead to an increase of both the deformation and the amounts decrease of alloyed elements and the mechanical properties of the weld.

3. In samples welded with M8 and M18 shielding gases, fewer inclusions are observed in the welds. This is due to the fact that the O<sub>2</sub> content that takes part in the weld is lower than for other shielding gases. For this reason, less oxides and other gaseous compounds are formed, which are unable to escape from the liquid phase of the weld.

4. The Mn content was higher in the welds of the samples made with M8 mixture at higher parameters (320A). Nevertheless, the hardness measurements did not reach the highest values. This can be explained by the uneven microstructure of the joint, as well as the reduced Ni content at higher parameters.

5. Smaller and relatively stable changes in Mn content were observed in welded samples with M25 mixture. However, the hardness test results were not observed to be higher than in the other welded samples.

6. The lowest amount of Mn as an alloying material was observed in all samples welded with C3 mixture. This can be explained by the presence of O<sub>2</sub> in the welding process, as a result of which the alloying elements in the seam are actively burned out. On the other hand, the presence of O<sub>2</sub> in the shielding gas does not significantly affect the changes in the Ni content, and as the current increases, its composition in the joint increases. However, this phenomenon does not ensure the hardness of the weld material, which decreases with increasing welding parameters. Therefore, the use of C3 alloy is not recommended for welding high strength steels at high welding parameters.

7. The best combination of weld shape, penetration and hardness parameters was achieved with M8 mixture at 280A welding parameters. Thus, the previously established hypothesis that welding results in a shielding gas environment at spray-arc transfer parameters for high-strength structural steels is achieved with a shielding gas with a lower percentage of CO<sub>2</sub>.

8. All samples made with M8 mixture achieved higher hardness values against other shielding gases at the same welding parameters. Sample 280A achieved the highest hardness value among all samples welded in spray-arc transfer modes. Although losses of Mn were observed at lower parameters, no decrease in Ni content was observed in the samples welded with M8 mixtures. This explains the relatively stable hardness values in welded joints.



9. A mathematical model was generated and validated to calculate the predicted hardness of weld metal.

10. The hardness of the weld metal in HAZ was achieved lower than the base material for all samples that were welded. It means that the influence of high welding parameters on non-melted welding pool metal is high and decreases its mechanical properties. Therefore, it might not be recommended to use spray-arc in welding of low alloyed high-strength steel or not to over increase these parameters during the welding process.

## REFERENCE LIST

1. Gas Metal Arc Welding [accessed on 10th of January 2022]. Available at: [http://www.itw-welding.com/media/Pdf/Welding\\_Support](http://www.itw-welding.com/media/Pdf/Welding_Support).
2. Grill J., MIG Welding (GMAW) Process Techniques & Tips [accessed on 10th of January 2022]. Available at: <https://weldguru.com/mig-welding/>.
3. MIG vs TIG Welding: The Main Differences [accessed on 2nd of June 2022]. Available at: <https://weldguru.com/mig-vs-tig-welding/>.
4. MAG Welding [accessed on 2nd of June 2022]. Available at: <https://rime.de/en/welding/mag-welding/>.
5. Kah P. & Martikainen J., Influence of shielding gases in the welding of metals (2011).
6. Knovel (Firm), ASM International. Handbook Committee. ASM handbook. Volume 6, Welding, brazing, and soldering (1993).
7. Gertsovich N. Svanberg M., Analysis of MIG welding with aim on quality, M.Sc. Thesis, Dept. Signal Processing, Blekinge Institute, Sweden (Jul. 2008).
8. Karadeniz E., Ozsarac U., and Yildiz C., The effect of process parameters in gas metal arc welding process, *Materials and Design*, vol. 28, 649–656 (Sep. 2005).
9. Kuk J.M., Jang K.C., Lee D.G., Kim I.S., Effects of temperature and shielding gas mixture on fatigue life of 5083 aluminum alloy, *J Mater Process Technol* 155(156): 1408–1414., (2004).
10. Chern T-S., Tseng K-H., Tsai H-L., Study of the characteristics of duplex stainless steel activated tungsten inert gas welds. *Mater Des* 32(1): 255–263 (Available on: [doi:10.1016/j.matdes.2010.05.056](https://doi.org/10.1016/j.matdes.2010.05.056)) (2011).
11. ПАТОН Б. Е., Кирсанов А. В., Подгаецкий В. В. и др., а. с. 448106 СССР, в 23 к 35/38. Защитная газовая смесь - приор. 26.06.72. Опубл. 30.10.74; бюл. № 40.
12. *SAGOS 3: Ein schutzgas fuer zwei Werkstoffgruppen*, *Stahlmarkt*, No. 11.: 66 (2001).
13. Pfeiffer G., Zuend- und spritzeruntersuchungen beim MAG-Impulsschweißen, *ZIS-Mitteilungen*, No. 6.: 545–549 (1989).
14. ПАТОН Б. Е., РИМСКИЙ С. Т., ГАЛИНИЧ В. И., Применение Защитных Газов в Сварочном Производстве (Обзор) (2014).
15. Рошупкин Н. П., Близнец Н. А., Свединский В. Г. и др. Опыт производственного применения газовых смеси на основе аргона заводами ВО «Союзстальконструкция», там же. № 3. 51–53 (1984).
16. Свединский В. Г., Римский С. Т., Галинич В. И. Сварка сталей в защитных газовых смесях на основе аргона в промышленности Украины, автомат. сварка. № 4. 41–44 (1994).
17. Свединский В. Г., Римский С. Т., Кирьян В. И. Оценка вязкости разрушения швов, сваренных в защитных газах и под флюсом, там же. № 8. 16–19 (1982).
18. Римский С. Т. Управление свойствами металла шва путем урегулирования уровня окисленности сварочной ванны при сварке в защитных газах, автомат. сварка. № 12. – с. 20–23 (2011).
19. Римский С. Т., Свединский В. Г., Шейко П. П. и др. импульсно-дуговая сварка низколегированных сталей плавящимся электродом в смеси аргона с углекислым газом, автомат. сварка. — № 2. – с. 38–41 (1993).
20. Ameye M. Einfluss der verschiedenen schutzgase im Zusammenwirken mit schweissverfahren und Werkstoffen, *Der Praktiker*. No. 7, s. 271–273 (2011).
21. Lyttle K., Stapon G. simplifying shielding gas selection, *Practical Welding today*. No. 1. 22–25 (2005).
22. Das schutzgas macht's, *Blech. Rohre Profile*. No. 8/9. 28–30 (2005).
23. Ernst M. Lichtbogen stabil gehalten, *Produktion*. No. 8. 23 (1999).
24. Church J. G., Imaizumi H. Welding characteristics of a new welding TIME-process, *IIW Doc. XII-1199*.
25. Lahnsteiner P. T.I.M.E.-Prozess ein neues MAG-schweißverfahren, *schweißtechnik*. No. 12. 182–186 (1991).
26. Lucas W. Choosing a shielding gas. Pt 2, *Weld. and Metal Fabr*. No. 6. 269–276 (1992).
27. Dixon K. shielding gas selection for GMAW of steels, *Weld. and Metal Fabr*. No. 5. 8–13. (1999).
28. Oeteren K.-A. «Neues schutzgas» metal-aktivgasgeschwift – ein wirtschaftlicher vorteil, *Der Praktiker*. No. 2. 90–94 (1992).
29. Gadallah<sup>1,\*</sup>, R. Fahmy<sup>1</sup> R., Khalifa<sup>1</sup> T., Sadek<sup>2</sup> A., Influence of Shielding Gas Composition on the Properties of Flux-Cored Arc Welds of Plain Carbon Steel (2012).
30. Moreira A.F. Gallego J. Tokimatsu R.C. & Ventrella V.A.\*. THE EFFECT OF SHIELDING GAS MIXTURE ON INCLUSION DISTRIBUTION FOR MIG WELDING PROCESS.

31. Çevik B., The effect of pure argon and mixed gases on microstructural and mechanical properties of S275 structural steel joined by flux-cored arc welding (2018).
32. Ghazvinlo H. R., Honarbakhsh Raouf A.: Journal of Applied Science, p. 658, (10, 2010), (Available on: [doi:10.3923/jas.2010.658.663](https://doi.org/10.3923/jas.2010.658.663) ).
33. Gülenç B., Develi K., Kahraman N., Durgutlu A.: International Journal of Hydrogen Energy, 30, 2005, p. 1475. (2005) (Available on: [doi:10.1016/j.ijhydene.2004.12.012](https://doi.org/10.1016/j.ijhydene.2004.12.012) ).
34. Aloraier A., Ibrahim R., Thomson P.: International Journal of Pressure Vessels and Piping, 83, 2006, p. 394. (2006), (Available on [doi:10.1016/j.ijpvp.2006.02.028](https://doi.org/10.1016/j.ijpvp.2006.02.028) ).
35. Kiliñçer S., Kahraman N.: Journal of the Faculty of Engineering and Architecture of Gazi University, 24, p. 23 (2009).
36. Boiko I., Avisans D., Study of Shielding Gases for MAG Welding, (2013).
37. Kou S., Welding Metallurgy Handbook, 2nd ed. New York, USA: John Wiley and Sons, 2002.
38. Gouda M., Takahashi M., Ikeuchi K., Microstructures of gas metal arc weld metal of 950 MPa class steel, Institute of Materials, Minerals and Mining (2005).
39. Fleming D. A., Bracarense A. Q., Liu S. and Olson D. L.: Weld. Journal 75 (6), 171–183 (1996).
40. Peng Y., Peng X., Zhang X., Tian Z., Eang T., Microstructure and Mechanical Properties of GMAW Weld Metal of 890 MPa Class Steel, Journal of Iron and Steel Research, International, 21 (5), 539-544 (2014).
41. Zhao Y., Shi H., Yan K., Wang G., Jia Z., He Y., Effect of shielding gas on the metal transfer and weld morphology in pulsed current MAG welding of carbon steel, Journal of Materials Processing Tech., 2018.
42. Tonbang A., Jinshan W., Jiguo S., Zhiling T., Influence of Shielding Gas Composition on Microstructure Characteristics of 1000 MPa Grade Deposited Metals (2018).
43. Keehan E., Karlsson L., Andren H.-O. and Bhadeshia H.K.D.H., New Developments with C-Mn-Ni High-Strength Steel Weld Metals, Part A – Microstructure, (September, 2006).
44. Lord M., Design and modeling of ultrahigh strength steel weld deposits. *Materials Science and Metallurgy*. University of Cambridge: Cambridge, U.K. (1999).
45. Kang, B.Y., Kim, H. J., and Hwang, S. K., Effect of Mn and Ni on the variation of the microstructure and mechanical properties of low-carbon weld metals. *ISIJ International* (Japan) 40(12): 1237- 1245 (2000).
46. Francis R. E., Jones J. E. and Olson D. L., Effect of Shielding Gas Oxygen Activity on Weld Metal Microstructure of GMA Welded Microalloyed HSLA Steel, *Welding Research Supplement*, 408 – 415 (1990).
47. Kikuta Y., Araki T., Honda K. and Sakahira S., The metallurgical properties of electroslag weld metal using CeF3 addition wire. *Proceedings of International Conference on Welding Research in the 1980s*, Session B, 131-136 (1980).
48. O. Pärtersons, J. Priednieks, MIG/MAG Metināšana, Part 2, AGA SIA (2010).
49. Product range offer home page of company Zultnermetall [accessed on 15<sup>th</sup> of March 2022]. Available at: <https://www.zultnermetall.com/en/fronius-tps-500i-mig-mag-schweissgeraet-puls-wassergekuehlt>.
50. Product and software range of company Fronius [accessed on 15<sup>th</sup> of March 2022]. Available at: <https://www.fronius.com/en/welding-technology/innovative-solutions/weldconnect>.
51. Sergejevs, D., Tipainis, A., Gavrilovs, P. Restoration of Railway Turnout Elements with Manual Metal Arc Welding and Flux-Cored Arc Welding (2016) *Procedia Engineering*.
52. Sergejevs, D., Tipainis, A., Gavrilovs, P. The restoration of worn surfaces of railway turnout elements by a flux cored arc welding (FCAW) (2014) transport Means - Proceedings of the International Conference (2014-January).
53. Avisans D., Boiko I., In: *Proceedings of 7th International Symposium „Surface Engineering. New Powder Composition Materials. Welding”*, 2nd Part, March 2011 (Minsk, Belarus, 2011).
54. Herring D. H. , The Influence of Manganese in Steel, Academy of Digital Learning, April, 2010, Zultnermetall [accessed on 15<sup>th</sup> of March 2022]. Available at: <https://www.industrialheating.com/articles/89322-the-influence-of-manganese-in-steel>.
55. Ebrahimmia M., Goodarzi M., Nouri M., Sheikhi M., Study of the effect of shielding gas composition on the mechanical weld properties of steel ST 37–2 in gas metal arc welding. *Mater Des* 30 (9):3891–3895. doi:10.1016/j.matdes.2009.03.031, (2009)
56. Sonmez U., Ceyhun V.: Kovove, Materialy-Metallic Materials, 52, , p. 57. (2014).

57. Rizvi S. A., Tewari S. P., Effect of the Shielding Gas Flow Rate on Mechanical Properties and Microstructure of Structural Steel (IS2062) Welds, (2017).
58. Akay A. A., Kaya Y., Kahraman N., Sakarya University, Journal of Science, 17, p. 85, (2013).
59. Schatt W., Worch H., Werstoffwissenschaft, Weinheim: Wiley VCH Verlag GmbH (2002).
60. Oettel H., Schaumann H., Metallografie, Weinheim: Wiley VCH Verlag GmbH (2005).
61. Schuster J., Hot cracking in welds – Initiation, verification and prevention, DVS-News, Volume 233, Düsseldorf; Verlag für Schweißen un verwandte Verfahren DVS-Verlag GmbH (2004).
62. Böse U., Ippendorf F., Base material behaviour during welding – Part 2, Application Düsseldorf; Verlag für Schweißen un verwandte Verfahren DVS-Verlag GmbH (2001).
63. Matsuda F., Fukada Y., Okada H., Shiga C., Ikeuchi K., Horii Y. and Shiwaku T.: Weld. World, 37, 134–154 (1996).
64. Pratomo S. B., Oktadinata H. and Widodo T.W., Effect of nickel additions on microstructure evolution and mechanical properties of low-alloy Cr-Mo cast steel, International Seminar on Metallurgy and Materials, IOP Conf. Series: Materials Science and Engineering 541; [doi:10.1088/1757-899X/541/1/012050](https://doi.org/10.1088/1757-899X/541/1/012050) (2019).
65. Navidi W.C.. Statistics for engineers and scientists, [https://mirlyn.lib.umich.edu/Record/014865504 CN - QA 276.4 .N38 2015 \(2015\)](https://mirlyn.lib.umich.edu/Record/014865504%20CN%20-%20QA%20276.4%20.N38%202015%20(2015)).
66. Mason R. L., Gunst R. F., Hess J. L., Statistical Design and Analysis of Experiments, with Applications to Engineering and Science, Second edition, A JOHN WILEY & SONS PUBLICATION, New Jersey, <https://www.abebooks.com/9780471372165/Statistical-Design-Analysis-Experiments-Applications-0471372161/plp>, [accessed on 15<sup>th</sup> of July 2022].

## **ANNEXES**

1/3  
75525K-002  
11.06.2021

VASTAANOTTODISTUS INSPECTION CERTIFICATE

EN 10 204-3.1 (2004)

**SSAB**  
 Tuotteen myyjä / Consignee  
 TUUSULA  
 TUUSULANKATU 7  
 02800 HYINKÄÄ FINLAND  
 Tilauksen nro. / Order No. 4501282498  
 Toimitus / Certificate 31

Tuotteen lähettäjä / Shipper  
 TUUSULA  
 TUUSULANKATU 49  
 80100 SEINÄJOKI FINLAND  
 Asetuksen merkki / Shipping mark

Toimituspaikka / Destination  
 Laitos / Shipping  
 Laitosmerkki / Quality Marking  
 STRENX 650 MC D

Toimitustyyppi / Delivery type  
 REST DELIVERY  
 Tuote / Product  
 Putki / Pipe  
 Laji / Grade  
 Laitosmerkki / Quality Marking  
 Laitosmerkin kuvaus / Description of Quality Marking  
 HIGH STRENGTH FORMABLE STEEL MEETS REQ. OF EN10149-2 S650MC

Pöytäkirja / Mill sheet  
 Item Dimensions mm  
 060 10.00 X 1500 X 6000 4501282498 A005.A02832 STD

Toimituspaikan nimi / Name of Inspector  
 Vastatodistuksen laji / Type of Certificate  
 Vastatodistuksen numero / Certificate No.  
 Muut merkinnät / Remarks  
 Tekniset vaatimukset / Technical terms of Delivery and/or official regulations  
 SSAB TOLERANCE EN10051, THICKN. 1/2 CAT D

Vastatodistuksen laji / Type of Certificate  
 Vastatodistuksen numero / Certificate No.  
 Muut merkinnät / Remarks  
 Tekniset vaatimukset / Technical terms of Delivery and/or official regulations  
 SSAB TOLERANCE EN10051, THICKN. 1/2 CAT D

Item	Dimensions mm	Weight kg	SP No.	UT	MT
060 10.00 X 1500 X 6000 4501282498 A005.A02832 STD	4	2835	74638	011	011
	***	4	2835		

**Raabe Steel Works**  
 Testaus ja analyysi / Testing and Inspection  
  
 MINNA VALKAMA  
 Vastatodistuksen myyjä / Authorized Inspection representative  
 CASE Europe Oy  
 Korpilampi Registraatio Office: HÄMEENLINNA  
 Puhelin / Telephone: 030 8511 3557,20 5911  
 Osoite / Address: FIN-22101 RAAHJE FINLAND  
 Y-tunnus / Business ID: 23954457



# AINESTODISTUS TEST REPORT

2/3  
75525K-002  
11.06.2021

Tilaaja Purchaser: Vastaindaja Consignee: Paivämäärä Date: 14.06.2021 AMH  
 TILNOR OY TIBNOR OY  
 05800 HOVINKAARI FINLAND 80100 SEINÄJOKI FINLAND  
 Tilauksen / Order No.: 75525K Tilausvirhinen / Order Confirmation: Asiakkaan merkki / Shipping mark: Mark of the Manufacturer  
 4501282498  
 Laji Grade: STREXX 660 MC D  
 Lisävaatimukset / Additional requirements: Annettu / Approved: Käsittely / Treatment: Fully Alled. The grain practiced

Liikennepöytäkirja / Transport Certificate: **HIGH STRENGTH FORMABLE STEEL MEETS REQ. OF EN10149-2 S650MC**

Pos. Item	Subauskera / Cast. test No	Tähdä / Mark	Velvoite / Tensile test	K2 °C	702	RE202 MPa	RE302 MPa	RE1 MPa	RE4 MPa	RM MPa	1	2	3	50...80 A %	200 RE / RM	RM / AS	RM / AS	RAZ %	1	2	3	Keskiverto / Average	32	2	0	Huom / NO	Passo / Tempering °C
060	74638	011	TM	32	779																						
K2: 32-CENTRE LONGITUDINAL																											
K3: 32-120 MM WIDE BEND TEST																											
Pos. Item	Subauskera / Cast. test No	Reulioite / Impact test	K3 °C	1	2	3	Keskiverto / Average	W (mm)	FA %	1	2	3	Keskiverto / Average	LE (mm)	*Spidemen ulkoisen / External diameter		Erikoisovien / Special tests		K4 °C		1	2	Keskiverto / Average	Huom / NO	Passo / Tempering °C		
060	74638	011	135 -020	62	56	58	59	FA = Sikaumutuman oisus / Shear fracture appearance	LE = Polttainen laajenema / Lateral Expansion																		

K3: 135-CH-MISO-VUJ75X10,CENTRELONGIT,KV600

## Raabe Steel Works

Tietäjä ja tarkastus / Testing and Inspection

*M. Manninen*

MINNIA VALKAMA  
 Valvottu edustaja / Authorized inspection representative  
 Yhtiön nimi / Company Name: SSAB Europe Oy  
 Käsipöytäkirja / Registered Office: RAINEENLA

Osoite Address: PL 53, P.O. Box 53  
 FIN-22101 RAUHE, FINLAND

Puhelin Telephone: 020 9911  
 +358 20 3811

Y-tunnus Business ID: 2389445-7

Täällä todistamme, että biomitus on tilausvirhisen mukainen.  
 We hereby certify that the material described above has been tested and complies with the terms of the order confirmation.



**ANALYYSITODISTUS ANALYSIS CERTIFICATE**  
**ANALYSEBESCHEINIGUNG COMPOSITIO CHIMIQUE CERTIFICAT**  
**СЕРТИФИКАТ АНАЛИЗА**

3/3  
 75525K-002  
 11.06.2021

Päivämäärä Date Datum Date Date  
 14.06.2021

AMEI

Ratio C Mn P S AL NB V TI CU CR NI MO B  
 Analyysi % Chemisch Zusammensetzung % Composition Chimique % Анализа массов % (\*-ppm)

0.60 .35 .053 .17 1.67 .011 .003 .040 .047 .011 .096 .017 0.06 0.04 .005 .0004

74638  
 Ratio C Mn P S AL NB V TI CU CR NI MO B  
 Analyysi % Chemisch Zusammensetzung % Composition Chimique % Анализа массов % (\*-ppm)

0.60 .35 .053 .17 1.67 .011 .003 .040 .047 .011 .096 .017 0.06 0.04 .005 .0004

CEC=C-MnB(Cr-Mo-V)-Ni-Cu/15

**Raabe Steel Works**

Testlab ja Inspektio  
 Prüfung und Inspektion  
 Essais et Contrôle

Исследовательская лаборатория

Steel manufacturing and supplied by Raabe Steel Works in the form of plates.  
 Производство и поставка в виде листовых прокатов в Raabe Steel Works и поставка.  
 Заводской стан, не использовались.

*Minna*

**MINNA VALKAMA**  
 Valmistaja  
 Manufacturer  
 valmistaja

Yhteisö-omistaja  
 Jointly owned  
 yhteisö-omistaja

Authorized Inspection representative  
 Inspector  
 Inspecteur  
 Inspektör

Y-tunnus Business ID: 2386445-7

Postiosoite / Registered Office: RAABE, FINLAND  
 Puhelin / Telephone: 020 5911  
 Faksi / Fax: 020 5913



Annex No. 2  
Welding Electrode Wire Certificate



Specials elektrods, SIA

Gustava Zemgala 71 a  
1039 Riga

X **Werkzeugnis** 2.2  
(Test Report)

**Abnahmeprüfzeugnis** 3.1  
(Inspection Certificate)

nach EN 10204

<b>Bestellung Nr.:</b> (your order no.)	<b>Besteller:</b> (customer)	<b>Datum:</b> (date)	<b>Unsere Auftr.Nr.:</b> (works order no)						
	2381	16.08.2021	20210004343						
<b>Qualität:</b> (Quality)	<b>Abmessung:</b> (Diameter)	<b>Schmelze:</b> (Batch-cast-no.)	<b>Menge:</b> (Quantity)						
DT-NiMoCr EN ISO 16834: ~Mn3Ni1CrMo AWS: ER 100S-G	1,20 mm auf K300	210127	900,00 kg.						
<b>Chemische Analyse in %</b> Chemical composition in %									
	C	Si	Mn	P	S	Cr	Mo	Ni	Zr
	0,075	0,630	1,630	0,009	0,007	0,280	0,220	1,420	0,0170
	Cu	Fe	Al	Co	Sn	B	Nb	V	Ti
	0,160		0,006				0,0020	0,090	0,0010

Viederstraße 19  
47009 Krefeld (Linn)  
Telefon: 02151 / 51 625 0  
Telefax: 02151 / 51 625 55  
info@schwec.de

Niederlassung SÜD  
Maybachstr. 13  
71696 Remseck a.N.  
Telefon 07141 / 894747  
Telefax 07141 / 894749

GF: Olaf Post  
Dp(Lng) Thomas Post

www.DRATEC.de

AG Krefeld HRB 2820

Riga Technical university  
Transport institute



### Chemical Results

Probe Nr. / sample ID: PARAUGS 1

Grundwerkstoff / material:

Kunde / customer:

Abmessung / dimension:

Kom.-Nr. / commission:

Zusatzwerkstoff / filler metals:

Labor Nr. / lab-no.:

Wärmebehandlung / heat treatment:

PTQ-Nr. / PTQ-no.:

Schmelze-Nr. / heat-no.:

Spektralanalyse Foundry-MASTER Werkstoff / grade:

	Fe	C	Si	Mn	P	S	Cr	Mo
1	97,8	0,0581	0,157	1,56	0,119	0,0162	0,0451	< 0,0030
Ave	97,8	0,0581	0,157	1,56	0,119	0,0162	0,0451	< 0,0030

	Ni	Al	Co	Cu	Nb	Ti	V	W
1	0,0251	0,0191	0,0127	0,0078	0,0416	0,102	0,0165	< 0,0250
Ave	0,0251	0,0191	0,0127	0,0078	0,0416	0,102	0,0165	< 0,0250

	Pb	Zr
1	< 0,0100	< 0,0030
Ave	< 0,0100	< 0,0030

Ort / town

Datum / date  
09.11.2021

Prüfer / tester

Sachverständiger / expert: Dr.sc.ing. asoci. prof. P. Gavrilovs

RTU, Transport institute  
Paula Valdena 1  
Riga (Latvia)  
Tel.: +371 29247769  
Web: www.dzt.edu.lv  
e-mail: pavels.gavrilovs@rtu.lv



## Chemical Results

Probe Nr. / sample ID: PARAUGS 2\_II

Grundwerkstoff / material:

Kunde / customer:

Abmessung / dimension :

Kom.-Nr. / commission :

Zusatzwerkstoff / filler metals:

Labor Nr. / lab-no.:

Wärmebehandlung / heat treatment :

PTQ-Nr. / PTQ-no.:

Schmelze-Nr. / heat-no.:

Spektralanalyse Foundry-MASTER

Werkstoff / grav1.0986 S550MC

	Fe	C	Si	Mn	P	S	Cr	Mo
Min		0,0000	0,0000	0,0000	0,0000	0,0000	0,0000	0,0000
Max		0,120	0,500	1,80	0,0250	0,0150	0,200	0,100
1	97,7	0,0437	0,169	1,71	0,0120	< 0,0050	0,0410	< 0,0030
Ave	97,7	0,0437	0,169	1,71	0,0120	< 0,0050	0,0410	< 0,0030
	Ni	Al	Co	Cu	Nb	Ti	V	W
Min	0,0000	0,0150			0,0000	0,0000	0,0000	
Max	0,150	1,00			0,0900	0,150	0,200	
1	0,0312	0,0233	0,0115	0,0095	0,0424	0,101	0,0159	< 0,0250
Ave	0,0312	0,0233	0,0115	0,0095	0,0424	0,101	0,0159	< 0,0250
	Pb	Zr						
Min								
Max								
1	< 0,0100	< 0,0030						
Ave	< 0,0100	< 0,0030						

Ort / town

Datum / date  
09.02.2022

Prüfer / tester

Sachverständiger / expert: Dr.sc.ing. asoci. prof. P. Gavrilovs

RTU, Transport institute  
 Paula Valdena 1  
 Riga (Latvia)  
 Tel.: +371 29247769  
 Web: www.dzti.edu.lv  
 e-mail: pavels.gavrilovs@rtu.lv



### Chemical Results

Probe Nr. / sample ID: PARAGUS 4 SUVE

Grundwerkstoff / material:

Kunde / customer:

Abmessung / dimension :

Kom.-Nr. / commission :

Zusatzwerkstoff / filler metals:

Labor Nr. / lab-no. :

Wärmebehandlung / heat treatment :

PTQ-Nr. / PTQ-no. :

Schmelze-Nr. / heat-no. :

Spektralanalyse Foundry-MASTER Werkstoff / grade :

	Fe	C	Si	Mn	P	S	Cr	Mo
1	96,7	0,117	0,339	1,49	0,0981	0,0181	0,160	0,102
Ave	96,7	0,117	0,339	1,49	0,0981	0,0181	0,160	0,102

	Ni	Al	Co	Cu	Nb	Ti	V	W
1	0,721	0,0099	0,0133	0,0599	0,0233	0,0454	0,0588	< 0,0250
Ave	0,721	0,0099	0,0133	0,0599	0,0233	0,0454	0,0588	< 0,0250

	Pb	Zr
1	< 0,0100	< 0,0030
Ave	< 0,0100	< 0,0030

Ort / town

Datum / date

Prüfer / tester

Sachverständiger / expert: Dr.sc.ing. asoci. prof. P. Gavrilovs

09.11.2021

RTU, Transport institute  
Paula Valdena 1  
Riga (Latvia)  
Tel.: +371 29247769  
Web: www.dzti.edu.lv  
e-mail: pavels.gavrilovs@rtu.lv



### Chemical Results

Probe Nr. / sample ID: PARAUGS 2_III	Grundwerkstoff / material:
Kunde / customer:	Abmessung / dimension:
Kom.-Nr. / commission:	Zusatzwerkstoff / filler metals:
Labor Nr. / lab-no.:	Wärmebehandlung / heat treatment:
PTQ-Nr. / PTQ-no.:	Schmelze-Nr. / heat-no.:

Spektralanalyse Foundry-MASTER      Werkstoff / grade: St52.05

	Fe	C	Si	Mn	P	S	Cr	Mo
Min		0,0000	0,0000	0,0000	0,0000	0,0000		
Max		0,220	0,550	1,60	0,0400	0,0350		
1	96,9	0,0602	0,291	1,54	H 0,0451	0,0057	0,152	0,0904
Ave	96,9	0,0602	0,291	1,54	H 0,0451	0,0057	0,152	0,0904

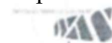
	Ni	Al	Co	Cu	Nb	Ti	V	W
Min								
Max								
1	0,697	0,0064	0,0119	0,0599	0,0208	0,0317	0,0522	< 0,0250
Ave	0,697	0,0064	0,0119	0,0599	0,0208	0,0317	0,0522	< 0,0250

	Pb	Zr
Min		
Max		
1	< 0,0100	< 0,0030
Ave	< 0,0100	< 0,0030

Ort / town	Datum / date	Prüfer / tester	Sachverständiger / expert: Dr.sc.ing. assoc. prof. P. Gavrilovs
	09.02.2022		

RTU, Transport institute  
Paula Valdena 1  
Riga (Latvia)  
Tel.: +371 29247769  
Web: www.dzti.edu.lv  
e-mail: pavels.gavrilovs@rtu.lv



## Chemical Results

Probe Nr. / sample ID: PARAUGS\_3\_II

Grundwerkstoff / material:

Kunde / customer:

Abmessung / dimension:

Kom.-Nr. / commission:

Zusatzwerkstoff / filler metals:

Labor Nr. / lab-no.:

Wärmebehandlung / heat treatment:

PTQ-Nr. / PTQ-no.:

Schmelze-Nr. / heat-no.:

Spektralanalyse Foundry-MASTER Werkstoff / grar1.0421 St52.05

	Fe	C	Si	Mn	P	S	Cr	Mo
Min		0,0000	0,0000	0,0000	0,0000	0,0000		
Max		0,220	0,550	1,60	0,0400	0,0350		
1	97,6	0,0466	0,210	1,59	0,0177	< 0,0050	0,0649	0,0057
Ave	97,6	0,0466	0,210	1,59	0,0177	< 0,0050	0,0649	0,0057
	Ni	Al	Co	Cu	Nb	Ti	V	W
Min								
Max								
1	0,195	0,0194	0,0142	0,0221	0,0381	0,0871	0,0245	< 0,0250
Ave	0,195	0,0194	0,0142	0,0221	0,0381	0,0871	0,0245	< 0,0250
	Pb	Zr						
Min								
Max								
1	< 0,0100	< 0,0030						
Ave	< 0,0100	< 0,0030						

Ort / town

Datum / date  
09.02.2022

Prüfer / tester

Sachverständiger / expert: Dr.sc.ing. asoc. prof. P. Gavrilovs

RTU, Transport institute  
Paula Valdena 1  
Riga (Latvia)  
Tel.: +371 29247769  
Web: www.dzti.edu.lv  
e-mail: pavels.gavrilovs@rtu.lv



## Chemical Results

Probe Nr. / sample ID: PARAUGS 1 SUVE

Grundwerkstoff / material:

Kunde / customer:

Abmessung / dimension :

Kom.-Nr. / commission :

Zusatzwerkstoff / filler metals:

Labor Nr. / lab-no. :

Wärmebehandlung / heat treatment :

PTQ-Nr. / PTQ-no. :

Schmelze-Nr. / heat-no. :

Spektralanalyse Foundry-MASTER Werkstoff / grade :

	Fe	C	Si	Mn	P	S	Cr	Mo
1	96,8	0,0629	0,290	1,44	> 0,125	0,0225	0,154	0,0890
Ave	96,8	0,0629	0,290	1,44	> 0,125	0,0225	0,154	0,0890

	Ni	Al	Co	Cu	Nb	Ti	V	W
1	0,725	0,0074	0,0111	0,0599	0,0201	0,0329	0,0533	< 0,0250
Ave	0,725	0,0074	0,0111	0,0599	0,0201	0,0329	0,0533	< 0,0250

	Pb	Zr
1	< 0,0100	< 0,0030
Ave	< 0,0100	< 0,0030

Ort / town

Datum / date  
09.11.2021

Prüfer / tester

Sachverständiger / expert: Dr.sc.ing. asoc. prof. P. Gavrilovs



## Chemical Results

Probe Nr. / sample ID: PARAUGS 3_III	Grundwerkstoff / material:
Kunde / customer:	Abmessung / dimension :
Kom.-Nr. / commission :	Zusatzwerkstoff / filler metals:
Labor Nr. / lab-no. :	Wärmebehandlung / heat treatment :
PTQ-Nr. / PTQ-no. :	Schmelze-Nr. / heat-no. :

Spektralanalyse Foundry-MASTER Werkstoff / grar1.0421 St52.0S

	Fe	C	Si	Mn	P	S	Cr	Mo
Min		0,0000	0,0000	0,0000	0,0000	0,0000		
Max		0,220	0,550	1,60	0,0400	0,0350		
1	96,8	0,0586	0,312	1,52	H 0,0501	0,0076	0,149	0,0858
Ave	96,8	0,0586	0,312	1,52	H 0,0501	0,0076	0,149	0,0858
	Ni	Al	Co	Cu	Nb	Ti	V	W
Min								
Max								
1	0,704	0,0073	0,0134	0,0585	0,0227	0,0368	0,0544	< 0,0250
Ave	0,704	0,0073	0,0134	0,0585	0,0227	0,0368	0,0544	< 0,0250
	Pb	Zr						
Min								
Max								
1	< 0,0100	< 0,0030						
Ave	< 0,0100	< 0,0030						

Ort / town	Datum / date	Prüfer / tester	Sachverständiger / expert: Dr.sc.ing. asoc. prof. P. Gavrilovs
	09.02.2022		

RTU, Transport institute  
Paula Valdena 1  
Riga (Latvia)  
Tel.: +371 29247769  
Web: www.dzti.edu.lv  
e-mail: pavels.gavrilovs@rtu.lv





### Chemical Results

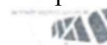
Probe Nr. / sample ID: PARAUGS 4_II	Grundwerkstoff / material:
Kunde / customer:	Abmessung / dimension:
Kom.-Nr. / commission:	Zusatzwerkstoff / filler metals:
Labor Nr. / lab-no.:	Wärmebehandlung / heat treatment:
PTQ-Nr. / PTQ-no.:	Schmelze-Nr. / heat-no.:

Spektralanalyse Foundry-MASTER      Werkstoff / grar1.0421 St52.0S

	Fe	C	Si	Mn	P	S	Cr	Mo
Min		0,0000	0,0000	0,0000	0,0000	0,0000		
Max		0,220	0,550	1,60	0,0400	0,0350		
1	96,8	0,0525	0,313	1,47	0,0345	< 0,0050	0,167	0,0974
Ave	96,8	0,0525	0,313	1,47	0,0345	< 0,0050	0,167	0,0974
	Ni	Al	Co	Cu	Nb	Ti	V	W
Min								
Max								
1	0,786	0,0056	0,0183	0,0620	0,0189	0,0287	0,0563	< 0,0250
Ave	0,786	0,0056	0,0183	0,0620	0,0189	0,0287	0,0563	< 0,0250
	Pb	Zr						
Min								
Max								
1	< 0,0100	< 0,0030						
Ave	< 0,0100	< 0,0030						

Ort / town	Datum / date	Prüfer / tester	Sachverständiger / expert: Dr.sc.ing. assoc. prof. P. Gavrilovs
	09.02.2022		

RTU, Transport institute  
Paula Valdena 1  
Riga (Latvia)  
Tel.: +371 29247769  
Web: www.dzti.edu.lv  
e-mail: pavels.gavrilovs@rtu.lv



### Chemical Results

Probe Nr. / sample ID: PARAUGS 3 SUVE

Grundwerkstoff / material:

Kunde / customer:

Abmessung / dimension :

Kom.-Nr. / commission :

Zusatzwerkstoff / filler metals:

Labor Nr. / lab-no. :

Wärmebehandlung / heat treatment :

PTQ-Nr. / PTQ-no. :

Schmelze-Nr. / heat-no. :

Spektralanalyse Foundry-MASTER Werkstoff / grade :

	Fe	C	Si	Mn	P	S	Cr	Mo
1	96,6	0,0656	0,342	1,45	> 0,125	0,0219	0,160	0,103
Ave	96,6	0,0656	0,342	1,45	> 0,125	0,0219	0,160	0,103

	Ni	Al	Co	Cu	Nb	Ti	V	W
1	0,800	0,0074	0,0132	0,0653	0,0204	0,0344	0,0595	< 0,0250
Ave	0,800	0,0074	0,0132	0,0653	0,0204	0,0344	0,0595	< 0,0250

	Pb	Zr
1	< 0,0100	< 0,0030
Ave	< 0,0100	< 0,0030

Ort / town

Datum / date  
09.11.2021

Prüfer / tester

Sachverständiger / expert: Dr.sc.ing. asoc. prof. P. Gavrilovs

RTU, Transport institute  
Paula Valdena 1  
Riga (Latvia)  
Tel.: +371 29247769  
Web: www.dztu.edu.lv  
e-mail: pavel.gavrilovs@rtu.lv



## Chemical Results

Probe Nr. / sample ID: PARAUGS 4\_III

Grundwerkstoff / material:

Kunde / customer:

Abmessung / dimension :

Kom.-Nr. / commission :

Zusatzwerkstoff / filler metals:

Labor Nr. / lab-no. :

Wärmebehandlung / heat treatment :

PTQ-Nr. / PTQ-no. :

Schmelze-Nr. / heat-no. :

Spektralanalyse Foundry-MASTER

Werkstoff / grar1.5403 17MnMoV6-4

	Fe	C	Si	Mn	P	S	Cr	Mo
Min		0,0000	0,200	1,40	0,0000	0,0000	0,0000	0,200
Max		0,190	0,500	1,70	0,0350	0,0350	0,200	0,500
1	96,6	0,0586	0,333	1,56	H 0,0539	0,0090	0,173	L 0,104
Ave	96,6	0,0586	0,333	1,56	H 0,0539	0,0090	0,173	L 0,104
	Ni	Al	Co	Cu	Nb	Ti	V	W
Min	0,0000	0,0000		0,0000	0,0000	0,0000	0,0000	0,0000
Max	1,00	0,100		0,400	0,0700	0,0500	0,190	0,100
1	0,849	0,0061	0,0142	0,0688	0,0197	0,0291	0,0618	< 0,0250
Ave	0,849	0,0061	0,0142	0,0688	0,0197	0,0291	0,0618	< 0,0250
	Pb	Zr						
Min	0,0000							
Max	0,0700							
1	< 0,0100	< 0,0030						
Ave	< 0,0100	< 0,0030						

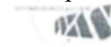
Ort / town

Datum / date  
09.02.2022

Prüfer / tester

Sachverständiger / expert: Dr.sc.ing. assoc. prof. P. Gavrilovs

RTU, Transport institute  
Paula Valdena 1  
Riga (Latvia)  
Tel.: +371 29247769  
Web: www.dzti.edu.lv  
e-mail: pavel.gavrilovs@rtu.lv



## Chemical Results

Probe Nr. / sample ID: PARAUGS 5\_II

Grundwerkstoff / material:

Kunde / customer:

Abmessung / dimension:

Kom.-Nr. / commission:

Zusatzwerkstoff / filler metals:

Labor Nr. / lab-no.:

Wärmebehandlung / heat treatment:

PTQ-Nr. / PTQ-no.:

Schmelze-Nr. / heat-no.:

Spektralanalyse Foundry-MASTER Werkstoff / grar1.0421 St52.05

	Fe	C	Si	Mn	P	S	Cr	Mo
Min		0,0000	0,0000	0,0000	0,0000	0,0000		
Max		0,220	0,550	1,60	0,0400	0,0350		
1	96,9	0,0527	0,276	1,37	0,0320	< 0,0050	0,171	0,107
Ave	96,9	0,0527	0,276	1,37	0,0320	< 0,0050	0,171	0,107
	Ni	Al	Co	Cu	Nb	Ti	V	W
Min								
Max								
1	0,862	0,0030	0,0123	0,0661	0,0170	0,0195	0,0602	< 0,0250
Ave	0,862	0,0030	0,0123	0,0661	0,0170	0,0195	0,0602	< 0,0250
	Pb	Zr						
Min								
Max								
1	< 0,0100	< 0,0030						
Ave	< 0,0100	< 0,0030						

Ort / town

Datum / date  
09.02.2022

Prüfer / tester

Sachverständiger / expert: Dr.sc.ing. assoc. prof. P. Gavrilovs



## Chemical Results

Probe Nr. / sample ID: PARAUGS 6 SUVE

Grundwerkstoff / material:

Kunde / customer:

Abmessung / dimension :

Kom.-Nr. / commission :

Zusatzwerkstoff / filler metals:

Labor Nr. / lab-no. :

Wärmebehandlung / heat treatment :

PTQ-Nr. / PTQ-no. :

Schmelze-Nr. / heat-no. :

Spektralanalyse Foundry-MASTER

Werkstoff / grade :

	Fe	C	Si	Mn	P	S	Cr	Mo
1	96,8	0,0557	0,289	1,40	> 0,125	0,0205	0,169	0,104
Ave	96,8	0,0557	0,289	1,40	> 0,125	0,0205	0,169	0,104

	Ni	Al	Co	Cu	Nb	Ti	V	W
1	0,758	0,0037	0,0116	0,0633	0,0161	0,0239	0,0583	< 0,0250
Ave	0,758	0,0037	0,0116	0,0633	0,0161	0,0239	0,0583	< 0,0250

	Pb	Zr
1	< 0,0100	< 0,0030
Ave	< 0,0100	< 0,0030

Ort / town

Datum / date

Prüfer / tester

Sachverständiger / expert: Dr.sc.ing. asoc. prof. P. Gavrilovs

09.11.2021

RTU, Transport institute  
Paula Valdena 1  
Riga (Latvia)  
Tel.: +371 29247769  
Web: www.dzti.edu.lv  
e-mail: pavel.gavrilovs@rtu.lv



## Chemical Results

Probe Nr. / sample ID: PARAUGS 1\_II

Grundwerkstoff / material:

Kunde / customer:

Abmessung / dimension :

Kom.-Nr. / commission :

Zusatzwerkstoff / filler metals:

Labor Nr. / lab-no. :

Wärmebehandlung / heat treatment :

PTQ-Nr. / PTQ-no. :

Schmelze-Nr. / heat-no. :

Spektralanalyse Foundry-MASTER Werkstoff / grar1.0421 St52.0S

	Fe	C	Si	Mn	P	S	Cr	Mo
Min		0,0000	0,0000	0,0000	0,0000	0,0000		
Max		0,220	0,550	1,60	0,0400	0,0350		
1	96,8	0,0595	0,299	1,52	< 0,0050	< 0,0050	0,155	0,0930
Ave	96,8	0,0595	0,299	1,52	< 0,0050	< 0,0050	0,155	0,0930
	Ni	Al	Co	Cu	Nb	Ti	V	W
Min								
Max								
1	0,794	0,0038	0,0094	0,0642	0,0188	0,0274	0,0553	< 0,0250
Ave	0,794	0,0038	0,0094	0,0642	0,0188	0,0274	0,0553	< 0,0250
	Pb	Zr						
Min								
Max								
1	< 0,0100	< 0,0030						
Ave	< 0,0100	< 0,0030						

Ort / town

Datum / date  
09.02.2022

Prüfer / tester

Sachverständiger / expert: Dr.sc.ing. assoc. prof. P. Gavrilovs

## ATBILSTĪBAS SERTIFIKĀTS

(Saskaņā ar LVS EN ISO/IEC 17050-1)

Datums 30.09.2021  
Sertifikāta Nr: 2067  
Kods/Produkts: 112967 MISON®25 10l/200bar  
Pavadzīmes/partijas Nr. 60976051  
Klienta nosaukums: SPECIĀLS ELEKTRODS SIA

Augstākminētais produkts atbilst Linde Gas SIA produkta specifikācijai:

Gāzes sastāvs	Daudzums	Mērvienība
Oglekļa dioksīds CO <sub>2</sub>	25 ± 2,5	tilpuma %
Slāpekļa monoksīds NO	275 ± 50	ppm*
Argons Ar	līdzsvarā	-
Mitrums H <sub>2</sub> O ne vairāk kā	10	ppm*
Slāpekļa dioksīds NO <sub>2</sub> ne vairāk kā	10	ppm*

\*ppm - tilpuma miljonā daļa

### Komentāri

Atbilst LVS EN ISO 14175 standarta prasībām

Metināšanā izlietojamie materiāli.

Gāzes un gāzu maisījumi kausēšanas metināšanai un radnieciskiem procesiem

Apzīmējums:

**LVS EN ISO 14175-Z-ArC+NO-25/0,03**

Pilnvarotās personas paraksts:

Paraksta atšifrējums:

Linde Gas SIA gāzu uzpildes stacija, Putnu iela 2, Zaķumuiža

  
Andris Ceplis

## ATBILSTĪBAS SERTIFIKĀTS

(Saskaņā ar LVS EN ISO/IEC 17050-1)

Datums 30.09.2021  
Sertifikāta Nr: 2068  
Kods/Produkts: 100968 MISON®18 20 L, 200 bar  
Pavadzīmes/partijas Nr. 60976051  
Klienta nosaukums: SPECIĀLS ELEKTRODS SIA

Augstākminētais produkts atbilst Linde Gas SIA produkta specifikācijai:

Gāzes sastāvs	Daudzums	Mērvienība
Oglekļa dioksīds CO <sub>2</sub>	18 ± 1,8	tilpuma %
Slāpekļa monoksīds NO	275 ± 50	ppm*
Argons Ar	līdzsvarā	-
Mitrums H <sub>2</sub> O ne vairāk kā	10	ppm*
Slāpekļa dioksīds NO <sub>2</sub> ne vairāk kā	10	ppm*

\*ppm - tilpuma miljonā daļa

### Komentāri

Atbilst LVS EN ISO 14175 standarta prasībām

Metināšanā izlietojamie materiāli.

Gāzes un gāzu maisījumi kausēšanas metināšanai un radnieciskiem procesiem

Apzīmējums: **LVS EN ISO 14175-Z-ArC+NO-18/0,03**

Pilnvarotās personas paraksts:

Paraksta atšifrējums:

Linde Gas SIA gāzu uzpildes stacija, Putnu iela 2, Zaķumuiža

  
Andris Ceplis



## ATBILSTĪBAS SERTIFIKĀTS

(Saskaņā ar LVS EN ISO/IEC 17050-1)

Datums 30.09.2021  
Sertifikāta Nr: 2070  
Kods/Produkts: 101638 MISON®8 20L/200bar  
Pavadzīmes/partijas Nr. 60976051  
Klienta nosaukums: 100968 MISON®18 20 L, 200 bar

Augstākminētais produkts atbilst Linde Gas SIA produkta specifikācijai:

Gāzes sastāvs	Daudzums	Mērvienība
Oglekļa dioksīds CO <sub>2</sub>	8 ± 0,8	tilpuma %
Slāpekļa monoksīds NO	275 ± 50	ppm*
Argons Ar	līdzsvarā	-
Mitrums H <sub>2</sub> O ne vairāk kā	10	ppm*
Slāpekļa dioksīds NO <sub>2</sub> ne vairāk kā	10	ppm*

\*ppm - tilpuma miljonā daļa

### Komentāri

Atbilst LVS EN ISO 14175 standarta prasībām

Metināšanā izlietojamie materiāli.

Gāzes un gāzu maisījumi kausēšanas metināšanai un radnieciskiem procesiem

Apzīmējums:

**LVS EN ISO 14175-Z-ArC+NO-8/0,03**

Pilnvarotās personas paraksts:

Paraksta atšifrējums:

Linde Gas SIA gāzu uzpildes stacija, Putnu iela 2, Zaķumuiža

  
Andris Ceplišs

## ATBILSTĪBAS SERTIFIKĀTS

(Saskaņā ar LVS EN ISO/IEC 17050-1)

Datums 30.09.2021  
Sertifikāta Nr: 2071  
Kods/Produkts: 101604 CORGON®3 50L/200bar  
Pavadzīmes/partijas Nr. 60976051  
Klienta nosaukums: SPECIĀLĀS ELEKTRODS SIA

Augstākminētais produkts atbilst Linde Gas SIA produkta specifikācijai:

Gāzes sastāvs	Daudzums	Mērvienība
Oglekļa dioksīds CO <sub>2</sub>	5 ± 0,5	tilpuma %
Skābeklis O <sub>2</sub>	5 ± 0,5	tilpuma %
Argons Ar	līdzsvarā	-
Mitrums H <sub>2</sub> O ne vairāk kā	20	ppm*

\*ppm - tilpuma miljonā daļa

### Komentāri

Atbilst LVS EN ISO 14175 standarta prasībām

Metināšanā izlietojamie materiāli.

Gāzes un gāzu maisījumi kausēšanas metināšanai un radnieciskiem procesiem

Apzīmējums: **LVS EN ISO 14175-M23-ArCO-5/5**

### Klienta paraksts:

Paraksta atšifrējums:

Pilnvarotās personas paraksts:

Paraksta atšifrējums:

  
Andris Ceplis

Linde Gas SIA gāzu uzpildes stacija, Putnu iela 2, Zaķumiža



COMPANY:	RTU Promocijas Padomei P-16
ATT:	
FROM:	GPOWER SIA

16.06.2022.

### **Vēstule.**

Uzņēmums SIA GPower daudzus gadus nodarbojas ar dažādu mobilo sakaru un cita veida aprīkojuma izgatavošanu. Viena no galvenajām prasībām uzņēmuma darbības virzienā ir izmantoto konstrukciju celtspēja un izturība, tai pašā laikā samazināta iekārtas kopējā masa. Kā vienu no risinājumiem SIA GPower ir izvēlēties aizvietot konstrukciju tēraudu ar augstas izturības tēraudu savos produktos.

Līdz šim gūtā pieredze metālapstrādē ir bijusi saistīta ar maz leģētu konstrukciju tēraudu produkciju izgatavošanu. Tomēr priekšrocības, ko sniedz augstas izturības tēraudi, būtiski atvieglotu izgatavojamās konstrukcijas, kā arī samazinātu paredzamās izgatavošanas un produkcijas transportēšanas izmaksas. Izgatavošanas tehnoloģijas, kuru skaitā ir arī metināšana, ir nepieciešams mainīt vai izstrādāt no jauna. Šī iemesla dēļ tika uzsākta sadarbība ar Rīgas Tehnisko Universitāti, piedaloties zinātniskā pētījumā par mums interesējošo augstas izturības tēraudu pusautomātisko metināšanu. Tieši šis process ir aktuāls SIA GPower ražošanā, jo to ir iespējams veikt gan izmantojot uzņēmuma darbiniekus, gan procesu mehanizējot. Viens no būtiskiem kritērijiem, kas ieinteresēja uzņēmumu, ir esošo metināšanas procesu optimizācija un ražības palielināšanas.

Iegūtā pētījuma rezultāti ir snieguši atbildes uz vairākiem jautājumiem, kas radušies augstas izturības tēraudu apstrādē. Ir veikti pirmie eksperimenti, balstoties uz pētījumā iegūtajiem rezultātiem, kas ir devuši iespēju metināšanas procesā uzlabot gan sametinātās šuves kvalitāti, gan procesa ražību.

SIA GPower arī turpmāk cer uz sekmīgu sadarbību ar Rīgas Tehnisko Universitāti, attīstot uzlabot un paplašinot pielietojamās tehnoloģijas, un ieviešot tās uzņēmuma ražošanas procesos.

Ar cieņu,  
Gpower SIA  
Valdes loceklis

Mārtiņš Grantiņš

Promocijas padomei P-16

Rīga,  
15.09.2022.

### Vēstule


Pirms vairāk nekā gada mūsu uzņēmumu, Speciāls elektrods, uzrunāja un piedāvāja iesaistīties zinātniskā pētījumā par specifiska materiāla – augstas izturības tērauda – metināšanu. Mūs, kā vienu no vadošajiem metināšanas iekārtu piegādātājiem Latvijā, kas izplata pasaulē zināma zīmola *Fronius International* metināšanas aprīkojumu, piekritām piedalīties šajā zinātniskā darba tapšanā.

Augstas izturības tēraudi ik gadu arvien biežāk ir sastopami dažādu Latvijas metālapstrādes uzņēmumu pasūtījumos. To metināšanas specifika atšķiras no ikdienā izmantoto materiālu metināšanas, kas ir viens no lēmumiem, kāpēc ir virkne uzņēmumu, kas, nepārzinot tehnoloģiskās iespējas un risinājumus, atsakās no pasūtījumiem, kuros ir sastopami iepriekš minētie tēraudi.

Pateicoties šim pētījumam arī mums, kā iekārtu un palīgmateriālu piegādātājiem, paveras iespēja sniegt risinājumus un ieteikumus metālapstrādes uzņēmumiem, lai veicinātu to izaugsmi un paplašināt ražošanas iespējas. Piedaloties zinātniskā pētījuma eksperimentos arī mūsu uzņēmuma darbinieki guva jaunu pieredzi un idejas, kas dotu uzlabojumus ikdienas darbā gan uzņēmumā esošajā darbnīcā, gan pie klientiem.

Pateicamies par sniegto iespēju sadarboties ar Rīgas Tehnisko Universitāti šajā pētījumā, kas vēlāk arī sniedza iespēju piedalīties Mašīnbūves, Transporta un Aeronautikas Fakultātes rīkotajā seminārā ar prezentāciju par šī brīža aktuālajām industrijas tehnoloģijām un to pielietojumu.

SIA Speciāls elektrods  
Valdes loceklis



O. Stepiņš

SIA «Speciāls Elektrods» • Reģ. Nr.: LV50003400101 • Brīvības iela 224, Rīga, LV-1039

Tālr.: +371 67 332 603 • E-pasts: info@specialelektrods.lv